Characterization of DPP4^{+} fibroadipogenic progenitors in skeletal muscle

by

Chun Wai Cheung

B.Sc., The Hong Kong University of Science and Technology, 2021

A THESIS SUBMITTED IN PARTIAL FULFILLMENT OF

THE REQUIREMENTS FOR THE DEGREE OF

MASTER OF SCIENCE

in

THE FACULTY OF GRADUATE AND POSTDOCTORAL STUDIES

(Medical Genetics)

THE UNIVERSITY OF BRITISH COLUMBIA

(Vancouver)

August 2023

The following individuals certify that they have read, and recommend to the Faculty of Graduate and Postdoctoral Studies for acceptance, the thesis entitled:

Characterization of DPP4^{+} fibroadipogenic progenitors in skeletal muscle

submitted by Chun Wai Cheung in partial fulfilment of the requirements for

the degree of Master of Science

in Medical Genetics

Examining Committee:

Fabio Rossi, Professor, Medical Genetics, UBC
Supervisor

Gordon Francis, Professor, Medical Genetics, UBC
Supervisory Committee Member

Marco Marra, Professor, Medical Genetics, UBC
Additional Examiner

Michael Underhill, Professor, Biomedical Engineering, UBC
Additional Examiner

Additional Supervisory Committee Members:

Freda Miller, Professor, Medical Genetics, UBC
Supervisory Committee Member

Abstract

Muscle regeneration is a highly orchestrated process in which multiple tissue-resident and infiltrating cells actively participate to ensure optimal repair and functional recovery. More than a decade ago, we reported a muscle resident, non-myogenic mesenchymal stromal cell type which we termed fibroadipogenic progenitors (FAPs) for their ability to spontaneously differentiate into mature fibroblasts or adipocytes. FAPs regulate multiple aspects of muscle biology, including maintenance of basement membrane, provide trophic support for muscle satellite cells, and recruitment of immune cells in response to injury. Recently, advent in single cell technologies unveiled previously unappreciated heterogeneity within FAPs. We and others identified *dipeptidyl peptidase 4* (*Dpp4*) as a putative marker for one of the FAP subsets that is present in homeostasis. In this study, we first demonstrated a robust flow cytometry workflow to purify $DPP4^+$ FAPs from steady state skeletal muscles, and implemented a variety of biological assays to comprehensively characterize this FAP subset. $DPP4^+$ FAPs are more proliferative, display a stronger capacity of undergoing adipogenic differentiation without sacrificing their fibrogenic potential, and have a higher frequency of colony forming units (CFUs), compared with their DPP4-negative counterparts. *In vitro* culturing further showed that $DPP4^+$ FAPs are the precursors of $DPP4^-$ FAPs, while $DPP4^-$ FAPs have negligible contribution to $DPP4^+$ FAPs. We also revealed a potential role of $DPP4^+$ FAPs as a niche for a recently discovered population of $LYVE1^+$ skeletal muscle self-renewing resident macrophages. Lastly, we employed a newly developed transgenic $DPP4^{CreERT2}$ mouse model to ablate DPP4-expressing cells and showed that they are critical for survival. Together, this project provided a detailed description of a novel FAP subset that has important roles in steady state muscles.

Lay Summary

Muscle regeneration is a complex process involving different cell types that work together to repair and restore muscle function. In some diseases muscles are replaced by scars or fats, both coming from a cell type within muscle known as fibroadipogenic progenitors (FAPs). Interestingly, FAPs are also found in healthy muscles and are needed for them to stay healthy. Therefore, understanding how FAPs switch from supporting healthy muscles to hindering them by forming fat and scar tissues will help us manage degenerative diseases. Here, we described the functions of a specific subset of FAP. They can form both scar and fat, but they are also needed to support muscle cells.

Preface

My contributions in the thesis include development of the concept, performing experiments and analyzing data. Lin Wei Tung assisted in analyze of bulk and single cell RNA sequencing data.

Chapter 1 is modified from a manuscript under preparation. I wrote the majority of the section with scientific inputs from Dr. Morten Ritso, Dr Marine Theret, Dr. Fabio Rossi and Lin Wei Tung.

Chapter 3.7 is modified from a manuscript under preparation titled *DPPIV+ fibro-adipogenic progenitors form the niche of adult skeletal muscle self-renewing resident macrophages*. I performed relevant experiments and analyzed the data in the session.

All research involving animals was conducted following the protocols approved by the UBC Animal Care Committee (protocols A19-0316, A18-0314, and A22-0245).

Table of Contents

List of Tables

List of Figures

List of Abbreviations

4ebp1	Eukaryotic Translation Initiation Factor 4E-Binding Protein 1
Acta2	Actin Alpha 2
ACVR1	Activin A Receptor Type 1
ADA	Adenosine Deaminase
ADAM12	A Disintegrin And Metalloproteinase Domain-Containing Protein 12
ADP	Adenosine Diphosphate
Akt	Ak Strain Transforming
ANOVA	Analysis Of Variance
ATP	Adenosine Triphosphate
bFGF	Basic Fibroblast Growth Factor
BMP	Bone Morphogenetic Protein
CCR	CC Chemokine Receptor
CD	Cluster of Differentiation
CDK	Cyclin Dependent Kinase
CFU	Colony Forming Unit
ChIP	Chromatin Immunoprecipitation
CSF1	Colony Stimulating Factor 1
Ctgf	Connective Tissue Growth Factor
CXCL	Chemokine (C-X-C Motif) Ligand
DM	Diabetes Mellitus
DMD	Duchenne Muscular Dystrophy

Dpp4	Dipeptidyl Peptidase 4
DTA	Diphtheria Toxin Fragment A
DUX4	Double Homeobox 4
ECM	Extracellular Matrix
ERK	Extracellular Signal-Regulated Kinase
FACS	Fluorescence-Activated Cell Sorting
FAP	Fibroadipogenic Progenitor
FGF2	Fibroblast Growth Factor 2
Fn1	Fibronectin 1
FOP	Fibrodysplasia Ossificans Progressiva
FOXO1	Forkhead Box Protein O1
FSHD	Facioscapulohumeral Muscular Dystrophy
Gdf10	Growth Differentiation Factor 10
GFP	Green Fluorescent Protein
GLP-1	Glucagon-Like Peptide-1
HDAC	Histone Deacetylase
HIC1	Hyper-Methylated in Cancer 1
HO	Heterotopic Ossification
HPF	Hepatocyte Growth Factor
Hprt	Hypoxanthine-Guanine Phosphoribosyltransferase
IFNγ	Interferon Gamma
Ig	Immunoglobulin

IGF	Insulin-Like Growth Factor
IL	Interleukin
IMAT	Intramuscular Adipose Tissue
IRAK1	Interleukin 1 Receptor Associated Kinase 1
JAK/STAT	Janus Kinase/Signal Transducers And Activators Of Transcription
kDA	Kilodalton
LGMD2B	Limb Girdle Dystrophy 2B Muscular Dystrophy
Ly6A	Lymphocyte Antigen 6 Family Member A
LYVE1	Lymphatic Vessel Endothelial Receptor 1
MAPK	Mitogen-Activated Protein Kinase
miR	microRNA
MMP	Matrix Metalloproteinase
MRF4	Muscle Specific Regulatory Factor 4
MSC	Mesenchymal Stromal/Stem Cell
mTOR	Mammalian Target Of Rapamycin
MuSC	Muscle Satellite Cell
Myf5	Myogenic Factor 5
MyoD	Myoblast Determination Protein 1
n.s.	Not Significant
NF-κB	Nuclear Factor Kappa B
NID1	Nidogen1
NO	Nitric Oxide

NTX	Notexin
OSM	Oncostatin M
Osr1	Odd Skipped-Related 1
PAX7	Paired Box 7
PBS	Phosphate-Buffered Saline
PDGFRα	Platelet Derived Growth Factor Receptor Alpha
Pi16	Peptidase Inhibitor 16
PI3k	Phosphoinositide 3-Kinase
PLIN	Perilipin
PPARγ	Peroxisome Proliferator Activated Receptor Gamma
RTqPCR	Reverse Transcription Quantitative Polymerase Chain Reaction
Sca-1	Stem Cell Antigen-1
SDF1α	Stromal Cell Derived Factor 1 Alpha
SMAD	Small Mothers Against Decapentaplegic
SRRM	Self-Renewing Resident Macrophage
TA	Tibialis Anterior
TAK1	Transforming Growth Factor-B-Activated Kinase 1
Tcf4	Transcription Factor 4
TGFβ	Transforming Growth Factor Beta
THBS1	Thrombospondin 1
TIM4	T-Cell Immunoglobulin And Mucin Domain Containing 4
TIMP	Tissue Inhibitor of Metalloproteinase

TMX	Tamoxifen
TNFα	Tumor Necrosis Factor Alpha
UMAP	Uniform Manifold Approximation and Projection
VCAM1	Vascular Cell Adhesion Molecule 1
WISP1	Wnt1-Inducible-Signaling Pathway Protein 1
αSMA	Alpha Smooth Muscle Actin

Acknowledgements

It is my greatest honour to be able to work under my incredible supervisor, Dr. Fabio Rossi. He has been an amazing supervisor throughout my study, always kind and humorous that made me believe that I had joined the right lab for my postgraduate study. He provided me with important insights at the time when I was struggling the most. Thank you so much for taking me as your student. I would also like to express my sincere gratitude to the members of my supervisory committee, Dr. Gordon Francis and Dr. Freda Miller, for the valuable discussions, providing supports and guidance.

I also need to thank my mentors in the lab throughout my study, Dr. Farshad Babaeijandaghi, Dr. Morten Ritso, and Dr. Marine Theret, for your excellent mentorships. All three of you are always helpful with my experiments, data analyses and interpretations. You are a knowledge hub that I can always count on whenever I encounter scientific and technical questions. I would also like to thank the other members of the Rossi Lab, Vittoria Canale, Chihkai Chang, Ian Coccimiglio, David Guo, Mark Hamer, Nasim Kajabadi, Bruce Lin, Dr. Ashok Narasimhan, Dr. Sandeep Saxena, Laura Stankiewicz, Henry Tung, and Lin Yi. Thank you all for creating the most amazing lab environment.

Many of the works would not be possible without the help from the following people: Takahide Murakami at the BRC Genotyping Facility; Krista Ranta, Wei Yuan and Jaspreet Rai at the BRC Animal Facility; Tara Stach at the BRC Sequencing Facility; Michael Williams at AbLab; Andy Johnson and Justin Wong at the UBC Flow Cytometry Facility.

Last but not least, I thank all my dear family and friends for your continuous support and love, even many of you are at the other side of the globe.

Dedication

To all my loved ones.

Chapter 1: Introduction

1.1 Skeletal Muscle Anatomical and Molecular Organization

Skeletal muscles contribute to about 40% of total body mass, making it the largest organ in human body (Janssen et al., 2000). Voluntary contraction of skeletal muscle confers locomotion and breathing (Dumont et al., 2015). They also play key roles in thermoregulation, maintaining balance, and glucose homeostasis. (Leon, 2017).

Skeletal muscles are composed of individual multinucleated myofibers that are bundled together into fascicles. Each fascicle is enclosed by a continuous layer of connective structure called perimysium. Within each fiber bundle, individual muscle fibers are surrounded by another connective tissue layer called the endomysium. Both perimysium and endomysium create continuous three-dimensional frameworks between and within the fascicles, which links neighboring muscle fibers together. Multiple fasicles form a skeletal muscle, which is covered in a layer of extracellular matrix-rich structure known as the epimysium. (Figure 1.1) (Purslow, 2020).

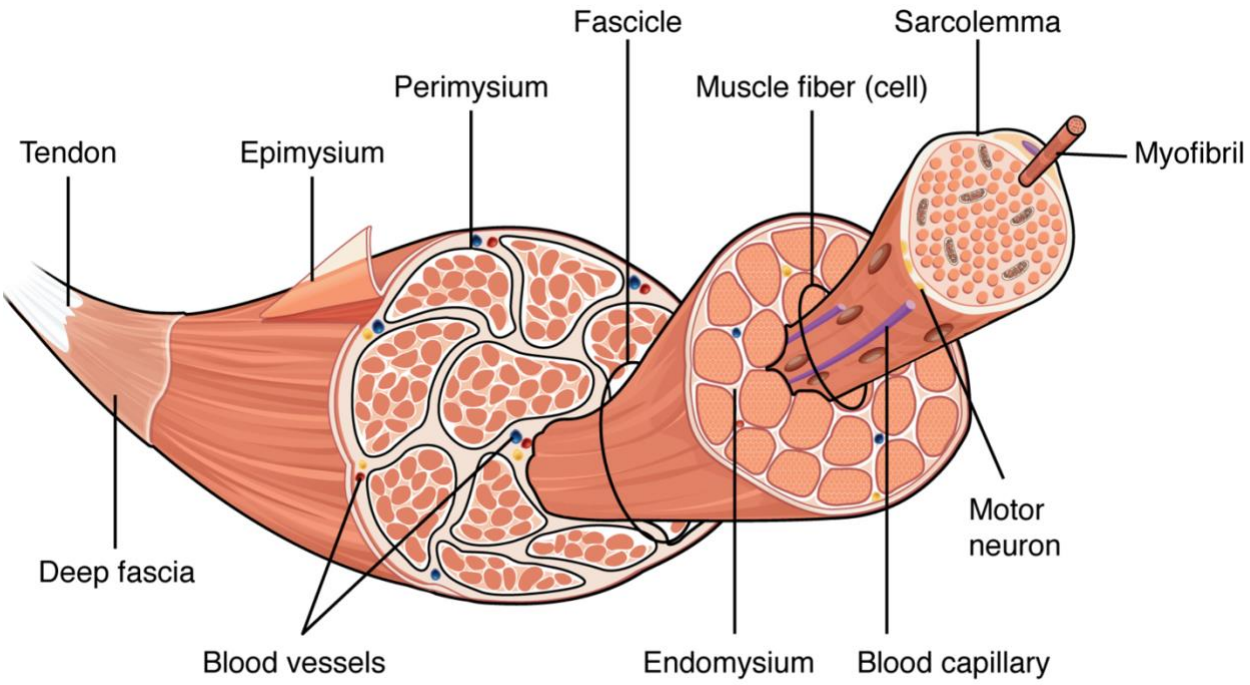

Figure 1.1 Connective tissues enclosing skeletal muscles

Adapted from *Anatomy & Physiology* (Biga et al., 2020), licensed under a Creative Commons Attribution-ShareAlike 4.0 International License.

A sarcomere is the basic contractile unit of a skeletal muscle, where thousands of them stack on top of each other and form cylindrical myofibrils, giving skeletal muscle its striated appearance (Au, 2004). It is composed of a network of thin filaments (primarily made of actin), thick filaments (primarily made of myosin), and cytoskeleton associating proteins, such as troponin and tropomyosin (Figure 1.2) (Au, 2004). Upon binding to Ca^{2+} ions, troponin undergoes a conformational change and releases tropomyosin from steric hindrance, which enables myosin to interact with the previously-occupied F-actin filament for force generation and transmission (Sweeney & Hammers, 2018).

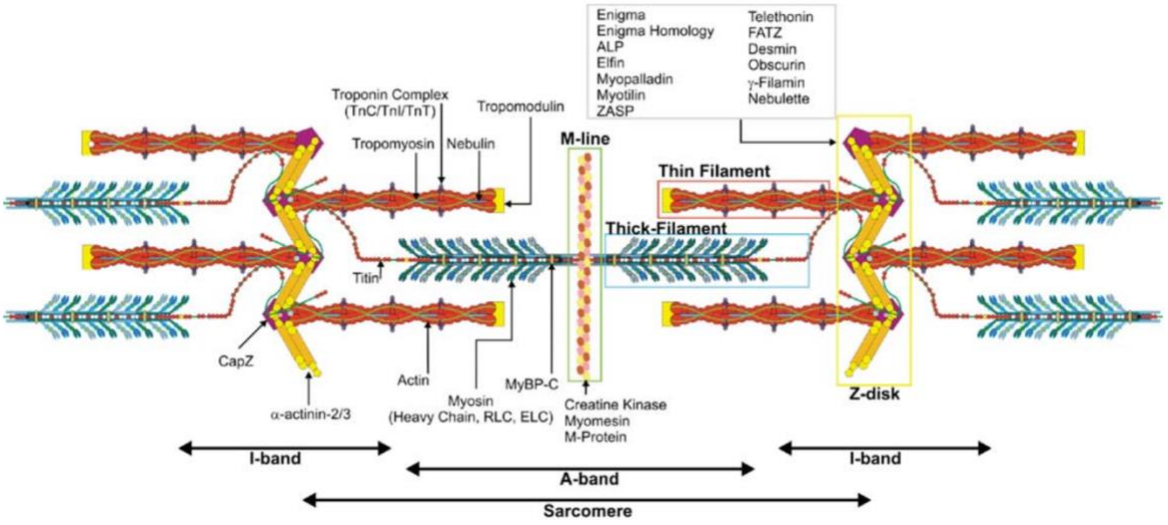

Figure 1.2 Schematic representation of sarcomere

Adapted from *The muscle ultrastructure: a structural perspective of the sarcomere* (Au, 2004).

Myosin is a type of motor protein that can "walk" on actin filaments using energy from ATP hydrolysis. In the beginning of the power stroke cycle, ATP binding to myosin would lead to its dissociation from actin. This triggers ATPase activity of myosin, hence ATP undergoes hydrolysis and gives rise to ADP and a phosphate group. Myosin in ADP-bound form rapidly rebounds to actin and releases the hydrolyzed phosphate group, at the same time inducing conformation changes in myosin, causing the level arm to move forward (Figure 1.3) (Sweeney & Holzbaur, 2018). In skeletal muscle, the re-engagement of myosin to actin moves the thin filament towards the M-line, shortening the sarcomere to generate force, which contracts the muscle (Sweeney & Hammers, 2018).

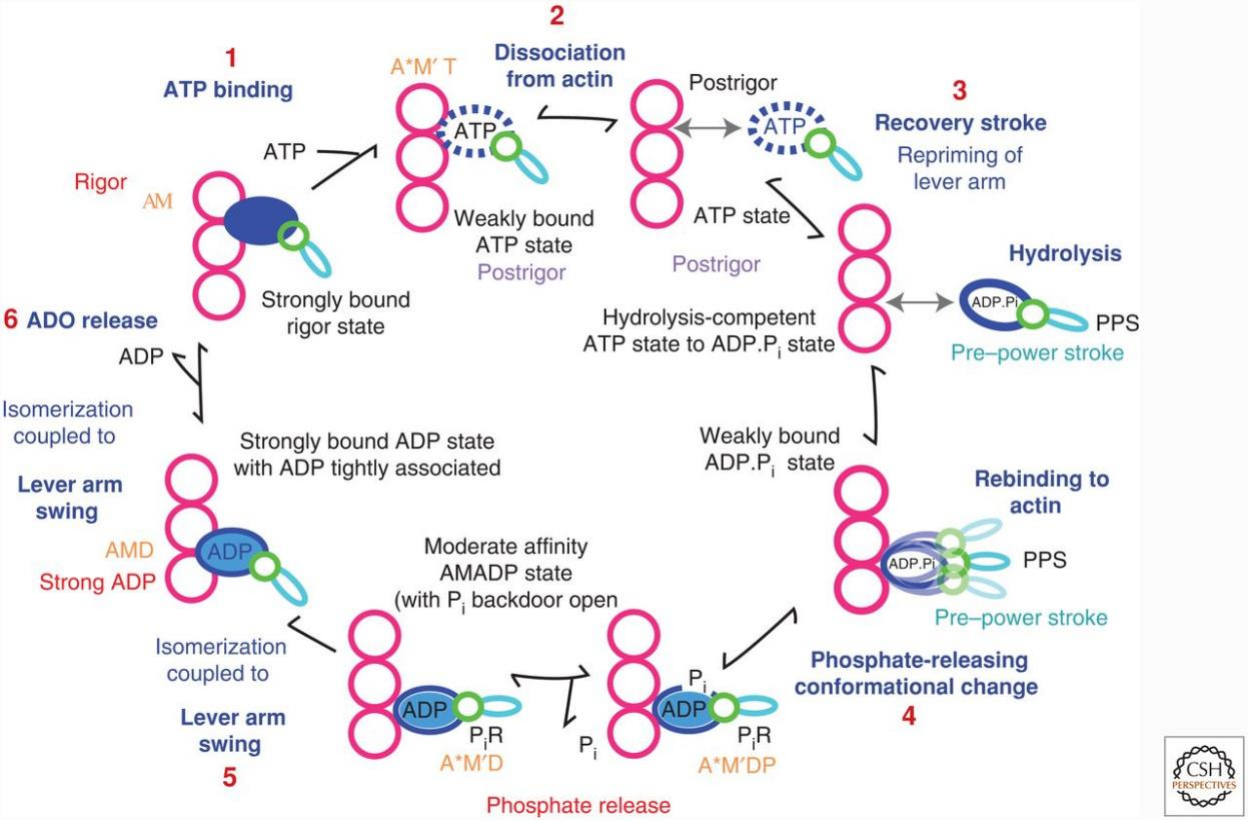

Figure 1.3 Myosin power stroke cycle

Adapted from *Motor Proteins* (Sweeney & Holzbaur, 2018).

1.2 Muscle Regeneration: An Orchestrated Process

Given the importance of muscle tissue, and the fact that muscles are under constant perturbations arising from daily usage, it is critical for them to maintain anatomical and functional integrity by endogenous regeneration. The incredible regenerative potential of skeletal muscle is conferred on the resident muscle stem cells (MuSCs), also known as satellite cells. While MuSCs are the principal contributor to repairing and rebuilding myofibers, muscle regeneration is a tightly regulated process that involves additional cell populations, such as muscle-resident and infiltrating immune cells, stromal, mural, as well as endothelial cells (Figure 1.4) (Wosczyna & Rando, 2018).

All of these populations are required to ensure the regeneration process is both efficient and complete. A brief overview of the roles of muscle stem cells and immune cells in the regenerative process will be provided, while fibroadipogenic progenitors (FAPs) will be discussed in more detail in section 1.3 as it is the primary scope of the thesis.

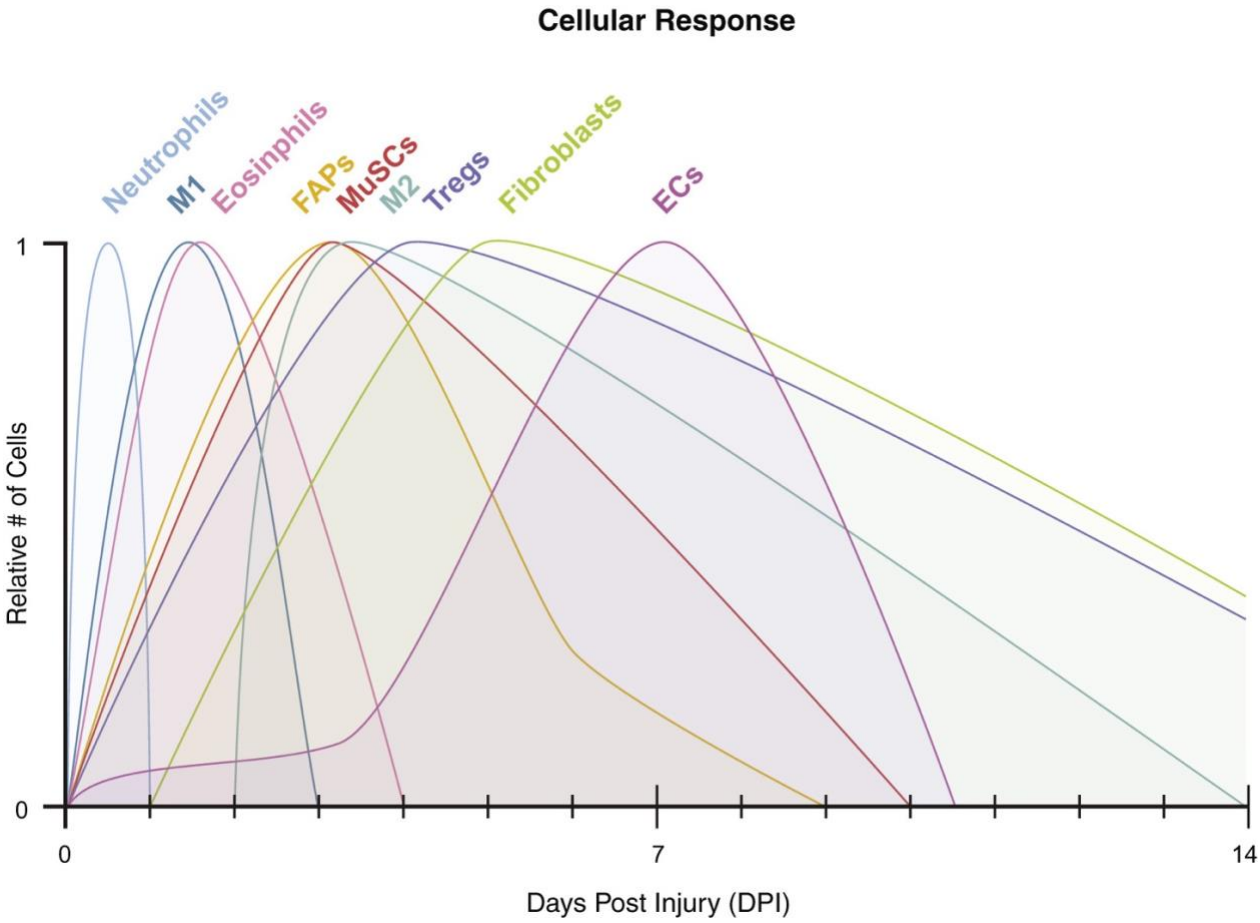

Figure 1.4 Dynamics of different cell types spanning muscle regeneration process

Adapted from A Muscle Stem Cell Support Group: Coordinated Cellular Responses in Muscle Regeneration (Wosczyna & Rando, 2018).

1.2.1 Muscle Satellite Cell

In 1961, Alexander Mauro first reported the presence of a rounded cell type residing between the plasma membrane and the basal lamina using electron microscopy, hence naming this cell type "satellite cell" (Mauro, 1961). Direct experimental evidence of satellite cells' contribution to new myonuclei emerged as Moss and Leblond proved that their progenies were incorporated into existing myofibers (Moss & Leblond, 1970). This led to the speculation that they could serve as the stem cell of skeletal muscle. Indeed, subsequent studies reported self-renewal and differentiation capabilities of MuSCs, which confirmed their identity as muscle-resident stem cells (Collins et al., 2005; Kuang et al., 2007; Sacco et al., 2008).

In adult muscle, MuSCs are uniquely marked by the expression of nuclear transcription factor Pax7 (Seale et al., 2000). $Pax7^+$ MuSCs was shown to be required for the muscle regeneration process (Sambasivan et al., 2011). Importantly, MuSCs differentiate both asymmetrically and symmetrically, whereas the former generates one committed myogenic progenitor ($Pax7^+/Myf5^+$) and one satellite stem cell ($Pax7^+/Myf5^-$), while the latter one result in either stem cell poll expansion (if both daugther cells remain $Myf5^-$) or depletion (if both daughter cells became $Myf5^+$) (Figure 1.5) (Chang et al., 2016; Kuang et al., 2007).

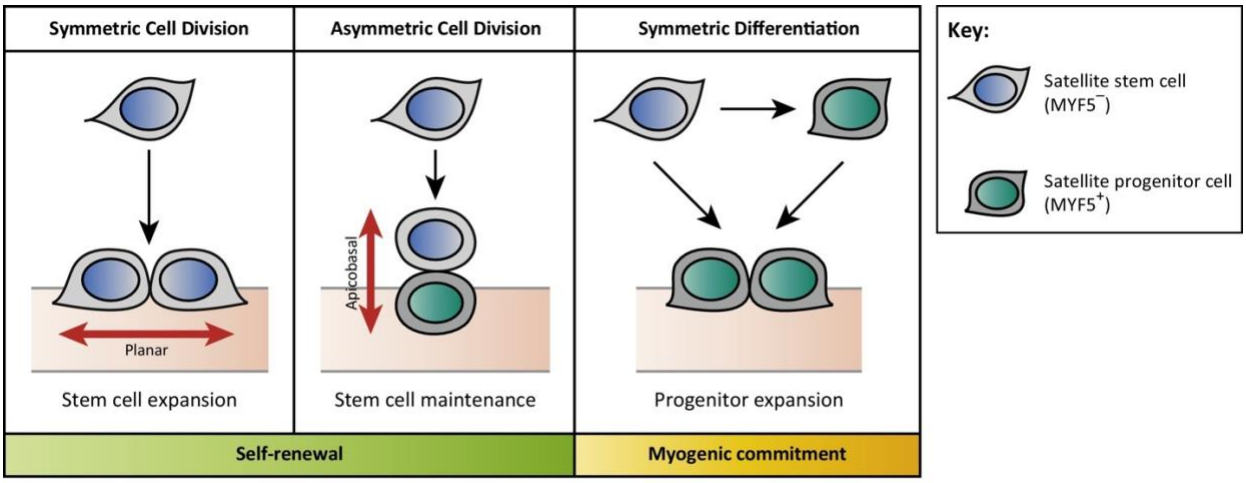

Figure 1.5 Symmetric and asymmetric division of satellite cells are critical mechanisms governing the maintenance of stem cell pool and regenerative success

Adapted from *Satellite Cells in Muscular Dystrophy – Lost in Polarity* (Chang et al., 2016).

Under homeostatic conditions, MuSCs are in a quiescent state, also known as G_0 phase, which is a critical mechanism for them to maintain genomic integrity, while preserving the ability to rapidly respond to external insults (Cheung & Rando, 2013). Upon injury, several growth factors, such as FGF2/bFGF (DiMario et al., 1989) and HGF (Tatsumi et al., 1998) are released from the damaged ECM, which serve as activation signals for MuSCs. FGF2 stimulates MuSC quiescence exit and activation by p38α/β MAPK (Jones et al., 2005). Other cells residing in the muscle stem cell niche also participate in the activation process. For example, IGF-1 secreted by fibroblast and myofiber downregulates FOXO1, which inhibits the activity of cell cycle inhibitor $p27^{kip}$, resulting in MuSC cell cycle re-entry (Machida et al., 2003; Perrone et al., 1995). Cytokines such as TNF-α released from immune cells were also shown to activate quiescent MuSCs (Acharyya et al., 2010; Li, 2003).

After the activation and proliferation phase, MuSCs begin to differentiate into committed $MyoD^+$ myoblasts. MyoD is a master regulator of the myogenic program as it possesses the ability to reprogram fibroblasts into myogenic cells (Davis et al., 1987). MyoD-null MuSCs display defective regeneration, inability to differentiate, and fail to upregulate late myogenic factors such as MRF4 and myogenin (Cornelison et al., 2000; Megeney et al., 1996; Rudnicki et al., 1993; Sabourin et al., 1999). MyoD represses cell cycle activity by inducing the expression of cyclin dependent kinase (CDK) inhibitors p21 (Halevy et al., 1995). To enable myogenic progression, MyoD further induces the expression of myogenin, a basic helix-loop-helix transcription factor, whose activity precedes the activation of downstream myogenic factors (Hollenberg et al., 1993). Myogenin triggers the expression of multiple genes involved in muscle contractile functions, such as α-actinin, troponin, myosin heavy chain and voltage-gated calcium channel (Davie et al., 2007; Dumont et al., 2015).

Myoblasts can then either fuse with each other to form multinucleated myofibers, or fuse with existing myofibers, which expand the pool of myonuclei within the myofiber, and allow the fiber to increase in size (Sampath et al., 2018). The cell-cell fusion mechanism was first investigated in a fly model. A ring-like structure called fusion-restricted myogenic-adhesive structure (FuRMAS) was formed by the interaction between Dumbfoudned (Duf) and Sticks and stones (Sns) proteins upon myoblast contact. Fusion proteins then accumulate at the cell-cell junction from intracellular perfusing vesicles and this leads to formation of fusion pores, which subsequently enlarge and dissolve to give rise to multi-nucleated cells (Dumont et al., 2015; Rochlin et al., 2010). The candidates regulating the myogenic fusion process remain poorly understood until fairly recently. Millay et al. reported Myomaker, a key membrane protein regulating myogenic fusion (Millay et al., 2013). Myomaker is a muscle specific trans-membrane

protein that is only expressed transiently during the fusion process and is rapidly downregulated afterwards (Millay et al., 2013). Myomaker is necessary for myogenic fusion, as a knock-out mice model resulted in early lethality because of skeletal muscle deficiency. Importantly, mono-nucleated myosin-positive cells were observed during the embryonic development process in muscle longitudinal section, which implies that muscle differentiation was not affected in Myomaker-null mice. The authors also demonstrated that Myomaker sufficiently induces cell fusion as over-expression in non-fusogenic C3H 10T1/2 fibroblasts resulted in fusion with myoblasts (Millay et al., 2013). However, Myomaker^{+} fibroblasts are only fusion-competent, meaning that they can fuse with existing fusogenic muscle cells, but cannot fuse with themselves. This implied that there should exist additional factors regulating the fusion process. Three independent groups subsequently reported another pivotal moderator named Myomixer/Minion/Myomerger (Bi et al., 2017; Quinn et al., 2017; Zhang et al., 2017). Similar to Myomaker, Myomixer/Minion/Myomerger-deficient mice exhibited perinatal death and marked increase in mono-nucleated myosin^{+} cells, again indicating that this protein does not affect differentiation and only impact myogenic fusion (Bi et al., 2017; Quinn et al., 2017; Zhang et al., 2017). Gain-of-function experiments were performed in non-fusogenic fibroblasts, proving that Myomixer/Minion/Myomerger overexpression could induce fusion with Myomaker^{+} cells (Bi et al., 2017; Quinn et al., 2017; Zhang et al., 2017). Therefore, both proteins are necessary and sufficient for myogenic fusion process. Myomaker is required for mixing of lipids on the plasma membrane, a process known as hemifusion, and Myomerger drives the fusion toward completion by inducing fusion pore formation and expansion between hemifusion intermediate (Figure 1.6) (Leikina et al., 2018). In this process, elastic stresses generated by Myomerger-induced membrane

positive curvature transmit to the hemifusion diaphragm, expediting the formation of the fusion pores (Golani et al., 2021).

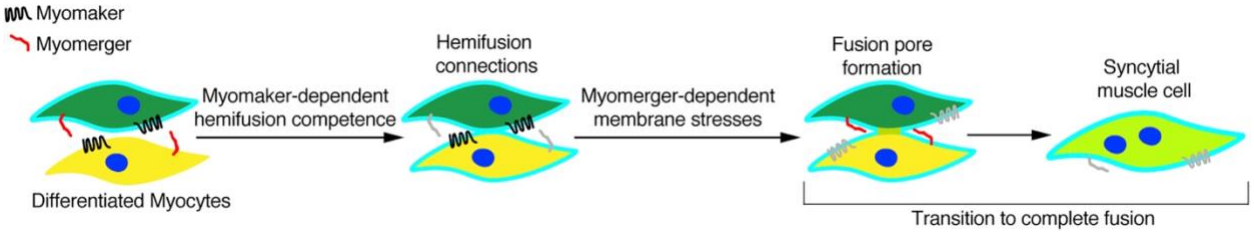

Figure 1.6 Myomaker and Myomerger work synergistically for myoblast fusion

Adapted from *Myomaker and Myomerger Work Independently to Control Distinct Steps of Membrane Remodeling during Myoblast Fusion* (Leikina et al., 2018).

Finally, *de novo* myofibers undergo maturation process by further fusing with each other. The PI3K/Akt/mTOR pathway plays a pivotal role in myotube maturation. IGF-1 binding to its canonical receptor IGFR leads to activation of PI3K, which activates the Akt and donwstream mTOR pathway (Rommel et al. 2001). Activated mTOR kinase activity is required for the late phase fusion to give rise to mature myotube (Park & Chen, 2005), whereas the kinase-independent activity mediated by IGF-2 is involved in the initiation of myogenic differentiation and early stage fusion for the formation of nascent myotubes (Erbay et al., 2003). Akt activation also promoted skeletal muscle hypertrophy through phosphorylation of downstream effectors $p70^{S6K}$, which stimulates protein synthesis by activating ribosomal protein S6. Meanwhile, mTOR attenuates the activity of translation repressor 4E-BP1 (Bodine et al., 2001; Dumont et al., 2015). In addition, Akt signaling prevents protein catabolism via the inhibition of FOXO, which induces the expression of E3-ubiquitin ligases *MuRF1* and *MAFbx* (Stitt et al., 2004).

1.2.2 Immune Cell

Immune cells are relatively rare in unpertubed muscle, but once an acute injury arises, they rapidly migrate towards the site of injury and perform a wide range of actions for the resolution of injury and regeneration process. The first responders are neutrophils that infiltrate the damaged region within 2 hours and reach peak numbers in less than 24 hours post damage (Tidball, 2017). Neutrophils are critical for the clearance of the damaged tissues by releasing reactive oxygen species (Wosczyna & Rando, 2018). They also secrete pro-inflammatory cytokines as such IFNγ and TNFα for the recruitment, activation and modulation of other immune cells, most notably, macrophages (Tidball, 2017). In the meantime, muscle-resident macrophages phagocytize the injury-induced apoptotic cells (Babaeijandaghi, Cheng, et al., 2022).

Macrophages are perhaps the most important player in the regeneration process. Their ubiquitous involvement in multiple aspects of the process include debris clearance, modulation of MuSCs proliferation and differentiation, regulation of FAP survival, etc (Figure 1.8) (Juban & Chazaud, 2017). Circulating macrophages arriving in the degenerative milieu secrete a myriad of cytokines, including IFNγ, IGF-1, IL-6, IL-1β and TNFα, which stimulate MuSC expansion and block their commitment further down the myogenic hierarchy (e.g. differentiation and fusion) (Wosczyna & Rando, 2018). These pro-inflammatory macrophages are crucial for scavenging the debris resulting from muscle damage, also creating space for repopulating muscle cells to grow in. In addition to the inflammatory response, macrophage-secreted TNFα directs apoptosis of tissue-resident FAPs to prevent them from aberrantly differentiating into ECM-laying fibroblasts that could result in permanent fibrosis within the muscle (Lemos et al., 2015), therefore compromising muscle strength. At later stage of injury, macrophages progressively transition from a pro-inflammatory to an anti-inflammatory phenotype. This switch in macrophage polarization is

thought to be dependent on IL-10 (Deng et al., 2012; Villalta et al., 2011), although a recent study suggests that the joint activity of IFNγ and TNFα is required (Babaeijandaghi, Paiero, et al., 2022). Anti-inflammatory macrophages produce high level of IGF-1 to stimulate MuSC proliferation (Tonkin et al., 2015). They also secrete low level of TGFβ and TNFα to enhance myoblast differentiation and fusion with nascent/existing myotubes (Saclier et al., 2013), This implies the secretory program of macrophages is under tight control so that a high concentration of TNFα can inflict FAP apoptosis (Lemos et al., 2015), while a low level promotes myogenic differentiation.

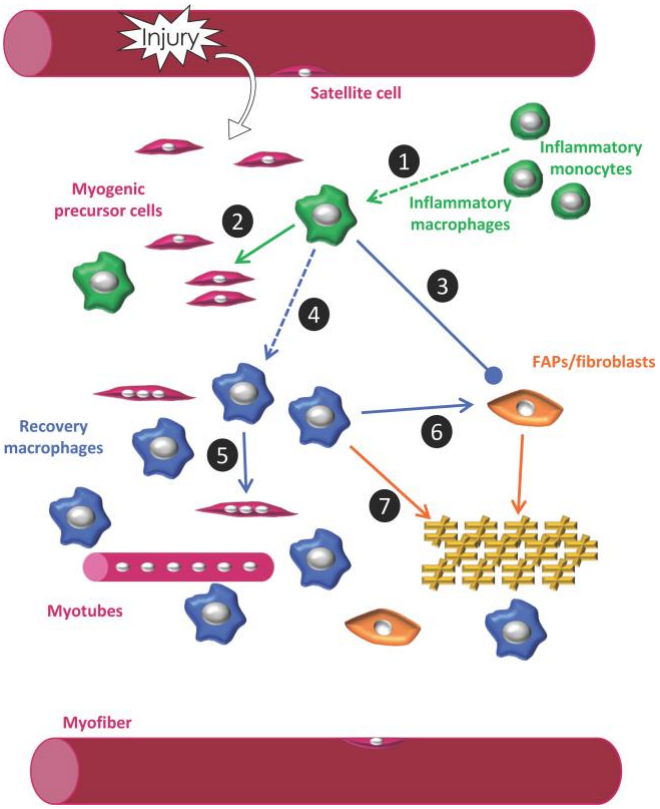

Figure 1.7 Involvement of macrophages in different stages in muscle degeneration/regeneration process

Adapted from *Metabolic regulation of macrophages during tissue repair: insights from skeletal muscle regeneration* (Juban & Chazaud, 2017).

Recently, regulatory T cells (Tregs) and eosinophils were found to play active roles in regenerating muscle. When Tregs were selectively ablated, muscle displayed an impaired regeneration phenotype as interstitial fibrosis and lower number of regenerating myofibers, two hallmarks of regenerative success, were observed (Burzyn et al., 2013). Importantly, accumulation

of Tregs at injured region is dependent on FAP-secreted IL-33 (Kuswanto et al., 2016), highlighting the sophisticated crosstalk among different cell types as a critical requirement for efficient and complete regeneration. Similarly, infiltrating eosinophils secrete IL-4 and directly act on FAPs through IL4 receptor on FAPs to stimulate their proliferation (Heredia et al., 2013). The importance of FAP expansion at early stage of regeneration will be discussed in subsequent section. In addition, IL-4 was shown to repress adipogenic differentiation of FAPs (Heredia et al., 2013), hence FAP-derived intramuscular adipose tissue is relatively rare in healthy regenerated muscle. This once again accentuates the delicate interactions between different cell types and signaling pathways in the regeneration process.

1.3 Fibroadipogenic Progenitor

1.3.1 FAPs in regeneration and homeostasis

Fibroadipogenic progenitors (FAPs) were first reported by two individual research groups in 2010. In the initial reports, murine muscle FAPs were characterized by their interstitial location, expression of platelet-derived growth factor receptor α (PDGFRα) and stem cell antigen-1 (Sca-1) (Joe et al., 2010; Uezumi et al., 2010). FAPs were shown to have bi-lineage differentiation potential by spontaneously differentiating into fibroblasts and adipocytes *in vitro*. In the years that followed, much research effort has been invested in the field, rapidly expanding our knowledge on FAPs in skeletal muscle. We now know that FAPs also possess osteogenic and chondrogenic potential under specific induction conditions, further reinforcing their identity as multipotent progenitors (Eisner et al., 2020; Tseng et al., 2022; Wosczyna et al., 2012). Due to their intrinsic differentiation potentials, FAPs have been linked to numerous chronic diseases with signs of fibro-

fatty degeneration. Multiple human FAP studies have also been reported, where their mediatory role in the pathogenesis of muscle diseases has been confirmed.

In response to injury, FAPs rapidly proliferate and are believed to support regeneration by facilitating myogenic differentiation of MuSCs via the release of pro-regeneration signals and trophic factors such as IL-6 (Joe et al., 2010; Serrano et al., 2008) and IL-33 (Kuswanto et al., 2016). During the process, activated FAPs acquire odd skipped-related 1 (Osr1) expression that resembles the embryonic development program (E11.5-13.5) (Stumm et al., 2018; Vallecillo-García et al., 2017). $Osr1^{+}$ FAPs direct macrophage polarization for the resolution of injury and promote myogenic via TGFβ signaling (Kotsaris et al., 2023). FAPs also release cytokines, such as CXCLl5, CCL2, and CCL7 to recruit immune cells to the injured region, facilitating the rapid clearance of necrotic fibers and cellular debris (Scott et al., 2019). In addition, FAPs secrete various ECM components such as collagen and fibronectin (Scott et al., 2019), forming a transient scaffold that stabilizes and provides mechanical supports for repopulating myofibers, likely a similar mechanism to that of "ghost fibers" (Webster et al., 2016). This temporary process, referred to as "regenerative fibrosis", is eventually resolved through downregulation of the provisional matrix genes, apoptosis of FAPs, and ECM-specific proteases such as matrix metalloproteinase 11 (MMP11) secreted by FAPs (Scott et al., 2019). To ensure optimal regeneration outcome, the number of FAPs are tightly controlled. A recent study identified hyper-methylated in cancer 1 (HIC1) as a marker of quiescent FAPs in muscle, and deletion of HIC1 resulted in injury-free proliferation of FAPs and a partially activated phenotype, such as a marked upregulation of *Ccl2* and *Ccl7*, resembling that following injury (Scott et al., 2019). After the initial expansion phase induced by acute injury (72–96 hours post injury), FAPs undergo rapid, macrophage-dependent, TNFα-mediated apoptosis (Lemos et al., 2015). Pharmacological blockage of FAP expansion by

a tyrosine kinase inhibitor Nilotinib; suppression of FAP apoptosis in Ccr2-knockout mouse model lacking infiltrating macrophages; or inhibiting TNFα pathway with TNFα-neutralizing antibodies, all led to impaired regeneration and persistence of fibrotic scars in muscle (Fiore et al., 2016; Lemos et al., 2015). Consistently, depletion of FAPs in PDGFRα^{CreERT2};diphtheria toxin fragment A (DTA) mouse model significantly reduced immune cell recruitment and delayed regeneration progress, further elucidating the requirement of FAPs in efficient muscle regeneration (Wosczyna et al., 2019). Ablation of Tcf4^{+} fibroblasts in muscle, which partially overlap with FAPs, similarly led to defective muscle regeneration (Murphy et al., 2011). Importantly, FAPs not only play a role in modulating the regenerative progress, but also actively maintain skeletal muscle mass in homeostasis. This was first demonstrated by Roberts *et al.* in 2013, where they observed muscle atrophy in the absence of external perturbations in ablated fibroblast activation protein α (FAP)-expressing stromal cells (Roberts et al., 2013). These FAP^{+} stromal cells uniformly express Sca-1, and to a large extent, PDGFRα, indicating they are indeed FAP cells. However, potentially due to the confusing nomenclature, there is limited literature characterizing the expression and function of the FAP protein in FAP cells. In 2019, Wosczyna *et al.* provided compelling experimental evidence for the necessity of FAPs in homeostatic maintenance of skeletal muscle. They depleted muscle FAPs using the PDGFRα^{CreER};DTA system, which specifically ablates cells expressing PDGFRα. Muscle atrophy was observed in ablated mouse as reflected by reduction of cross-sectional myofiber area, muscle mass and strength (Wosczyna et al., 2019). This was confirmed by Uezumi *et al.*, who elucidated that Bmp3b from FAPs as the potential candidate for muscle maintenance (Uezumi et al., 2021). We also reported the aberrant activation of FAPs by HIC1 deletion or β-catenin could lead to defective muscle regeneration and muscle atrophy, respectively (Scott et al., 2019; Kajabadi et al., 2023). Collectively, FAPs are non-myogenic mesenchymal

progenitors residing in the interstitial space of skeletal muscle, and are crucial to efficient muscle regeneration and homeostatic maintenance.

1.3.2 FAPs in diseases

Given the intrinsic fibrogenic and adipogenic capabilities of FAPs, it is not surprising that they are involved in the manifestations of numerous diseases with symptoms of fibrofatty infiltration. Similarly, FAP dynamics are crucial in ensuring complete and efficient muscle regeneration, hence altered FAP behaviors are often seen in multiple diseases with impaired regeneration. In fact, these two aspects are tightly coupled that FAPs less vulnerable to apoptosis or aberrantly activated are the direct source of the ectopic scars and fats. Understanding the contributions of FAPs to different diseases would therefore be valuable for development of novel therapies.

1.3.2.1 Muscular dystrophies

Duchenne muscular dystrophy (DMD) is the most common and severe type of muscular dystrophy in humans, affecting one in every 5000 male births. It is an X-linked recessive disease whereby the nonsense mutation of *DMD* gene destabilizes skeletal muscles and leads to chronic injury-regeneration cycles, eventually exhausting the resident MuSC pool (Dowling et al., 2021). FAPs actively participate in the degenerative process through several mechanisms. First, $TCF4^{+}$ muscle interstitial cells, which significantly overlap with FAPs, were shown to be enriched in fibrotic muscles in mdx mice, a commonly used experimental model for DMD (Contreras et al., 2016). Direct contribution of FAPs to intramuscular fibrotic and adipose tissue in DMD has also been demonstrated (Uezumi et al., 2011, 2014). Remarkably, adipogenic differentiation of FAPs

in mdx mice is inhibited by the hedgehog signaling pathway, whereas tissue inhibitor of metalloproteinase 3 (TIMP3) secreted from FAP represses MMP14-induced adipogenesis, suggesting a potential therapy against DMD (Kopinke et al., 2017). Another possible remedy of fatty degeneration is the administration of nitric oxide (NO) donor drug. NO blunts adipogenic differentiation by inhibiting the master adipogenic regulatory factor PPARγ via secretion of miR-27b (Cordani et al., 2014). DMD FAPs were also shown to impair myogenic capacity of MuSCs (Sohn et al., 2015). In terms of cellular dynamics, FAPs in mdx mice are refractory to the wave of macrophage-dependent apoptosis after the rapid proliferation phase (Juban et al., 2018; Lemos et al., 2015). Persistent FAPs subsequently differentiate along fibrogenic and adipogenic lineages and result in fibrofatty infiltration. FAP composition is also affected by DMD. Several FAP subpopulations were reported to have important roles in regulating the local environment. For example, a marked loss of adipogenic-regulating $CD142^{+}$ FAPs was observed in DMD, which act by blocking adipogenesis through the secretion of GDF10 in healthy individuals, resulting in excessive adipocyte deposition in DMD muscles (Camps et al., 2020). Another FAP subset that is being affected in DMD is $VCAM1^{+}$ FAPs. They are only present in the muscle of healthy individuals after acute injury and display a pro-fibrotic profile, which is a transient state critical for efficient regeneration (Fiore et al., 2016). These FAPs are eventually removed from injured muscle in a macrophage-dependent mechanism (Malecova et al., 2018). $VCAM1^{+}$ FAPs were found to be enriched in the diaphragm of mdx mice, which strongly suggests that the elevated level of intramuscular fibrosis is a result of the enrichment of this FAP subset. DMD also alters FAPs on an epigenomic level, evident by the fact that histone deacetylase (HDAC) inhibitor could rescue muscle regeneration defect in mdx mice in a FAP-secreted follistatin-dependent manner (Mozzetta et al., 2013). Indeed, ChIP-seq of mdx FAPs revealed a global alteration in histone acetylation

pattern in mdx mouse and led to elevated activity of fibrosis-associated pathways such as the TGFβ-SMAD axis (Consalvi et al., 2022). In a more severe DMD mouse model (D2-mdx), calcification is occasionally observed in muscles, which can be attributed to the elevated TGFβ signaling activity that drives FAPs into osteogenic lineage (Mázala et al., 2020). In addition, mitochondrial metabolism in mdx mouse-isolated FAPs were altered, leading to enhanced proliferation and adipogenic differentiation *in vitro*. This suggested a disease-causing mechanism of FAPs contributing to DMD pathogenesis (Reggio et al., 2020).

FAPs are also responsible for muscle functional deterioration of limb girdle dystrophy 2B muscular dystrophy (LGMD2B), a disease caused by dysferlin deficiency which led to poor membrane repair after sarcolemma injuries (Bansal et al., 2003; Bashir et al., 1998). LGMD2B patients presented pelvic and shoulder girdle muscle atrophy and could eventually result in loss of ambulation (Fernández-Eulate et al., 2021). Adipose tissues were found to accumulate in dysferlin-deficient muscles (Grounds et al., 2014), highlighting a possible involvement of FAPs in the degeneration process. Indeed, adipogenic differentiation of FAPs is unrepressed due to the accumulation of Annexin 2A in the ECM of surrounding myofibers (Hogarth et al., 2019).

Similarly, FAPs were postulated to be associated with facioscapulohumeral muscular dystrophy (FSHD). FSHD is an autosomal dominant disorder caused by the loss of D4Z4 macrosatellite repeats which leads to ectopic expression of DUX4 gene within the locus (Tawil et al., 2014). DUX4 expression in myogenic cells resulted in disruption of myogenic differentiation, including downregulation of key myogenic genes MYOD and MYF5 (Bosnakovski et al., 2018). FSHD is characterized by asymmetric muscle weakness in face and shoulder muscles, which progressively propagates to the trunk and lower extremities (Tawil et al., 2014). A recent study showed that FAPs in a FSHD mouse model acquired a distinctive transcriptional signature, which

is comparable to that of FSHD human patients' muscle biopsies (Bosnakovski et al., 2020), suggesting a possible association between FAPs and FSHD. More recently, a report demonstrated a positive correlation between of accumulation of FAPs and the clinical severity of FSHD (Di Pietro et al., 2022). The direct contribution of FAPs to FSHD pathogenesis and pathoprogression remain to be proven.

1.3.2.2 Obesity and diabetes

It is estimated that 425 million people are suffering from diabetes mellitus (DM) worldwide (Forouhi & Wareham, 2019), and that for overweight/obesity is at a staggering level of 2.5 billion, representing one-third of the global population (Chooi et al., 2019). Importantly, muscle fibrosis and fatty infiltration are common hallmarks in diabetes and obesity, in both injury and injury-free settings, likely mediated by muscle-resident FAPs. For example, drastic upregulation of ECM-related genes and pronounced skeletal muscle fibrosis are observed in overfed, obese and diabetic individuals (Berria et al., 2006; Tam et al., 2014). Although the identity of the ECM-depositing cells was not tackled in the studies, it is plausible to assume FAPs are the principal contributor, given their known ability of fibrogenic differentiation within skeletal muscle (Joe et al., 2010; Uezumi et al., 2010, 2011). Similarly, FAPs were believed to be the precursors of intramuscular adipose tissues (IMAT) in obese patients. Indeed, $CD56^{-}/CD15^{+}$ adipogenic progenitors from obese human donors, whose cell-surface immunophenotype is equivalent to $PDGFR\alpha^{+}$ FAPs (Arrighi et al., 2015), gave rise to mature white adipocytes (Laurens et al., 2016). In addition, FAPs robustly gave rise to adipocytes following cardiotoxin injury in both diet-induced and genetic-induced obesity models, once again suggested a detrimental role of FAPs in obesity (Takada et al., 2022). Recently, it is shown that FAP-derived fibroblasts and adipocytes underlie diaphragmatic

collagen deposition and fatty degeneration in high fat diet-fed mice, leading to reduced respiratory dysfunction induced by THBS1 (Buras et al., 2019). FAP-secreted NID-1 also primed them for fibrogenic differentiation, and concomitantly impaired MuSCs proliferation in obese mouse model (Pérez-Díaz et al., 2022).

FAPs also have indispensable roles in exacerbating the symptoms of DM. As in obese individuals, IMATs are also commonly found in DM patients (Goodpaster & Wolf, 2004; van Loon & Goodpaster, 2006). Similarly, fibrosis is another common finding in DM (Farup et al., 2021; Rasmussen et al., 2018). Fibro-fatty degeneration compromises muscle strength in DM (Moore et al., 2016), hence determining the cellular source driving the pathological remodeling of muscle is necessary to combat the disease. Fatty infiltration after acute muscle injury resulted from FAP adipogenic differentiation in diabetic mouse was documented (Mogi et al., 2016), implicating that FAPs could also be the source of IMAT in uninjured diabetic patients. FAPs were also determined to contribute to intramuscular fibrosis (Farup et al., 2021). Notably, Farup and colleagues identified a $CD90^+$ FAP subpopulation that was poised for fibrogenic differentiation enriched in type 2 DM patients, which established a possible causal role of $CD90^+$ FAPs in fibrotic degeneration (Farup et al., 2021).

1.3.2.3 Heterotopic ossification and Fibrodysplasia Ossificans Progressiva

Heterotopic ossification (HO) is a disease condition characterized by ectopic bone formation in skeletal muscles and soft tissues (Eisner et al., 2020; Wosczyna et al., 2012). It can be caused by external insults such as orthopedic injuries (Nauth et al., 2012) and surgeries (Amar et al., 2015), spinal cord injury (Tseng et al., 2022), or inherited as a genetic disease (Shore et al., 2006). Early studies showed that $Tie2^+$ cells are the source of ectopic bone formation in BMP-

induced and genetic HO model (Lounev et al., 2009; Medici et al., 2010). However, as Tie2 is expressed by different cell types (Wosczyna et al., 2012), the authors did not uncover the exact identity of osteogenic progenitors. Notably, Tie2 labels a FAP subpopulation in steady state (Malecova et al., 2018), highlighting an unappreciated role of this particular FAP subset. A subsequent study by Wosczyna and colleagues revealed that in different $Tie2^{+}$ cell subfractions, only non-endothelial and non-hematopoietic cells that express PDGFRα and Sca1, the two definitive markers of FAPs, contribute to heterotopic bone, suggesting a causal role of FAPs in HO pathogenesis (Wosczyna et al., 2012). We consolidated this notion by lineage tracing of a more reliable and specific Cre driver mouse model of muscle FAPs ($PDGFR\alpha^{CreERT2}$;tdTomato), demonstrating that muscle resident $PDGFR\alpha^{+}$ cells (i.e. FAPs) are indeed the source of osteogenic cells in heterotopic bone lesions (Eisner et al., 2020). Mechanistically, osteogenic differentiation of FAPs could be triggered by an altered local immune environment that leads to FAP accumulation and aberrant activation of osteogenic pathways. Muscle injury alone in mice with defective capability to clear FAPs (infiltrating monocyte/macrophage-null $CCR2^{KO}$ mouse) can occasionally cause HO (Eisner et al., 2020). Similarly, neurological HO induced by spinal cord injury (SCI) resulted in reduced FAP apoptosis and enhanced proliferation (Tseng et al., 2022). On the other hand, SCI exacerbated inflammatory response in injured muscle along the JAK/STAT axis through the secretion of OSM (Alexander et al., 2019; Torossian et al., 2017), and ablating phagocytic macrophages by clodronate injection conferred protection against neurological HO (Genêt et al., 2015). In summary, these studies reveal key interactions between FAPs and inflammatory cells in HO pathogenesis.

A prevalent type of inherited HO is Fibrodysplasia Ossificans Progressiva (FOP), an autosomal dominant disease caused by bone morphogenetic protein (BMP) receptor ACVR1

R206H mutation (Hatsell et al., 2015; Shore et al., 2006). Similarly, it has been demonstrated that FAPs govern the pathogenesis of FOP in an activin-A-dependent manner, as systemic inhibition of activin-A reverses the HO phenotype (Lees-Shepard et al., 2018). Fate mapping of *Mx1*-Cre mouse, which labelled a fraction of muscle interstitial cells residing outside basal lamina (an anatomical location where FAPs are found) and are capable of adipogenic differentiation, revealed that the $Mx1^{+}$ interstitial cells committed a chondrogenic fate and formed intramuscular ossified lesions (Dey et al., 2016). In the genetic model of FOP ($Acvr1^{R206H}$-knockin mouse), FAPs were resistant to apoptosis after injury and they inhibited MuSCs differentiation *in vitro* (Stanley et al., 2022). It is therefore reasonable to hypothesize that the prolonged presence of FAPs in an injury setting could force them to adopt an osteogenic fate, leading to FOP onset.

1.3.3 FAP heterogeneity

Prior to introduction of single cell technologies, limited studies had attempted to analyze FAP subsets with significant physiological implications. With the recent advancements in single cell omics in the past few years, we are now able to examine individual cells at transcriptomic, epigenomic and proteomic levels by using various single cell technologies, such as single cell and single nuclei RNA sequencing, single cell ATAC sequencing, and single cell mass cytometry. As a consequence, a plethora of studies in recent years utilized these techniques to decipher the roles and interactions of myogenic and non-myogenic cells in maintenance and regeneration of skeletal muscle. Two critical insights are that FAPs, previously defined by the co-expression of Sca-1 and PDGFRα, are a heterogeneous population. This means thatdifferent subpopulations emerge at distinct stages of regeneration and disease. Some FAP subsets are predisposed to differentiate into a specific lineage, suggesting that they may be the precursors of fibrofatty infiltration in disease

context. In this section, we summarize the FAP subpopulations existing in steady and activated states. It is worth noting that, despite the differences in naming conventions by different authors, such as fibroblasts, interstitial stromal cells (ISCs), mesenchymal stem cells, and mesenchymal progenitors (MPs), these cells are *bona fide* FAPs as reflected by their expression of the defining markers Sca-1 and PDGFRα in the lineage (CD31, CD45 and α7-integrin) negative fraction.

1.3.3.1 Steady State

The first study that demonstrated the heterogeneity and dynamics of FAPs in different stages using single cell technology was by Malecova and colleagues in 2018. Through flow cytometry and single cell RT-qPCR, they showed that in their uninjured state, FAPs can be segmented into $Tie2^{high}$ and $Tie2^{low}$ populations. $Tie2^{high}$ FAPs, which represent only 10% of the total population, are enriched in *Igfbp5, Wnt11* and *Bmp6,* and displayed high activity in forming focal adhesion. In contrast, the transcriptional signature of $Tie2^{low}$ FAPs is associated with chemotactic ability. Similarly, analysis of the transcriptome of quiescent $Hic1^{+}$ FAPs revealed that they can be divided into 2 subsets (FAP1 and FAP2) (Scott et al., 2019). FAP1 is characterized with the expression of *Cxcl14* and numerous ECM-associated genes, such as *Col15a1* and *Col4a1*, whereas FAP2 expresses high level of *Dpp4*, *Pi16*, *Igfbp5* and *Wnt2*. Intriguingly, FAP2 are also high in *Tek* expression, gene encoding for Tie2 protein. This suggested that FAP2 and $Tie2^{high}$ FAPs could belong to the same family of FAP subset. A subsequent report by Oprescu *et al.* also confirmed the existence of $Cxcl14^{+}$ and $Dpp4^{+}$ FAPs in uninjured and 21 days post injury (resembling steady state) muscle that displayed very similar transcriptional signatures to FAP1 and FAP2, respectively, further suggesting the existence of the two FAP subsets in skeletal muscle in steady state (Oprescu et al., 2020). Notably, $Dpp4^{+}$ FAPs are present or overlap significantly

with a specific FAP subset reported in other single cell studies, including Tabula Muris Senis (Almanzar et al., 2020), *Cd55*$^{+}$ FAPs (Fitzgerald et al., 2023), SCA-1^{high} FAPs (Giuliani et al., 2021), *Gap43*$^{+}$ FAPs (Leinroth et al., 2022), interstitial progenitor cells (Yang et al., 2022), and ISC1 (Camps et al., 2020). The study by Camps and colleagues also unveiled a population of CD142^{+} FAPs (ISC2), which has the ability to regulate adipogenic differentiation by the release of GDF10/Bmp3b (Camps et al., 2020), deemed to be crucial in maintaining muscle integrity (Uezumi et al., 2021). Since CD142^{+} stromal cells have been found in adipose tissues and their ability to regulate adipogenesis has been well-documented in previous studies (H. Dong et al., 2022; Merrick et al., 2019; Schwalie et al., 2018; Yang et al., 2022), it is therefore plausible to assume that CD142^{+} FAPs in muscle are also responsible for the same function. Additionally, the number of CD142^{+} FAPs in limb grindle muscular dystrophic mouse and Duchenne muscular dystrophic human patients has been found to be lower compared to healthy controls (Uezumi et al., 2021). This provides evidence for a possible connection between this specific FAP subset and the pathophysiology of muscular dystrophies.

Similar degree of FAP heterogeneity is also seen in human. Single RNA sequencing of human muscle mononucleated cells revealed two FAP subpopulations, namely *FBN1/PRG4*$^{+}$ FAPs and *LUM*$^{+}$ FAPs (Rubenstein et al., 2020). Strikingly, these two human FAP subsets are also found in mice and are characterized by genes that largely overlap with the top differentially expressed genes in the corresponding mouse subpopulations, including *Cd55* and *Cxcl14*, respectively. Further analysis fortified this hypothesis as their transcriptomic signatures are highly correlated to that of *Dpp4*$^{+}$ *and Cxcl14*$^{+}$ FAP subtypes in mouse (Fitzgerald et al., 2023). This finding is in conformity to another independent study (De Micheli, Spector, et al., 2020). Although the authors adopted different terminology (fibroblast), cells belonging to the fibroblast 2 subset integrate into

the same cluster with *Cd55*$^{+}$ FAPs (Fitzgerald et al., 2023), and express the defining FAP marker PDGFRα. The biological significance of this FAP subset that exists in both mouse and human remains largely elusive.

1.3.3.2 Activated State

In this section activated FAPs are referred to as those that have undergone changes triggered by any type of disturbance, such as acute or chronic injuries. By lineage tracing, a population of ADAM12^{+} FAPs was identified as the fraction with greater tendency to differentiate into myofibroblast, but with limited adipogenic capacity (Dulauroy et al., 2012). Fate mapping further confirmed their role as the primary source of collagen-depositing cells in response to muscle injury. More recently, a pro-adipogenic FAP subset was discovered. This group of FAPs is marked by *Mme* (CD10), and was shown to be the predominant source of infiltrating adipocytes in skeletal muscle (Fitzgerald et al., 2023). Interestingly, *Mme*$^{+}$ FAPs were also found to be more prone to apoptosis following the expansion phase (Fitzgerald et al. 2023). The differential vulnerability to apoptosis and the differing propensity for differentiation into a mature lineage of the two FAP subsets, collectively suggest that there may exist a FAP subpopulation that is preferentially preserved during the wave of apoptosis and more refractory to injury-induced pro-differentiation signals. This implies that in chronic injuries such as DMD, other FAP subpopulations would have been diminished or terminally differentiated, while this presumed subset prevails, alluding to a possible disease-causing mechanism.

Aside from those that are primed for differentiation, some FAPs also play crucial roles in regulating of the local environment after acute damage. A subset of FAPs upregulated immunomodulatory genes, such as *Ccl7* and *Cxcl5*, was observed as soon as 12 hours post injury, before fading out within 3 days (De Micheli, Laurilliard, et al., 2020; Oprescu et al., 2020; Scott

et al., 2019). From 3.5 to 5 days post injury (dpi), *Wisp1*$^+$ FAPs emerged and exhibited ECM remodeling capacity, by the expression of associated genes such as *Postn*, *Adam12* and *Acta2*. At 4 dpi, a small set of *p16*$^+$/*p21*$^+$/*Acta2*$^+$ FAPs appeared and were believed to contribute to muscle regeneration by senescence-associated secretory phenotype (Saito et al., 2020; Takada et al., 2022). *Dlk1*$^+$ FAPs arose at 10 dpi with upregulated imprinting genes such as *H19* and *Igf2* (Oprescu et al., 2020). At 21 dpi, *Osr1*$^+$ FAPs showed up, and pseudotemporal analysis suggested that they bifurcate into *Dpp4*$^+$ and *Cxcl14*$^+$ FAPs, which are the two FAP subsets in unperturbed muscle (Oprescu et al., 2020). Since muscle is capable of regenerating after repeated round of damages once the previous injury has resolved, we reasoned that the trajectory forms a closed loop (Contreras et al., 2021), allowing *Dpp4*$^+$ and *Cxcl14*$^+$ FAPs, positioned at the ends of the trajectory, to be re-activated and aid in regeneration in future muscle insults.

FAP diversity is also apparent in various disease conditions. For instance, a study by Farup *et al.* found that a subpopulation of CD90-expressing FAPs is enriched in human type 2 diabetic patients with muscle fibrosis (Farup et al., 2021). These FAPs were poised for ECM deposition as reflected by their pro-fibrotic transcriptional landscape. Similarly, in mdx mice, an animal model for the DMD, a subpopulation of VCAM1$^+$ FAPs was found to be present (Malecova et al., 2018). VCAM1 expression in FAPs is nearly absent in uninjured muscle, but is strongly upregulated in response to injury, suggesting that VCAM1 may serve as an activation marker. Crucially, VCAM1$^+$ FAPs from steady state mdx mouse muscle possess similar transcriptional profile as VCAM1$^+$ FAPs from wildtype mice 3 days post damage, reflecting that FAPs in mdx mice adopted a chronic activation state that could contribute to DMD pathogenesis. This finding is corroborated by the fact that VCAM1$^+$ FAPs in mdx mice express high level of pro-fibrotic genes such as *Col1a1* and *Adam12*. Moreover, ectopic fat accumulation in the injured muscle of high fat diet-

induced obese mice was found to originate from 2 small subsets of FAPs that respond to galectin-3 secreted by macrophages, leading to the activation of PPARγ signaling and adipogenic differentiation (Takada et al., 2022).

1.4 Dipeptidyl peptidase 4

Dipeptidyl peptidase 4 (EC:3.4.14.5, also known as CD26) is a 110kDa protease that can cleave a peptide at the N-terminal penultimate proline/alanine residue (Boonacker & Van Noorden, 2003). It is expressed by multiple tissues and cell types in mammals, such as kidney, lung, liver in human (Biftu & SinhaRoy, 2017; Wu et al., 2016), and small intestine, T cells, and spleen in mouse (Wu et al., 2016). Because of its proteolytic property, DPP4 could regulate the biochemical activity and availability of a wide range of substrates (Boonacker & Van Noorden, 2003), with incretin hormones glucagon-like peptide-1 (GLP-1) being the most famous target (Gilbert & Pratley, 2020). GLP-1 stimulates insulin secretion and suppresses glucagon production as an important means to regulate blood glucose level (Müller et al., 2019), hence DPP4-mediated GLP-1 cleavage would render it completely ineffective. As such, DPP4 inhibitors like sitagliptin are commonly prescribed for type 2 diabetes to control hyperglycemic condition (Ahrén, 2019). Inhibition of DPP4 activity also finds potential application in the field of stem cell transplantation for its role in coordinating the migration and engraftment of transplanted cells via the CXC chemokine receptor type 4-stromal cell derived factor 1α (CXCR4-SDF1α) signaling axis, as SDF1α is a substrate of DPP4 and is essential in cell chemotaxis (Christopherson et al., 2002, 2004).

DPP4 also participates in processes independent of its proteolytic function. For example, hepatic DPP4 promotes inflammation in visceral adipose tissue by inducing phosphorylation of components of caveolin-1 pathway (IRAK1 and TAK1), which in turn induces the expression of

ERK1/2 and NK-κB and hence results in inflammation (Ghorpade et al., 2018). DPP4 can function as costimulatory component of T cell activity by direct interaction with caveolin-1. DPP4/caveolin-1 binding results in caveolin-1 phosphorylation, which leads to IRAK1 and Tollip dissociation; dissociated IRAK1 then translocates to the cytosol of monocytes, where it activates NK-κB to upregulate the expression of cell surface CD86, and this enhances T cell proliferation in response to antigen stimulation (Ohnuma et al., 2005). Another binding partner of DPP4 is adenosine deaminase (ADA). DPP4 binding to ADA activates catalytic activity of ADA, promoting T cell activation and proliferation by lowering adenosine concentration, a metabolite that functions to inhibit T cell activation (R. P. Dong et al., 1996). On the other hand, it has been shown that ADA on antigen presenting dendritic cells could bind directly with DPP4 on T cell surface, which triggers costimulation and promotes an augmented T cell activation, producing more proinflammatory cytokine such as IFNγ, TNFα and IL-6 (Pacheco et al., 2005).

1.5 Research Aim

While many of the *in-silico* studies reviewed above have demonstrated the existence of multiple FAP subsets, their physical presence *in vivo*, either by flow cytometry or histology, has yet to be confirmed. For example, there is no direct evidence that the two FAP subpopulations exist in steady state (*Dpp4*$^{+}$ FAPs and *Cxcl14*$^{+}$ FAPs). In addition, whether or not distinct FAP subsets possess different biological functions or contribute to different pathological conditions remain largely elusive, as there lacks direct proof of functionality or pathogenicity. The lineage relationship between different FAP subtypes has yet to be resolved. Therefore, we sought to provide a comprehensive characterization of FAP subsets, and FAP2 identified in our previous study (Scott et al., 2019), has attracted our particular attention. Firstly, as detailed above, such

subpopulations were universally reported in multiple single cell studies across different platforms (CYTOF, droplet-based and FACS-based scRNAseq), hence it is unlikely an *in-silico* artifact. Secondly, *Pi16* and *Dpp4* were discovered to label a primitive fibroblast subtype in a fibroblast atlas (Buechler et al., 2021), which also happened to be two commonly used marker genes for the specific FAP subset. The fact that it is present across tissues could be indicative of important biological functions. Last, DPP4 was used in adipose tissue to identify the interstitial progenitor population of tissue-resident MSCs (Merrick et al., 2019). Critically, the authors performed transplantation and lineage tracing, providingcompelling experimental evidence that $DPP4^+$ MSCs in fat give rise to mature adipocytes (Merrick et al., 2019; Stefkovich et al., 2021), which is the first-of-its-kind study that has validated its presence *in vivo*. Therefore, we reasoned that $DPP4^+$ FAPs are present in skeletal muscle and is an equivalent cell type to $DPP4^+$ MSCs in fat. We attempted to characterize this FAP subset to understand its role in the steady state muscle and upon injury.

Chapter 2: Methods

2.1 Animals

Animal maintenance and experimental procedures were conducted in accordance with the University of British Columbia Animal Care Committee guideline. Mice were housed under 12:12 light-dark cycle in a pathogen-free facility. Food and water were provided *ad libitum.* C57BL/6J (JAX stock #000664), B6.129S4-Pdgfratm11(EGFP)Sor/J (PDGFRa-EGFP, JAX stock #007669), B6.129P2-Gt(ROSA)26Sortm1(DTA)Lky/J (Rosa-DTA) and B6.Cg-Gt(ROSA)26Sortm9(CAG-tdTomato)Hze/J (Rosa-tdT, JAX stock #007909) mice were purchased from the Jackson Laboratory. DPP4^{CreERT2} mice are kindly provided by Patrick Seale (University of Pennsylvania). They were interbred with Rosa-DTA mice to yield DPP4^{CreERT2};DTA mice. PDGFRα^{CreERT2};tdTomato mice was produced by crossing PDGFRa^{CreERT2} mice, which is a gift from Brigid L.M. Hogan (Duke University), with Rosa-tdT mice. Cre recombination was induced by intraperitoneal (IP) injection of 0.3 mg tamoxifen (TMX, Sigma-Aldrich T5648) in 100μL of corn oil for 5 consecutive days (3 days for PDGFRα^{CreERT2};tdTomato mice). Mice administered with TMX were given at least 10 days of washout period before further experiments. Muscle injury was induced by intramuscular injection of 0.07μg Notexin snake venom (LATOXAN L8104) into the tibialis anterior (TA) muscle. All experimental mice were maintained on a C57BL/6 background and were 2-6 months in age. Littermates of both sexes were randomly assigned to different experimental groups wherever applicable. No blinding was performed and no data was excluded.

2.2 Tissue preparation

Mouse are euthanized by CO_2 followed by cervical dislocation. Hindlimb muscles were carefully dissected, washed in cold PBS, and finely minced with a pair of scissors. The slurry was then digested in 4mL of Collagenase D (1.5 U/mL, Roche 11088882001)/Dispase II (2.4 U/mL, Roche 04942078001) with 10mM $CaCl_2$ at 37°C with gently rocking for 1 hour, vortexing briefly every 15 minutes to ensure even digestion. The digestion was quenched with 40mL of cold FACS buffer (2% fetal bovine serum [FBS], 2mM EDTA in PBS). The solution was then sequentially filtered through 70μm (Falcon 352350) and 40μm (Falcon 352340) cell strainers, and centrifuged at 4°C at 500g for 10 minutes. Wash was discarded and cells were treated with ACK lysis buffer (Gibco A1049201) to remove contaminating red blood cells, incubated on ice for 5 minutes, and then quenched with 20mL cold FACS buffer. The lysate was centrifuged at 500g for 5 minutes and the pellet was resuspended in 3mL cold FACS buffer, and once again filtered through a 40μm cell strainer cap (Falcon 352235) and spun down.

2.3 Flow cytometry (FC) and fluorescent activated cell sorting (FACS)

Mononucleated cells were incubated with primary antibodies cocktail on ice for 30 minutes. Detailed information of antibodies used can be found in table 2.1. To eliminate dead cells, cells were stained with 1μg/mL propidium iodide (PI, Sigma-Aldrich P4170) before sorting. Compensations and gating were performed using appropriate single colour controls and fluorescence minus one (FMO) for the first time the panel is developed, or when the separation of positive-negative population is not well-defined. FC was performed on CytoFLEX flow cytometer (Beckman Coulter) equipped with 5 lasers, and FACS was performed on Influx (BD), CytoFLEX

SRT (Beckman Coulter) or MoFlo Astrio EQ sorter (Beckman Coulter). Analyses were performed with CytExpert 2.4 (Beckman Coulter) or FlowJo 10.8.1 (BD).

2.4 Cell culture

Cells were grown in a 37°C incubator with 5% CO_2. Sorted FAPs were cultured in high glucose DMEM (DMEM, Gibco 11965-092) supplemented with 10% FBS (Gemini 100-500 or Sigma-Aldrich F1051), 100U/mL Penicillin-Streptomycin (Gibco 15140-122), 1mM sodium pyruvate (Gibco 11360070), and 2.5ng/mL bFGF (Gibco 13256029). This is referred to as "growth media". Cells were allowed to adhere in incubator for 3 days and fresh growth media were added, and either switched into differentiation media on the next day, or new fresh growth media were added every 3 days. FAPs stayed in fibrogenic differentiation medium, containing DMEM, 5% FBS and 1ng/mL human TGFβ (eBioscience™ 14-8348-62) for 3 days. Adipogenic differentiation of FAPs was induced using mouse MesenCult™ Adipogenic Differentiation Kit (STEMCELL Technologies 05505). Half of adipogenic medium were refreshed every 2 days and cells were harvested after 5 days of adipogenic differentiation. Mouse fibroblast cell line C3H/10T1/2 (ATCC CCL-226) were cultured in DMEM supplemented with 10% FBS and 100U/mL Penicillin/Streptomycin.

2.5 Limiting dilution analysis

C3H 10T1/2 cells were irradiated with X-ray using an X-RAD 320 machine (Precision X-ray) at a fixed dosage of 4000cGy, then seeded at 7000 cells/well density into individual well of 96-well plates. Sorted FAPs were reconstituted to a concentration of 2×10^4 cells/100uL, and then serially diluted so that each well contain 2-250 cells. Fresh growth media were added every

3 days, and the number of wells with colonies formed at different density were counted after 10 days. Frequency of colony forming unit was estimated by single hit Poisson model (see Statistics).

2.6 Immunocytochemistry

Culture medium was aspirated, and cells were washed with PBS. They were then fixed with 4% paraformaldehyde (PFA, Sigma-Aldrich P6148) for 10 minutes and washed with PBS for 3 times, followed by permeabilization/blocking in 3% donkey serum (Sigma-Aldrich S30-M), 4% MOM blocking reagent (V/V, Vector Laboratories BMK-2202), 0.3% Triton X-100 (V/V, Sigma-Aldrich T8787) in PBS for 30 minutes. Cells were stained with primary antibody in the permeabilization/blocking buffer at 4°C overnight. On the second day, cells were washed with PBST for 3 times and incubated with fluorescent-conjugated secondary antibody in permeabilization/blocking buffer protected from light at RT for 1 hour.

2.7 RNA isolation and RT-qPCR

Total RNA from sorted or cultured cells was isolated using RNAzol® RT solution (Sigma-Aldrich R4533) following manufacturer's instruction. Reverse transcription was performed using the High-Capacity cDNA Reverse Transcription Kit (Applied Biosystems 4368813). Gene expression analysis was performed using Taqman Gene Expression Assays on a Viia7 Real Time PCR system (Applied Biosystems). Taqman *Acta2* (Mm01546133_m1), *Col1a1* (Mm00801666_g1), *Col3a1* (Mm00802300_m1), *Fn1* (Mm01256744_m1) probes were purchased from ThermoFisher Scientific. Relative gene expression was calculated by the ΔΔCt method normalized to hypoxanthine-guanine phosphoribosyltransferase (*Hprt,* Mm00446968_m1).

2.8 RNA sequencing

Sample quality was assessed using the Agilent 2100 Bioanalyzer. RNA samples with an RNA Integrity Number > 8 were used to prepare libraries following the standard protocol for the TruSeq Stranded mRNA library kit (Illumina 20020595) on the Illumina Neoprep automated microfluidic library prep instrument. Paired-end sequencing was performed on the Illumina NextSeq 2000 using the NextSeq 100-cycles P3 Reagent Kit (Illumina 20040559).

2.9 RNA-seq bioinformatics analysis

Illumina base call files were de-multiplexed by bcl2fastq2 (v. 2.20) on Basespace. Adaptor sequences were trimmed and low-quality reads (< 35 base pairs) were discarded. Additionally, Bowtie was used to remove read pairs that aligned against abundant sequences. Demultiplexed read sequences were then aligned to the mm10 genome reference using STAR aligner. The number of aligned reads to each annotated gene was tallied with RnaReadCounter to generate read-count matrices for all samples, which were used as inputs for downstream analyses. Bowtie, STAR, and RnaReadCounter are tools built under RNA-Seq Alignment (v 1.1.1). Downstream analyses of read-count data were performed in R (v 4.2.2). Genes with less than 2 counts per million (CPMs) in at least three samples were filtered out. Filtered counts were processed and analyzed using DESeq2 (v 1.38.2) (Love et al., 2014). This included count normalization, principal component analysis (PCA), and differential expression analysis. Over representation analysis was performed using DAVID (v 2021) (Huang et al., 2009; Sherman et al., 2022) with all significant genes considered to inform enriched biological processes under Gene Ontology (GO DIRECT). Bars

associated with top enriched GO terms reflect log-transformed adjusted P-values. All P-values were adjusted by Benjamini-Hochberg correction.

2.10 Single cell RNA-seq analyses

Publicly available single cell RNA-seq datasets were directly downloaded from the Gene Expression Omnibus (GEO), a genomics data repository commonly used alongside publications. These published datasets include GSE110037 (Scott et al., 2019), GSE138826 (Oprescu et al., 2020), and GSE143437 (De Micheli, Laurilliard, et al., 2020). As the data were previously aligned by the respective research groups, we extracted and loaded gene-barcode matrices into R (v. 4.1.2). Data processing and differential expression analysis were performed using the Seurat R package (v.4.1.1) (Hao et al., 2021). Filtering of data is performed in two rounds. Firstly, genes that are not expressed in at least 3 cells and cells that do not express at least 200 genes are removed. Secondly, quality control is enforced to isolate viable singlets based on two parameters: 1) the number of unique molecular identifiers (UMIs or unique sequences incorporated into transcripts during library generation to minimize PCR amplification bias); 2) the proportion of mitochondrial UMIs per cell ("percent.mt"). "Cells" with high UMI counts are likely "doublets" generated during gel-in-emulsion (GEM) formation where multiple cells are incorporated into the same gel droplet, whereas those with low UMI counts are likely empty droplets filled with ambient RNA. Additionally, "cells" with high percent.mt are likely non-viable as mitochondrial RNA tends to be more stable than nuclear RNA when cells lyse. Both of these parameters are tailored to each respective dataset. scTransform-based normalization was performed as described in the published vignette (Hafemeister & Satija, 2019) with top 3000 variable genes selected. "Percent.mt" was

regressed out to minimize cell clustering by cell quality. To avoid batch variation, Seurat's "integration" approach is adopted to identify cells of similar biological states. This is applied to datasets of the same time point across the three studies or datasets of all time points but within the same study. The number of principal components (PCs) used for Louvain clustering and uniform manifold approximation and projection (UMAP) was determined by the inflection point of variances accounted by PCs (~20 PCs). Clusters were grouped into distinct annotated subsets as advised by identity markers reported in past literature. Differential gene expression is performed with Wilcoxon rank sum test with p-value adjustments by Bonferroni's correction.

2.11 Immunohistochemistry staining

Tissues were drop-fixed in 4% PFA in PBS overnight with constant shaking at 4°C. They were then switched to 30% sucrose solution before frozen in Tissue-Tek O.C.T. compound (Sakura 4583) in liquid nitrogen-cooled isopentane. 10μm tissue cryosections were prepared using a Leica cryostat. Cryosections were equilibrated to room temperature, rehydrated in PBS, and permeabilized in 0.5% Triton X-100/100mM glycine in TBS for 10 minutes. They were then blocked in 2% bovine serum albumin (w/V, Sigma-Aldrich A7906), 5% normal goat serum (GeneTex GTX73249) (or donkey serum) and 4% MOM blocking reagent, 0.1% Tween 20 (V/V, Sigma-Aldrich P1379) in TBS for 1 hour at RT. Sections were then stained in primary antibodies without the MOM reagent at appropriate dilution overnight in 4°C. On the second day, sections were rinsed with TBST and incubated with fluorescent-conjugated secondary antibodies in dark at RT for 1 hour. Nuclei were counterstained with 600nM DAPI (Invitrogen D3571). Slides were mounted with Fluoromount-G® reagent (Southern Biotech 0100-01). Imaging was performed with Nikon Eclipse, Echo Revolve, or Zeiss LSM900 Confocal microscope.

2.12 Image analysis

Image quantification was performed in ImageJ (NIH) software. Number of cells within a field was calculated by thresholding followed by watershed function in the DAPI channel. Adipogenicity was quantified by averaging the percentage of perilipin+ cells over all nuclei in 3 random fields and 2 technical replicate wells.

2.13 Statistical analysis

Statistical analyses were performed in Prism 9 (GraphPad). Limiting dilution analysis was performed on a web interphase developed by Walter and Eliza Hall Institute of Medical Research, Melbourne, Australia (https://bioinf.wehi.edu.au/software/elda/) (Hu & Smyth, 2009).

Antibody	Fluorophore	Clone	Dilution	Provider	Cat number
Anti-CD31	eFluor™ 450	390	1:500	eBioscience™	48-0311-82
Anti-CD31	APC	390	1:500	eBioscience™	17-0311-82
Anti-CD45	eFluor™ 450	30-F11	1:500	eBioscience™	48-0451-82
Anti-CD45	APC	30-F11	1:500	eBioscience™	17-0451-83
Anti-Ly-6A/E (Sca-1)	FITC	D7	1:1000	eBioscience™	11-5981-81
Anti-Ly-6A/E (Sca-1)	PE-Cyanine7	D7	1:4000	eBioscience™	25-5981-82
Anti-Ly-6A/E (Sca-1)	APC	D7	1:2000	eBioscience™	17-5981-83
Anti-DPP4	APC	H192-112	1:200	Biolegend	137807

Table 2.1 List of antibodies used in flow cytometry

Antibody	Fluorophore	Clone	Dilution	Provider	Cat number
Anti-DPP4		Polyclonal	1:200	R&D System	AF954

Anti-Laminin		Polyclonal	1:200	Abcam	ab11575
Anti-Laminin		Polyclonal	1:200	Abcam	ab11576
Anti-LYVE1		EPR21771	1:200	Abcam	ab218535
Anti-Perilipin		Polyclonal	1:200	Sigma Aldrich	P1873
Anti-Alpha-Smooth Muscle Actin		1A4	1:200	Invitrogen	14-9760-82
Goat anti-Rabbit IgG (H+L) Cross-Adsorbed Secondary Antibody	Alexa Fluor™ 568	Polyclonal	1:1000	Invitrogen	A11011
Goat anti-Rabbit IgG (H+L) Highly Cross-Adsorbed Secondary Antibody	Alexa Fluor™ 647	Polyclonal	1:1000	Invitrogen	A21245
Goat anti-Rat IgG (H+L) Cross-Adsorbed Secondary Antibody	Alexa Fluor™ 647	Polyclonal	1:1000	Invitrogen	A21247
Goat anti-Rabbit IgG (H+L) Cross-Adsorbed Secondary Antibody	Alexa Fluor™ 405	Polyclonal	1:1000	Invitrogen	A31556
Donkey anti-Rabbit IgG (H+L) Highly Cross-Adsorbed Secondary Antibody	Alexa Fluor™ 488	Polyclonal	1:1000	Invitrogen	A21206
Donkey anti-Goat IgG (H+L) Cross-Adsorbed Secondary Antibody	Alexa Fluor™ 647	Polyclonal	1:1000	Invitrogen	A21447
Donkey Anti-Rat IgG H&L (Alexa Fluor® 647) preadsorbed	Alexa Fluor® 647	Polyclonal	1:1000	Abcam	ab150155

Table 2.2 List of antibodies used in immunofluorescence staining

Chapter 3: Results

3.1 *Dpp4* marks a distinct FAP subset by single cell RNA sequencing

We first performed integrated analysis using three publicly available single cell RNA sequencing datasets of skeletal muscle that span different stages of muscle regeneration (Figure 1A-C). In each of the dataset, we subset only the mesenchymal stromal cells (MSCs), defined by the cell clusters co-expressing *Pdgfra* and *Ly6a* and re-clustered them. We performed differential gene analysis, and discovered that *Dpp4*, *Pi16* and *Cd55* were enriched in a subset of mesenchymal stromal cells. The expression patterns of these 3 genes are clearly distinct from *Cxcl14*, *Mme* and *Vcam1*, which were being used to identify other mesenchymal subpopulations in literature (Fitzgerald et al., 2023; Malecova et al., 2018; Oprescu et al., 2020) (Figure 1D-F). We further integrated all mesenchymal cells in resting stage (D0) from three datasets and performed re-clustering (Figure 1G). Clustering analysis identified a common group of mesenchymal stromal cells (clusters 1, 3, and 5) co-expressing *Dpp4, Pi16 and Cd55* (Figure 1H), indicating that *Dpp4* is a conserved marker for this specific FAP subset.

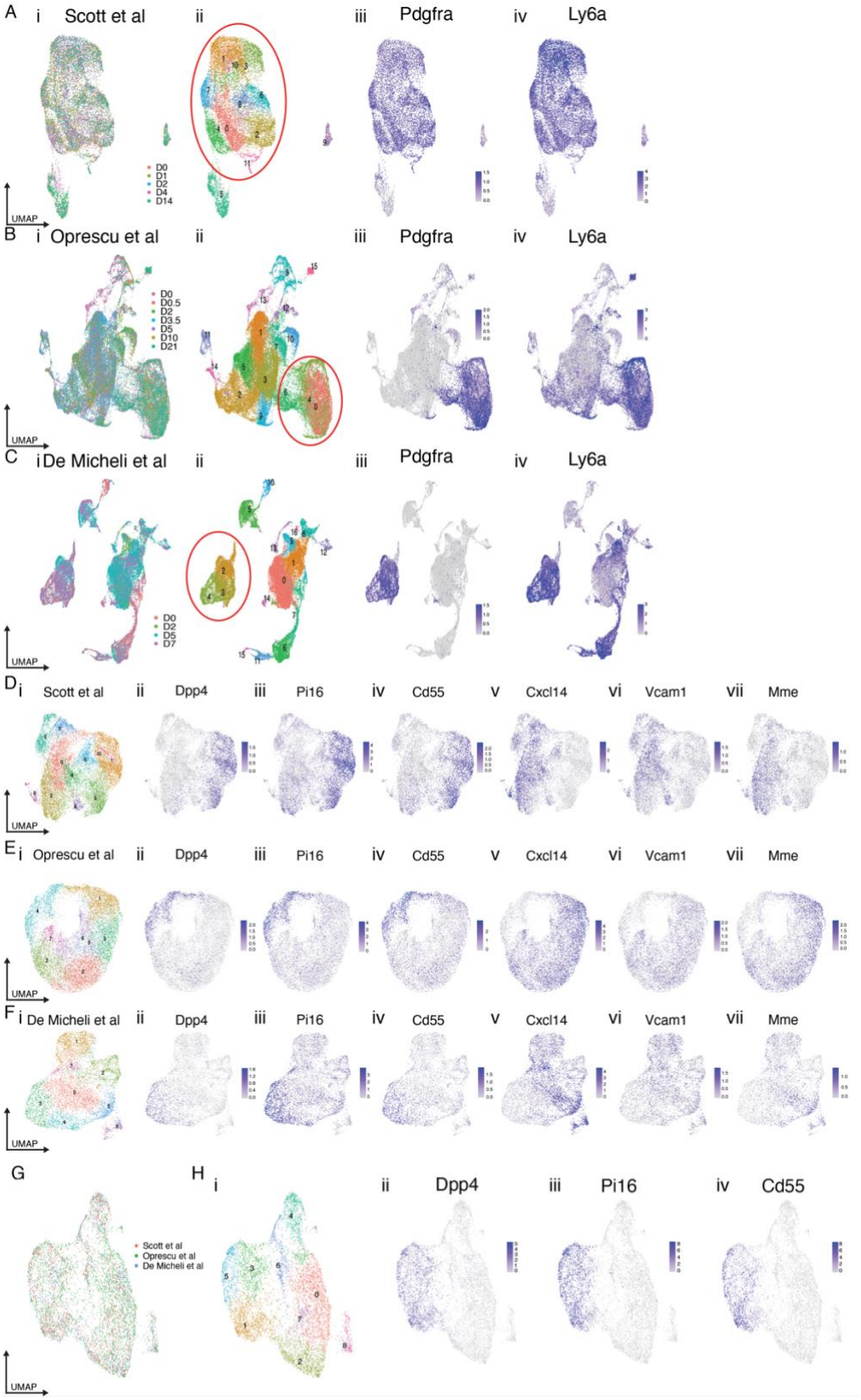
A
i Scott et al
ii
iii Pdgfra
iv Ly6a
D0
D1
D2
D4
D14
UMAP
B
i Oprescu et al
ii
iii Pdgfra
iv Ly6a
D0
D0.5
D2
D3.5
D5
D10
D21
UMAP
C
i De Micheli et al
ii
iii Pdgfra
iv Ly6a
D0
D2
D5
D7
UMAP
D
i Scott et al
ii Dpp4
iii Pi16
iv Cd55
v Cxcl14
vi Vcam1
vii Mme
UMAP
E
i Oprescu et al
ii Dpp4
iii Pi16
iv Cd55
v Cxcl14
vi Vcam1
vii Mme
UMAP
F
i De Micheli et al
ii Dpp4
iii Pi16
iv Cd55
v Cxcl14
vi Vcam1
vii Mme
UMAP
G
Scott et al
Oprescu et al
De Micheli et al
UMAP
H
i
ii Dpp4
iii Pi16
iv Cd55
UMAP

Figure 3.1 DPP4 marks a distinct FAP subset by single cell RNA sequencing

(A-C) Single cell RNA sequencing data of skeletal muscles at different timepoint post injury from (A) Scott et al., (B) Oprescu et al., and (C) De Micheli et al.

(i) UMAP plot coloured by the timepoint after injury depicting shared biological states across timepoints after batch correction

(ii) UMAP plot coloured by unsupervised Louvain clustering of cells highlighting the similarity of biological states captured throughout the regeneration cascade

(iii) Expression pattern of *Pdgfra* and (iv) *Ly6a* reveals the clusters corresponding to mesenchymal stromal cells (circled in red). Expression values represent SCT-normalized transcript counts with maximum threshold set to the 95th percentile across all cells.

(D-F) (i) UMAP plot of only FAPs subset from the original dataset revealing heterogeneity within cells. Analysis of the expression patterns of (ii) *Dpp4*, (iii) *Pi16*, (iv) *Cd55*, (v) *Cxcl14*, (vi) *Vcam1*, and (vii) *Mme* by FAPs at single cell resolution during muscle regeneration in the three datasets

(G) UMAP plot of the integration of murine *Pdgfra*$^{+}$/*Ly6a*$^{+}$ mesenchymal stromal cells in uninjured skeletal muscle from the three datasets, colour coded by the source of the dataset

(H) (i) UMAP plot showing the unsupervised clustering of the integrated dataset reveals a group of cells that co-express (ii) *Dpp4*, (iii) *Pi16* and (iv) *Cd55* at single-cell level.

3.2 Prospective isolation and characterization of DPP4$^+$ FAPs in steady state skeletal muscles

We next sought to confirm the physical presence of DPP4+ FAPs at steady state muscle, since it has only been shown as a transcriptionally distinct set of cells without direct proof of existence. By flow cytometry, we identified DPP4$^+$ FAPs as CD31$^-$CD45$^-$Sca1$^+$DPP4$^+$ cells in steady state skeletal muscle, which constitutes approximately 45% of all FAPs (Figure 2A). We complemented the results by immunohistochemical staining. DPP4 signals colocalized with PDGFRα-EGFP across the tibialis anterior (TA) muscle sections in interstitial space (Figure 2B), again confirmed the presence of DPP4$^+$ FAPs in physiological condition.

To further validate that the DPP4$^+$ FAPs we identified here are equivalent to the FAP subset identified in our previous single cell RNA sequencing study (Scott et al., 2019), we FACS-isolated DPP4$^+$ and DPP4$^-$ FAPs and performed bulk RNA sequencing. Principal component analysis (PCA) reflected that the majority of the differences can be explained by sorting strategy where DPP4$^+$ FAPs exhibit a clear distinction in transcriptome compared to DPP4$^-$ FAPs (Figure 2C). DESeq2 revealed differentially expressed genes (DEGs) between DPP4$^+$ and DPP4$^-$ FAPs, which significantly overlapped with the reported DEGs in the previous study (Figure 2D). In particular, *Dpp4*, *Pi16* and *Cd55*, the three genes that were used as markers for this specific MSC subset in literature, were upregulated in FACS-isolated DPP4$^+$ FAPs, while *Cxcl14* and *Mme*, two genes used to identify the other resting stage FAP subpopulation, were downregulated in DPP4$^+$ FAPs (Figure 2E). Intriguingly, we also noticed that *Ly6a* (the gene encoded for SCA1) was upregulated in DPP4$^+$ FAPs (Figure 2E). This was independently confirmed in flow cytometry (Figure 2F), which linked this subset to SCA-1^{high} FAPs previously identified by mass cytometry (Giuliani et al., 2021). Top 10 DEGs in DPP4$^+$ and DPP4$^-$ FAPs were shown in the heatmap below (Figure

2G-H). Collectively, we demonstrated that DPP4^{+} FAPs are present in skeletal muscle, and are congruent to a specific FAP subset identified in past single cell RNA sequencing studies.

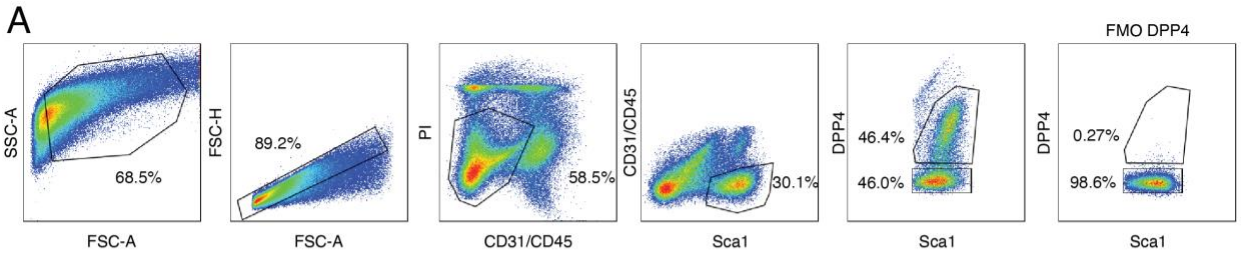
A
SSC-A
FSC-A
68.5%
FSC-H
FSC-A
89.2%
PI
CD31/CD45
58.5%
CD31/CD45
Sca1
30.1%
DPP4
Sca1
46.4%
46.0%
FMO DPP4
DPP4
Sca1
0.27%
98.6%

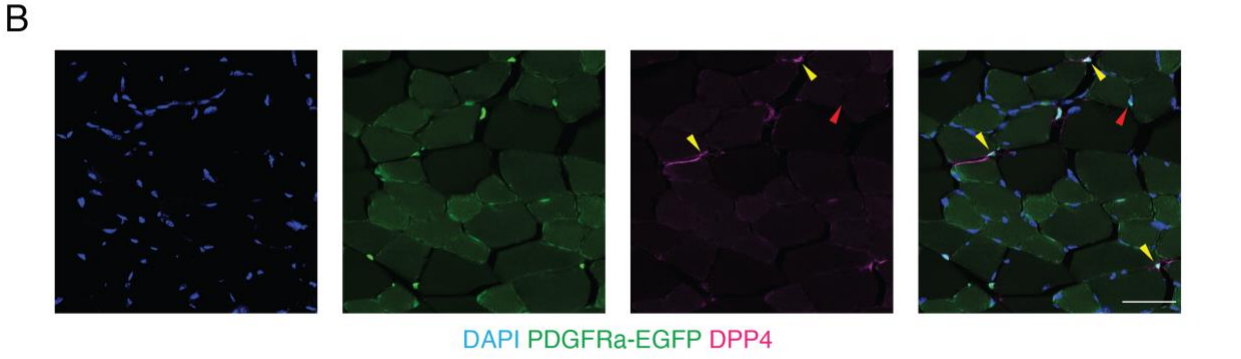
B
DAPI PDGFRa-EGFP DPP4

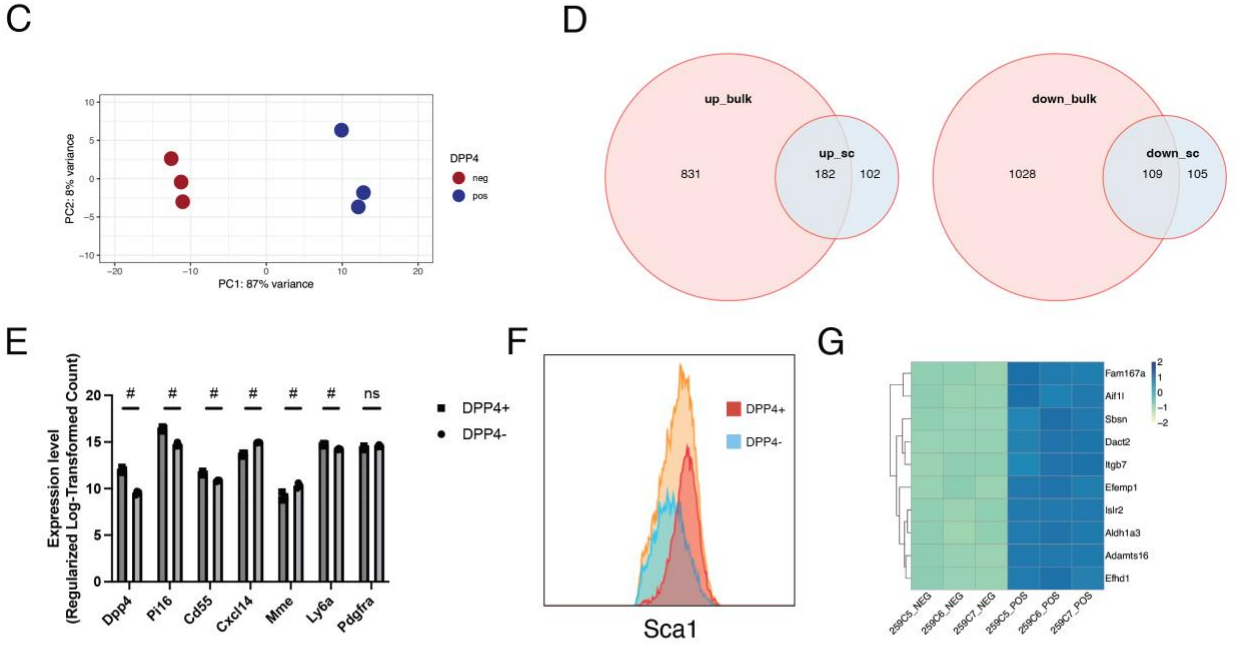
C
PC2: 8% variance
PC1: 87% variance
DPP4
neg
pos
D
up_bulk
831
up_sc
182
102
down_bulk
1028
down_sc
109
105
E
Expression level
(Regularized Log-Transformed Count)
#
#
#
#
#
#
ns
Dpp4
Pi16
Cd55
Cxcl14
Mme
Ly6a
Pdgfra
DPP4+
DPP4-
F
DPP4+
DPP4-
Sca1
G
Fam167a
Aif1l
Sbsn
Dact2
Itgb7
Efemp1
Islr2
Aldh1a3
Adamts16
Efhd1
259C5_NEG
259C6_NEG
259C7_NEG
259C5_POS
259C6_POS
259C7_POS
H
Lamc3
Crlf1
Pygm
Nrxn2
Crispld2
Esm1
Adamtsl2
Atp1a2
D630003M21Rik
Vwa1
259C5_NEG
259C6_NEG
259C7_NEG
259C5_POS
259C6_POS
259C7_POS

Figure 3.2 Prospective isolation and characterization of DPP4$^+$ FAPs in steady state skeletal muscles

(A) Gating strategy to identify DPP4$^+$ FAPs in steady state skeletal muscle. Cells were identified based on forward/side scatter, and singlets were selected for downstream analysis. CD31 and CD45 were used to exclude mature endothelial and hematopoietic cells (Lin), respectively, and propidium iodide (PI) was used to remove dead cells. DPP4$^+$ FAPs were identified as DPP4$^+$ cells out of the Lin$^-$ Sca1$^+$ fraction. The gating for DPP4$^+$ FAPs is drawn based on fluorescence minus one (FMO) control.

(B) Immunofluorescence staining of TA cross section from a PDGFRα-EGFP mouse. Yellow arrows indicate overlap of DPP4 and EGFP (FAPs) signals, and red arrows indicate FAPs that are negative for DPP4. Myofibers were shown by autofluorescence in FITC channel. Scale bar: 50 μm.

(C) PCA analysis of sorted DPP4$^+$ and DPP4$^-$ FAPs from uninjured C57BL/6J mice. Each dot represents biological replicate.

(D) Venn diagram showing the common differentially expressed genes in DPP4$^+$ FAPs from bulk and single cell RNA sequencing.

(E) Expression levels of selected genes from bulk RNA sequencing. The defining marker for FAP *Pdgfra* is included as reference. Gene expression levels are the regularized log-transformed counts normalized by DEseq2. $^{\#}$ $P < 0.05$. N.s.: not significant. Normalized expression level and adjusted p-value for the genes listed here can be found in Table 3.1 and Table 3.2 respectively.

(F) Histogram of SCA-1 expression level in FAPs with DPP4$^+$ and DPP4$^-$ FAPs overlayed on top

(G, H) Heatmap showing the top 10 (G) upregulated and (H) downregulated genes in DPP4$^+$ FAPs

3.3 DPP4^{+} FAPs retain bi-lineage differentiation potentials

FAPs were known for their ability to spontaneously differentiate into both mature adipocytes and fibroblasts. However, it is not known whether specific FAP subsets would possess different lineage potentials. To this end, we examined the lineage potentials of DPP4^{+} FAPs by single cell differentiation assay. Single DPP4^{+} and DPP4^{-} FAPs were purified by FACS and directly seeded on top of a feeder layer consisted of growth-arrested C3H 10T1/2 fibroblast, and allowed to proliferate and differentiate under standard growth condition (Figure 3A). FAPs were stained against αSMA and PLIN1 to assess their fibrogenic and adipogenic differentiation potential, respectively. We observed both DPP4^{+} and DPP4^{-} FAPs were able to form fibroblasts and adipocytes spontaneously in standard growth media (Figure 3b). Therefore, both DPP4^{+} and DPP4^{-} cells are bipotent fibroadipogenic progenitors in skeletal muscle.

A

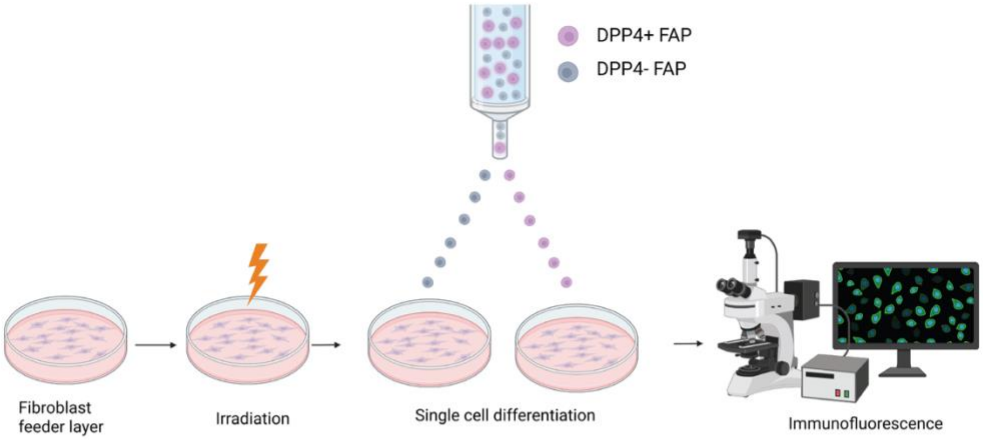
DPP4+ FAP
DPP4- FAP
Fibroblast feeder layer
Irradiation
Single cell differentiation
Immunofluorescence

B

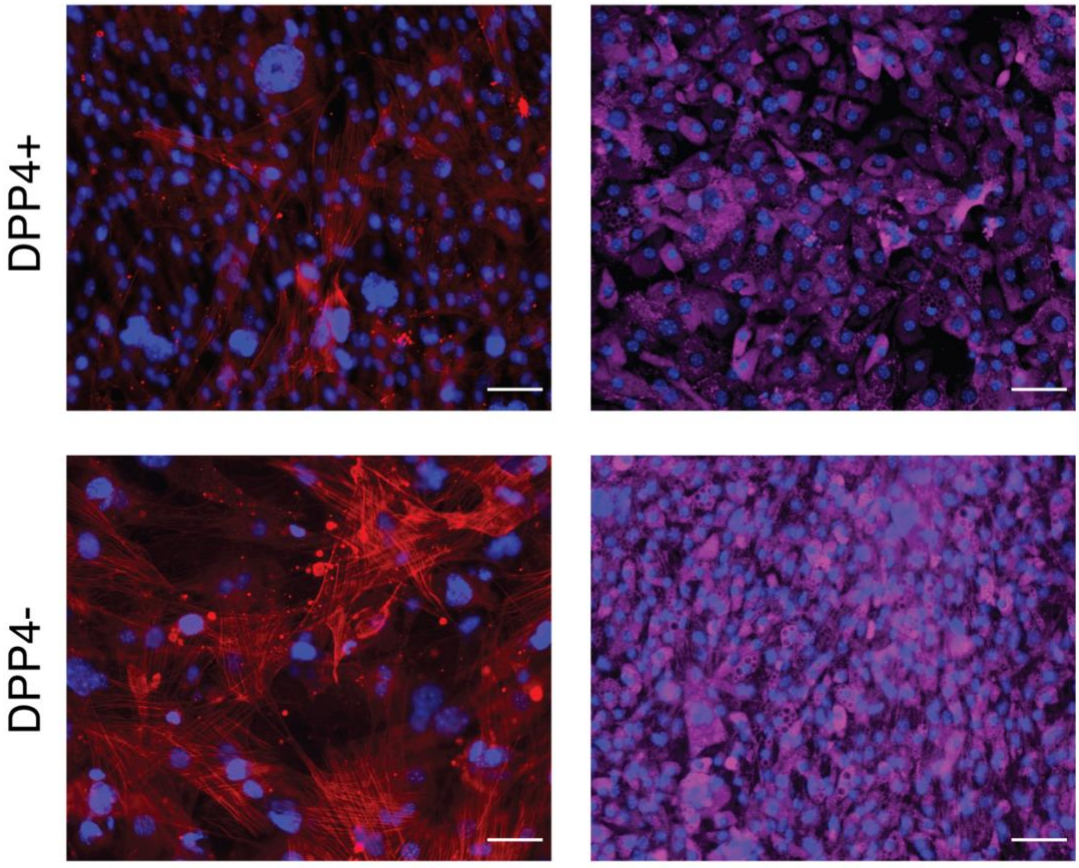
DPP4+
DPP4-
DAPI aSMA PLIN

Figure 3.3 DPP4^{+} FAPs retain bi-lineage differentiation potential

(A) Schematic diagram of the experimental design. Single DPP4^{+} or DPP4^{-} FAPs were sorted directly on top of irradiated C3H fibroblast feeder layer.

(B) Immunofluorescence staining revealed both DPP4^{+} and DPP4^{-} FAPs retained potential to spontaneously differentiate into αSMA^{+} mature fibroblast (left) and PLIN^{+} adipocyte (right). Scale bar: 100μm.

3.4 DPP4^{+} FAPs possess higher clonogenicity

We next assayed the clonogenicity of DPP4^{+} FAPs by limiting dilution analysis. We sorted DPP4^{+} and DPP4^{-} FAPs from tamoxifen-treated PDGFRα^{CreERT2}-tdTomato mice so that all FAPs were labelled by tdTomato fluorescent protein. Isolated cells were two-fold serially diluted so that each replicate well contain 2 to 250 cells. They were allowed to expand for 10 days on top of C3H 10T1/2 fibroblast feeder layer. Wells with tdTomato^{+} FAP colonies, defined as >32 cells, were counted (Figure 4A-B). Single-hit Poisson model estimated the frequency of colony-forming unit (CFU) in DPP4^{+} FAPs to be 11.6%, which is 2.5-fold higher than that of DPP4^{-} FAPs (Figure 4C-D). Hence, DPP4^{+} FAPs have higher clonogenicity.

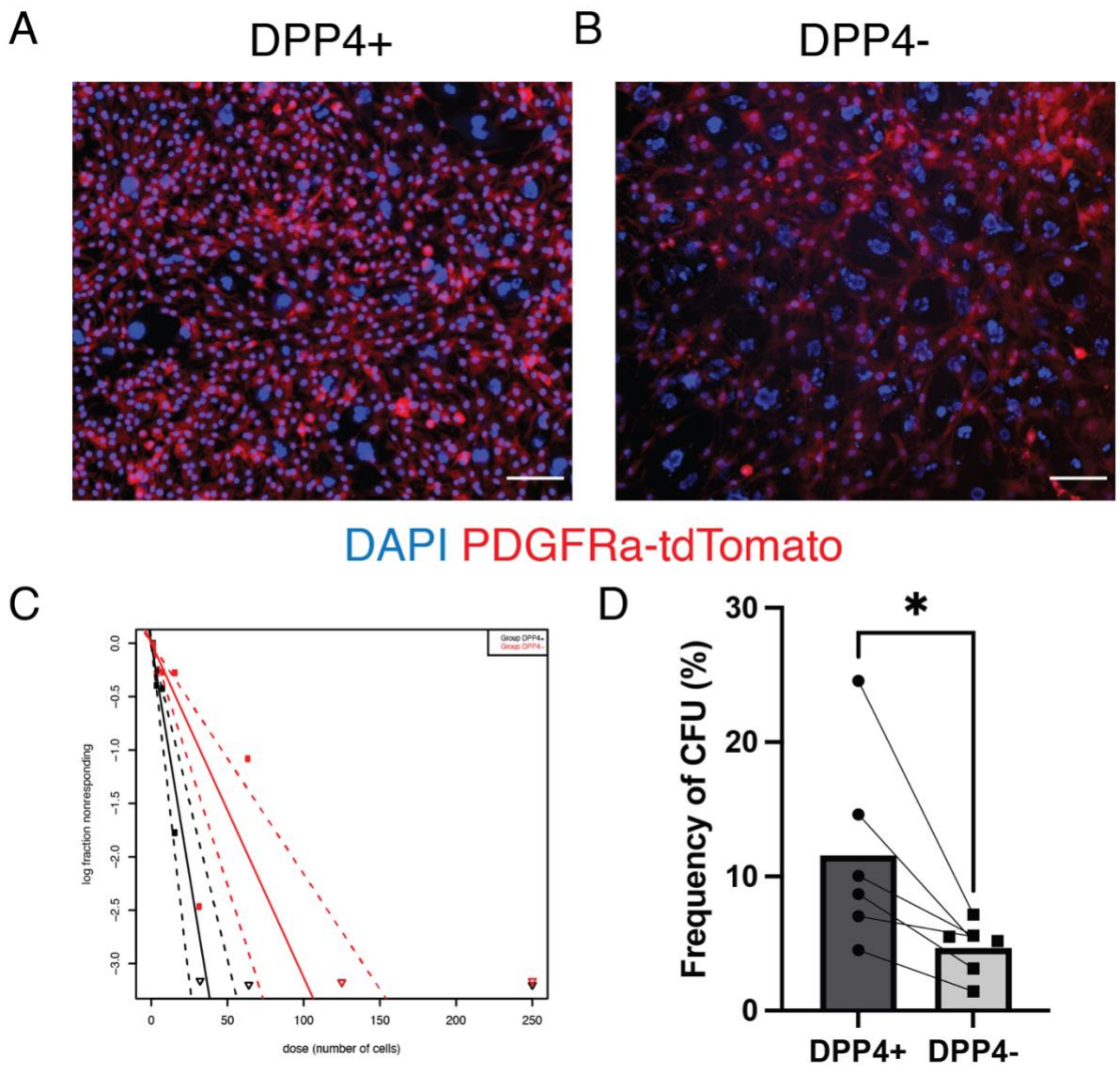
A
DPP4+
B
DPP4-
DAPI PDGFRa-tdTomato
C
log fraction nonresponding
dose (number of cells)
D
Frequency of CFU (%)
DPP4+
DPP4-
*

Figure 3.4 DPP4^{+} FAPs possess higher clonogenicity

(A, B) Representative fluorescence microscopy images of colonies developed from (A) DPP4^{+} and (B) DPP4^{-} FAPs. Nuclei were counterstained with Hoechst 33342. Scale bar: 100 μm.

(C) Representative figure for estimation of the frequency of CFU in DPP4^{+} and DPP4^{-} FAPs.

(D) Quantification of CFU frequency of DPP4^{+} and DPP4^{-} FAPs. N = 6. * $P < 0.05$ (two-tailed paired t test).

3.5 DPP4^{+} FAPs display distinct adipogenic profile *in vitro*

Having demonstrated that both DPP4^{+} and DPP4^{-} FAPs are capable of differentiating into adipocytes and fibroblasts, we move on to identify whether or not they would preferentially differentiate into one of the specific lineages under induction conditions. We treated FACS-isolated DPP4^{+} and DPP4^{-} FAPs with TGFβ which drove them to commit to fibrogenic lineage. Consistent with previous reports, we observed robust fibrogenesis, as seen by the αSMA^{+} stress fibers formation (Figure 5A-B). We compared the expression level of fibrogenic signature genes, namely *Fn1, Col1a1, Col3a1, Acta2,* and *Ctgf*, by RTqPCR. TGFβ-treated cells expressed a higher level of fibrogenic genes as anticipated; however, we did not observe a significant difference in the expression level between TGFβ-treated DPP4^{+} and DPP4^{-} FAPs (Figure 5C). Therefore, both of them are similarly prone to fibrogenesis *in vitro*. We also induced adipogenic differentiation of DPP4^{+} and DPP4^{-} FAPs. Similarly, we noticed pronounced intracellular fat droplets accumulation labelled by PLIN1 (Figure 5D-E). In contrast to fibrogenic differentiation, we found that DPP4^{+} FAPs exhibited stronger propensity towards adipogenesis, as 83.4% of cells DPP4^{+} FAPs committed to the adipogenic fate, while only 49.4% of DPP4^{-} FAPs-derived cells were PLIN1^{+} (Figure 5F). Importantly, in both conditions, we noticed that DPP4^{+} FAPs had a higher rate of proliferation (Figure 5G). This is consistent with the reported characteristics of DPP4^{+} interstitial progenitors in adipose tissue (Merrick et al., 2019), once again suggesting that DPP4^{+} FAPs could be an equivalent cell type of adipose tissue interstitial progenitors in muscle.

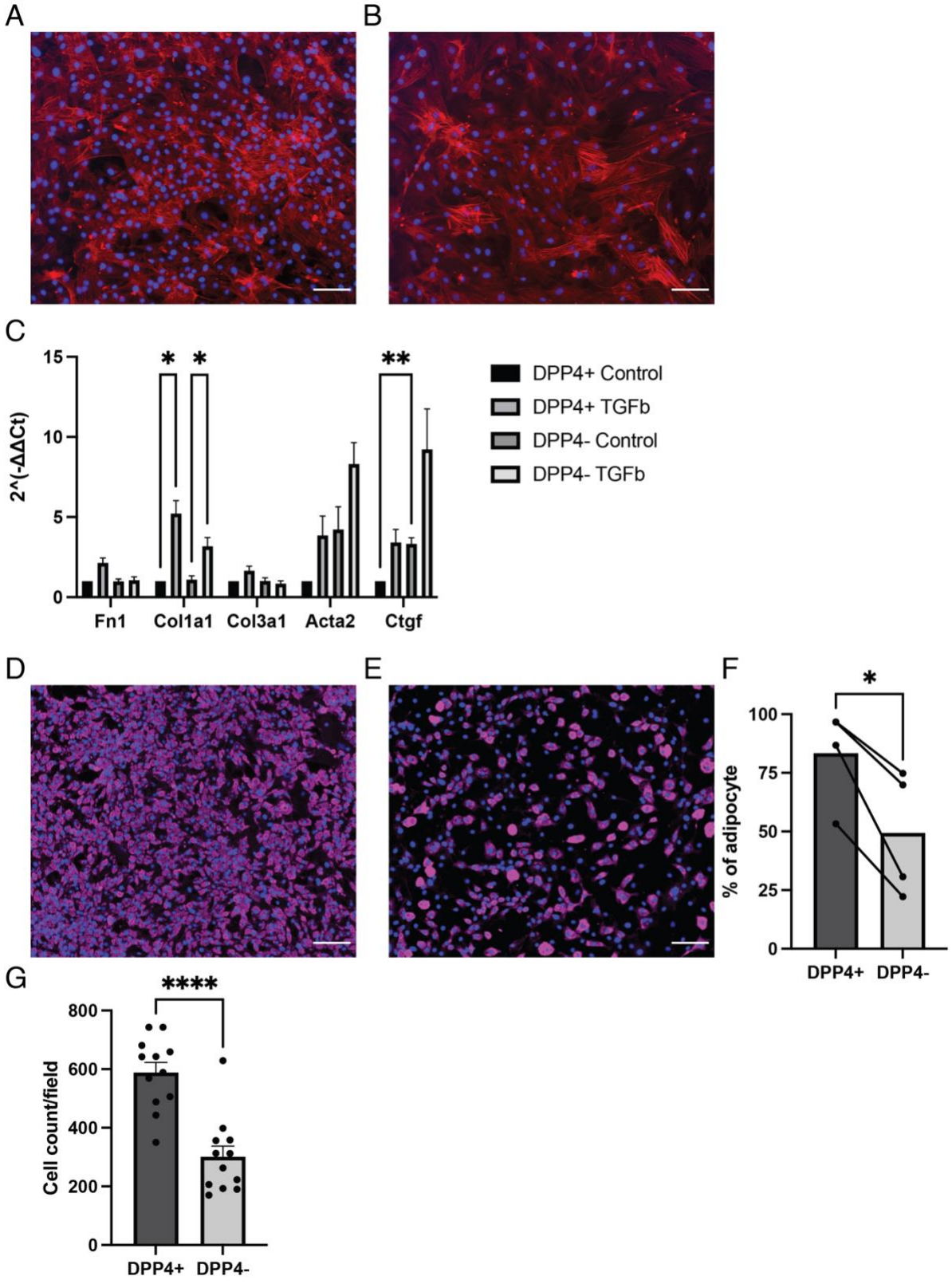
A
B
C
2^(-ΔΔCt)
15
10
5
0
* *
**
Fn1
Col1a1
Col3a1
Acta2
Ctgf
DPP4+ Control
DPP4+ TGFb
DPP4- Control
DPP4- TGFb
D
E
F
*
100
75
50
25
0
% of adipocyte
DPP4+
DPP4-
G
****
800
600
400
200
0
Cell count/field
DPP4+
DPP4-

Figure 3.5 DPP4^{+} FAPs display distinct adipogenic profile *in vitro*

(A-B) Immunofluorescence staining of TGFβ-treated (A) DPP4^{+} and (B) DPP4^{-} FAPs against αSMA. Scale bar: 100 μm.

(C) Expression level of selected fibrosis marker genes. Gene expression levels were first normalized to *Hprt*, and 2^(-ΔΔCt) values were computed by comparing to that of DPP4^{+} FAPs in control condition. * $P < 0.05$. ** $P < 0.01$ (RM two-way ANOVA with Geisser-Greenhouse correction. Multiple comparisons were performed using Šidák's multiple comparisons test).

(D, E) Immunofluorescence staining of (D) DPP4^{+} and (E) DPP4^{-} FAPs in adipogenic condition against PLIN1. Scale bar: 100 μm.

(F) Quantification of percentage of differentiated FAPs. N = 4. * $P < 0.05$ (two-tailed paired t test).

(G) Quantification of cells in 12 randomly selected fields from DPP4^{+} and DPP4^{-} FAP cultures treated with fibrogenic/adipogenic media. **** $P < 0.0001$ (unpaired t test).

3.6 DPP4^{+} FAPs are the precursors of DPP4- FAPs *in vitro*

We next sought to define the lineage relationship between DPP4^{+} and DPP4^{-} FAPs. We FACS-purified DPP4^{+} and DPP4^{-} FAPs, and cells were either immediately reprofiled for DPP4 expression by flow cytometry, or subjected to *in vitro* culture and were harvested 7 days later by trypsinization. Cultured FAPs were re-stained with antibodies for flow cytometry. 95.8% and 0.95% of freshly isolated DPP4^{+} and DPP4^{-} FAPs were positive for DPP4, confirming the purity of the FACS strategy (Figure 6A-B). After 7 days of culture, we observed a marked reduction of DPP4^{+} cells in cultured DPP4^{+} FAPs with only 32.8% of cells retaining DPP4 expression (Figure 6C). On the contrary, we did not notice a significant increase in the incidence of DPP4^{+} cells from the DPP4^{-} FAPs culture (Figure 6D). Collectively, these *in vitro* cultures suggested that there is a unidirectional flux of DPP4^{+} FAPs to DPP4^{-} FAPs.

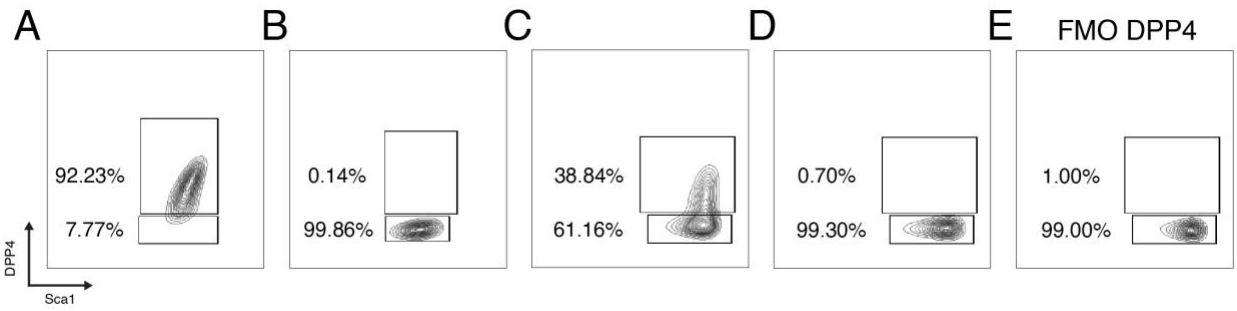
A
B
C
D
E
FMO DPP4
92.23%
7.77%
0.14%
99.86%
38.84%
61.16%
0.70%
99.30%
1.00%
99.00%
DPP4
Sca1

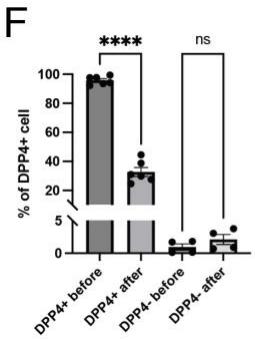
F
****
ns
% of DPP4+ cell
100
80
60
40
20
5
0
DPP4+ before
DPP4+ after
DPP4- before
DPP4- after

Figure 3.6 DPP4$^+$ FAPs are the precursor of DPP4$^-$ FAPs *in vitro*

(A-D) Representative flow cytometric analysis of DPP4 expression profile from (A) freshly isolated DPP4$^+$ FAPs, (B) freshly isolated DPP4$^-$ FAPs, (C) cultured DPP4$^+$ FAPs, and (D) cultured DPP4$^-$ FAPs.

(E) FMO control of DPP4 re-staining for (C) and (D)

(F) Quantification of DPP4 expression by flow cytometry in freshly isolated and cultured DPP4$^+$ and DPP4$^-$ FAPs. N = 6 for DPP4$^+$ FAPs and n = 4 for DPP4$^-$ FAPs. N.s.: not significant. **** $P < 0.0001$ (ordinary one-way ANOVA with Šidák's multiple comparison test).

3.7 DPP4$^+$ FAPs form the niche of skeletal muscle self-renewing resident macrophages

After characterization of DPP4$^+$ FAPs *in vitro*, we next attempt to understand their functions in steady state skeletal muscle. Recently, we found a population of skeletal muscle self-renewing resident macrophages (SRRMs) defined by TIM4 and LYVE1 expression (Babaeijandaghi, Cheng, et al., 2022). CSF1 signaling is critical for macrophage survival and proliferation (Lavin et al., 2015; Ryan et al., 2001), and depletion of SRRMs by CSF1R inhibition resulted in accumulation of necrotic fibers (Babaeijandaghi, Cheng, et al., 2022). Importantly, we found FAPs to be the only source of CSF1 in skeletal muscle (Figure 7A) (Babaeijandaghi, 2021). This raised a possibility that FAPs could play key roles in regulating the survival and activity of SRRMs. However, we observed a two-fold higher number of FAPs than LYVE1$^+$ SRRMs (Figure 7B) in skeletal muscle, which does not support the hypothesis that FAPs form the niche for SRRMs, as the number of niche cell is often limiting (Scadden, 2006). This in turn suggests that a subpopulation of FAPs, but not all FAPs, could form the niche of SRRMs. Intriguingly, upon analysis of the transcriptomic profiles of *Csf1*-expressing FAPs, we found that *Dpp4* to be upregulated in this subset (Figure 7C). This suggested that DPP4$^+$ cells could be the subset of FAPs that serve as the niche for SRRMs. Indeed, we examined the number of DPP4$^+$ FAPs and compared it to LYVE1$^+$ SRRMs and found that they are similar in number (Figure 7D). Histological analysis revealed that, despite only 34.8% of FAPs express DPP4, the majority of FAPs (60.0%) with LYVE1$^+$ SRRMs in close vicinity are DPP4-positive (Figure 7D-E). The over-representation of DPP4$^+$ FAPs in all *Csf1*-expressing cells (i.e. FAPs) that reside adjacent to SRRMs strongly suggested that they are the key contributor of CSF1 for survival of SRRMs, hence placing them a well-suited candidate as the niche component.

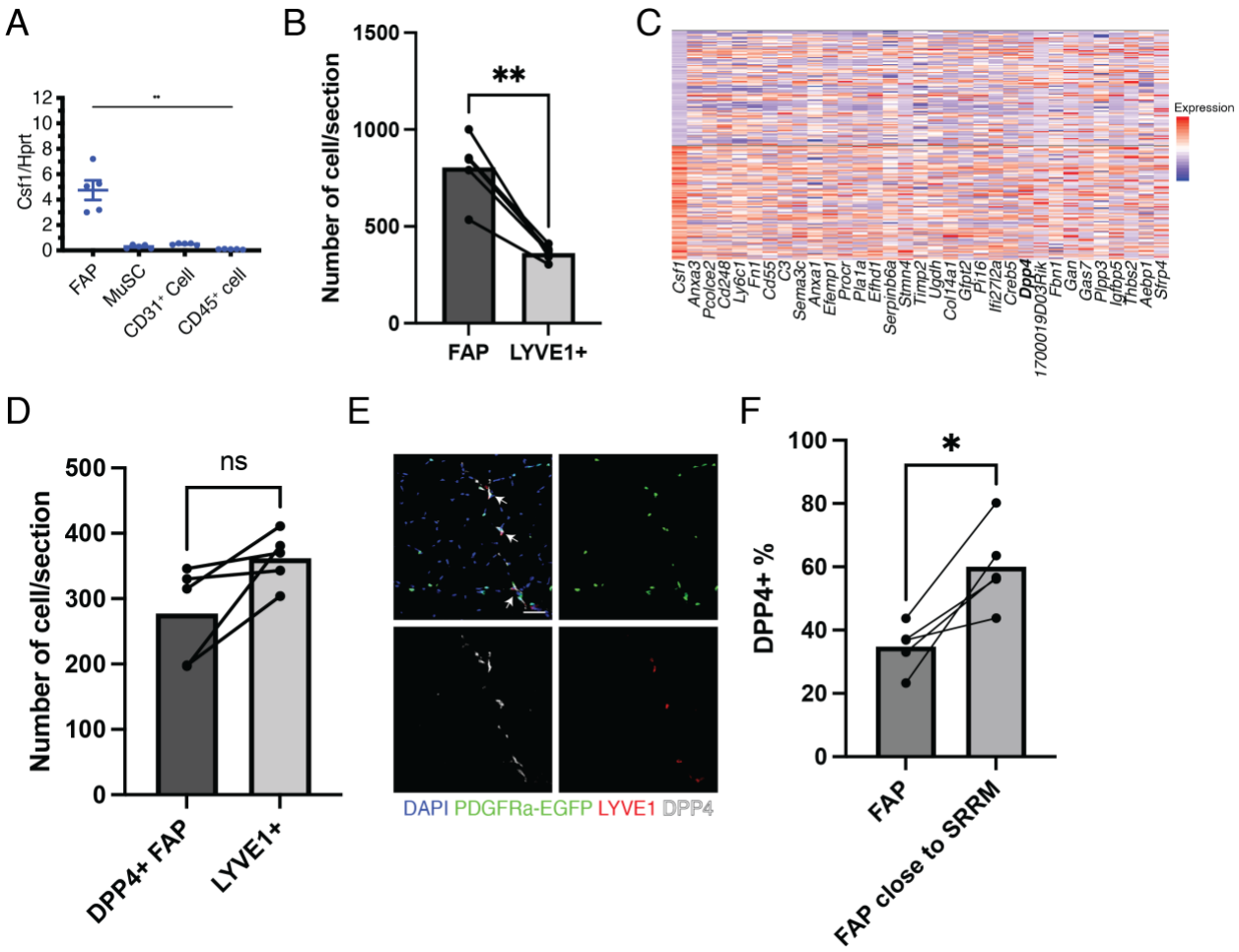
A
Csf1/Hprt
FAP
MuSC
CD31+ Cell
CD45+ cell
B
Number of cell/section
FAP
LYVE1+
C
Expression
Csf1
Anxa3
Pcolce2
Cd248
Ly6c1
Fn1
Cd55
C3
Sema3c
Anxa1
Efemp1
Procr
Pla1a
Efhd1
Serpinb6a
Stmn4
Timp2
Ugdh
Col14a1
Gfpt2
P116
Ifi27l2a
Creb5
Dpp4
1700019D03Rik
Fbn1
Gan
Gas7
Pipp3
Igfbp5
Thbs2
Aebp1
Sfrp4
D
Number of cell/section
ns
DPP4+ FAP
LYVE1+
E
DAPI PDGFRa-EGFP LYVE1 DPP4
F
DPP4+ %
FAP
FAP close to SRRM

Figure 3.7 DPP4$^+$ FAPs form the niche of skeletal muscle self-renewing macrophages

(A) Expression of *Csf1* in different muscle resident cell populations assessed by droplet digital PCR (n = 8 mice for FAPs, n = 5 mice for the other populations, Brown-Forsythe and Welch ANOVA tests). ** $P < 0.01$. Adapted from *Dissecting the role of innate immunity in muscle regeneration* (Babaeijandaghi, 2021).

(B) The number of LYVE1$^+$ SRRMs and PDGFRa-EGFP$^+$ FAPs in TA muscle sections. N = 5. ** $P < 0.01$ (paired t-test).

(C) Heatmap showing upregulated differentially expressed genes in *Csf1* expressing FAPs. Adapted from *Dissecting the role of innate immunity in muscle regeneration* (Babaeijandaghi, 2021).

(D) The number of LYVE1$^+$ SRRMs and PDGFRα-EGFP$^+$/DPP4$^+$ FAPs in TA muscle sections. N = 5. N.s.: not significant (paired t-test).

(E) Immunofluorescence staining of LYVE1$^+$ SRRMs and PDGFRa-EGFP$^+$/DPP4$^+$ FAPs in TA sections. Scale bar: 50 μm.

(F) Quantification of the percentage of DPP4$^+$ cells among all FAPs (PDGFRa-EGFP$^+$) or among PDGFRa-EGFP$^+$ FAPs with LYVE1$^+$ SRRMs in close vicinity. N = 5. * $P < 0.05$ (paired t-test).

3.8 DPP4CreERT2-DTA transgenic mouse model revealed the necessity DPP4$^+$ cells

We last attempted to understand the role of DPP4$^+$ FAPs in muscle regeneration by taking advantage of a newly developed DPP4^{CreERT2} transgenic mouse model (Figure 8A) (Stefkovich et al., 2021). We introduced the diphtheria toxin fragment A (DTA) transgene into their genome under the control of Rosa26 locus. Upon Cre induction, the floxed-STOP cassette is excised and will result in DTA expression in Cre-expressing cell, leading to a specific ablation of that cell type (Figure 8B). Indeed, 14 days after tamoxifen induction, we observed a lower proportion of DPP4$^+$ FAPs (20.2% vs. 45% in wildtype animals) in steady state skeletal muscle, suggesting the ablation strategy effectively eliminated DPP4-expressing cell (Figure 8C). We next moved on to test if DPP4$^+$ FAPs ablation would have any effect on muscle regeneration by comparing injured mice between control and ablated group 14 days after injury (Figure 8D). However, we observed massive weight loss in all mice with DPP4$^+$ cells depleted compared with the wildtype littermates (Figure 8E-F), which required us to euthanize most of the mice in compliance to the animal ethics protocol. Nonetheless, this experiment strongly suggests an absolute necessity of DPP4$^+$ cells in vital functions.

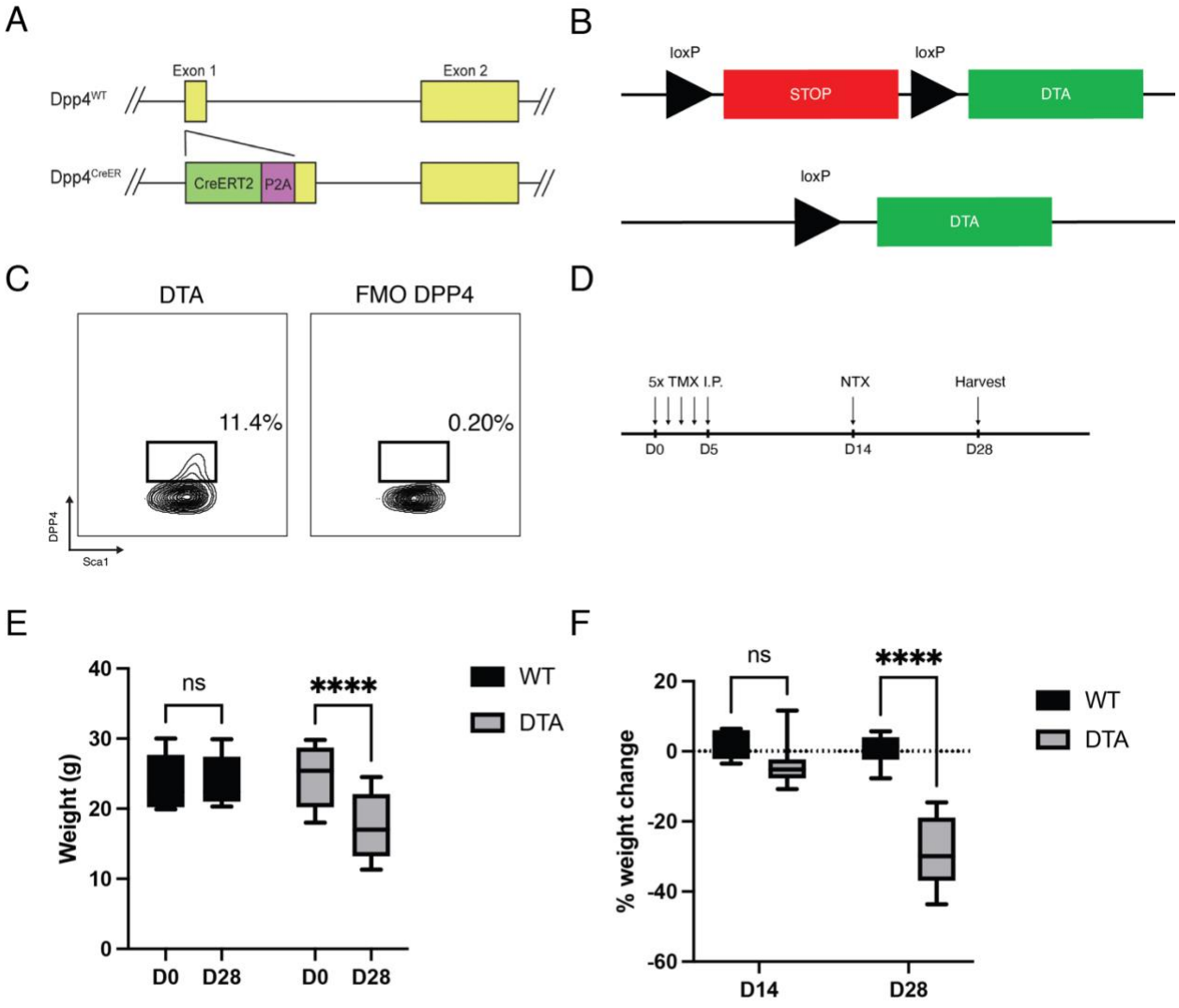
A
Exon 1
Exon 2
Dpp4WT
Dpp4CreER
CreERT2
P2A
B
loxP
STOP
loxP
DTA
loxP
DTA
C
DTA
FMO DPP4
11.4%
0.20%
DPP4
Sca1
D
5x TMX I.P.
NTX
Harvest
D0
D5
D14
D28
E
ns
****
WT
DTA
Weight (g)
40
30
20
10
0
D0
D28
D0
D28
F
ns
****
WT
DTA
% weight change
20
0
-20
-40
-60
D14
D28

Figure 3.8 DPP4CreERT2-DTA transgenic mouse model revealed the necessity DPP4$^+$ cells

(A) Schematic of DPP4-CreERT2 mouse line. Adapted from *Dpp4+ interstitial progenitor cells contribute to basal and high fat diet-induced adipogenesis* (Stefkovich et al., 2021).

(B) Schematics of DPP4-CreERT2 driven DTA expression.

(C) Representative flow cytometry analysis of DPP4-expressing cells depletion efficiency. Left: Tamoxifen-treated DPP4CreERT2-DTA mouse. Right: FMO control for DPP4 staining of the same mouse. N = 2.

(D) Experimental scheme. Mice received one dose of tamoxifen IP per day for 5 consecutive days, waited for 10 days for wash out before injuring the left TA with notexin. Mice were harvested 14 days post injury, which is 28 after the first dose of tamoxifen injection.

(E) Weight of WT and DTA mice before tamoxifen induction (D0) and at experimental endpoint (28 days after induction, 14 days after notexin injury). N = 16 for WT and N = 14 for DTA group. N.s.: not significant. **** $P < 0.0001$ (RM two-way ANOVA with Šidák's multiple comparison test). Box-and-whisker plot indicates the maximum and the minimum value of the data.

(F) Percentage weight change of WT and DTA mouse before notexin injury (D14) and 14 days after injury (D28, refer to Fig. 8C for time point indication) compared to pre-tamoxifen induction. N = 7-16. N.s.: not significant. **** $P < 0.0001$ (Mixed-effects analysis with Šidák's multiple comparison test). Box-and-whisker plot indicates the maximum and the minimum value of the data.

	259C5_NEG	259C6_NEG	259C7_NEG	259C5_POS	259C6_POS	259C7_POS
Dpp4	9.68741993	9.61301242	9.31684118	12.2729328	11.9986082	11.7338898
Pi16	14.5667058	14.6001536	14.963559	16.1796839	16.6088748	16.4869574
Cd55	10.8838178	10.8788044	10.7615217	11.8565849	11.5492942	11.475223
Cxcl14	14.9023299	14.9747161	14.9353086	13.4808971	13.8064402	13.7676886
Mme	10.5924634	10.3027178	10.0508912	9.6198616	9.10812381	8.77035611
Ly6a	14.1687915	14.230836	14.2956653	14.5970553	14.8385468	14.7684231
Pdgfra	14.6884146	14.5315444	14.4977642	14.5660561	14.2389542	14.1822753

Table 3.1 DESeq2 normalized expression level of selected genes from bulk RNA sequencing

	baseMean	log2FoldChange	lfcSE	stat	pvalue	padj
Dpp4	3370.27788	4.19171412	0.26573779	15.7738728	4.71E-56	2.50E-53
Pi16	68967.4973	2.73942938	0.23974883	11.4262469	3.09E-30	4.94E-28
Cd55	2639.10677	1.30344374	0.18492208	7.0486106	1.81E-12	7.15E-11
Cxcl14	24643.0939	-1.981299	0.17448082	-11.355397	6.97E-30	1.08E-27
Mme	1058.70057	-1.9010169	0.3799435	-5.00342	5.63E-07	1.02E-05
Ly6a	23746.7878	0.8021741	0.14056522	5.70677495	1.15E-08	2.75E-07
Pdgfra	22767.1202	-0.3680057	0.19259462	-1.9107787	0.05603303	0.19531226

Table 3.2 Differential expression analysis of selected genes by DESeq2

Chapter 4: Discussion

Emerging evidence from single cell studies in recent years continued to reveal the intrinsic heterogeneity within muscle FAPs. However, it is not known whether or not those subsets mostly arisen from performing unsupervised clustering and dimensionality reduction, are identifiable by current techniques, let alone if they possess any biological relevance. Here, we described and characterized a new subpopulation of muscle-resident fibroadipogenic progenitors labelled by DPP4 expression. By integrated analysis, we confirmed that *Dpp4*$^{+}$ FAPs from 3 different dataset that span different timepoints over the course of muscle regeneration are transcriptionally similar (Fig 1). In addition, accumulating experimental evidence from mesenchymal stromal cells in other organs, especially in heart (Soliman et al., 2020) and in fat (Merrick et al., 2019), which are defined by a very similar set of surface antigen profile in flow cytometry (CD31^{-}/CD45^{-}/Sca1^{+}) to that of muscle FAPs, could be fractionated in DPP4^{+} and DPP4^{-} populations. This significantly raised our confidence in attempting to purify this subset of cells by conventional flow cytometry and immunofluorescence staining in order to perform further characterizations. Indeed, we successfully isolated DPP4^{+} FAPs from skeletal muscles by FACS, with bulk RNA sequencing confirming that the transcriptomic profile of DPP4^{+} FAPs largely overlaps with those *Dpp4*$^{+}$ FAP subsets postulated in single cell studies (Fig 2D). Immunofluorescence staining further confirmed the existence of two distinct FAP subpopulations in skeletal muscle, and excluded the possibility of DPP4^{-} FAPs as an artifact inadvertently introduced during the enzymatic digestion for flow cytometry and FACS.

We next moved on to comprehensively characterize this new subset of DPP4^{+} FAPs via an array of biological assays. We first tested if DPP4^{+} and DPP4^{-} FAPs would possess different lineage potential by using a single cell differentiation assay. Both populations were able to

spontaneously differentiate into adipocytes and contractile myofibroblasts (Figure 3B), indicating that DPP4+/- fractionation does not alter their identity as fibroadipogenic progenitors. In the meantime, we attempted to compare the clonogenicity of $DPP4^+$ and $DPP4^-$ FAPs in the same assay. However, there could be a considerable proportion of cell culture wells that did not have a single cell deposited during FACS. Coupled with the inherent difficulty for a single cell to repopulate without the trophic support from adjacent cells, even in the presence of a feeder layer, the number of wells containing colonies outgrown from the deposited single DPP4+/- FAP remain too low (data not shown) to confidently deduce the actual frequency of colony-forming unit (CFU) in each of the population. Instead, we utilized a limiting dilution approach to assess the clonogenicity by single-hit Poisson statistics. Indeed, the number of wells containing colonies was much higher which allowed us to estimate the CFU frequency with higher statistical power. We observed that $DPP4^+$ FAPs have a higher frequency of CFU than $DPP4^-$ FAPs (Figure 4C-D), a property closely linked to the proliferation and differentiation abilities of a cell population (Rajendran & Jain, 2018). Intriguingly, $DPP4^+$ FAPs have higher expression levels of *Cd34* and *Ly6a*, two genes commonly associate with stemness in the field. In addition, we showed that $DPP4^+$ FAPs give rise to $DPP4^-$ FAPs *in vitro* (Figure 6), indicating that they have the potential to act as a progenitor population. However, whether $DPP4^+$ FAPs act as the true "stem cells" of FAPs require further study.

We then attempted to further understand the lineage potential of $DPP4^+$ FAPs. Importantly, they displayed differing propensity toward adipogenic fate when situated in a strong adipogenic induction condition, where $DPP4^+$ FAPs were able to differentiate into adipocytes at a much higher frequency than $DPP4^-$ FAPs (Fig 5D-F). This is consistent with the study conducted by Merrick and colleagues in adipose tissue, showing that $DPP4^+$ interstitial progenitors represent the source

of mature adipocytes (Merrick et al., 2019). It is worth noting that Fitzgerald *et al.* recently reported an MME^+ FAP subset which serve as the predominant contributor of fatty infiltration (Fitzgerald et al., 2023). From the transcriptomic characteristics, it appears that $DPP4^+$ FAPs and MME^+ FAPs represent two distinct sets of FAPs. In fact, it is probable that MME^+ FAPs belong to the same class of cells as $DPP4^-$ FAPs in this study, since *Cxcl14* and *Col15a1* are among two of the top upregulated genes in the subset, which are two commonly used markers to identify this particular FAP subset present in homeostasis (Oprescu et al., 2020; Scott et al., 2019). This apparent contradiction of adipogenicity of FAP subsets could be explained by two different theories. It may be that $DPP4^+$ FAPs first downregulate DPP4 and acquire MME expression, or vice versa, prior to differentiating into mature adipocytes. The second possible explanation is that $DPP4^+$ FAPs only constitute a part of MME^- FAPs, and similarly, that MME^+ FAPs only constitute a part of $DPP4^-$ FAPs. Therefore, when the adipogenic potential of $DPP4^+$ versus $DPP4^-$ FAPs were being compared, despite the presence of a pro-adipogenic MME+ FAPs population in $DPP4^-$ FAPs, other FAPs in $DPP4^-$ fraction that are less prone, or even anti-adipogenic, would result in an overall lower adipogenic phenotype. One such example is the $CD142^+$ FAPs, which are known to inhibit adipogenesis via the secretion of GDF10 that cluster differently as $Cd55^+$ cells (another upregulated gene in $DPP4^+$ FAPs). Lineage tracing with $DPP4^{CreER}$ and MME^{CreER} mouse models, or similar transgenic models that specifically labelled these two subsets, are required for definitive answer to the lineage relationship between the two FAP subsets. Similarly, while we demonstrated that $DPP4^+$ FAPs could turn into $DPP4^-$ FAPs in vitro, but not the other way around, it is not known if such lineage hierarchy is preserved *in vivo*. $DPP4^{CreER}$ mouse model-based lineage tracing, or transplantation of $DPP4^+$ and $DPP4^-$ FAPs would be necessary.

FAPs are known to play important regulatory roles in resolving muscle injury and promoting muscle regeneration. Here, we tested if DPP4^{+} FAPs would have any distinct function in the process by selective ablation of DPP4^{+} cells using the DTA system. Unfortunately, the mice behave poorly in response to the ablation as we observed massive weight loss, which forced us to end the experiment for ethical concerns. Since it is extremely unlikely that a single leg injury could have resulted in such massive weight loss, and the fact that the wildtype littermates that received the same tamoxifen treatment and injury did not display such phenotype, the weight loss can only be attributed to the depletion of DPP4-expressing cells. However, we were unable to explain the phenotype solely by the depletion of DPP4^{+} FAPs, as DPP4 is expressed by multiple cell types across organs, such as epithelial cells and endothelial cells in liver, lung, small intestine (Biftu & SinhaRoy, 2017; Wu et al., 2016). In addition, even though the weight loss in some of the DPP4^{+} cells-depleted mice is within tolerance, we reasoned that the displayed regenerative defects, if any, could not be deconvolved from their poor health condition. Nevertheless, we could still conclude that DPP4-expressing cells have indispensable roles in maintaining the physical well-being of the animal. In order to alleviate the effect of global DPP4^{+} cells ablation, we could employ a local depletion approach by surgically implanting a scaffold infused with endoxifen, an active tamoxifen metabolite, on top of the TA muscle (Kajabadi et al., 2023; Wosczyna et al., 2019). The scaffold would limit the scope of DTA ablation to only the tissue adjacent to the implanted area, thus avoiding the weight loss associated with global DPP4^{+} cell depletion. This would also enable us to precisely define the role of DPP4^{+} cells in skeletal muscle in regeneration.

We also reported an unexpected role for DPP4^{+} FAPs as the niche for SRRMs. As we were characterizing the recently discovered SRRMs in skeletal muscle, we found that CSF1 plays an important role in mediating their survival and activity (Babaeijandaghi, Cheng, et al., 2022).

Importantly, when we examined the cellular source of CSF1 in skeletal muscle, FAPs appeared to be the only cell population that can produce CSF1 (Fig 7A), which suggests that FAPs might form part of the niche of SRRMs to regulate their functions. As we further analyzed the transcriptomic profiles of *Csf1*-expressing FAPs, to our surprise, *Dpp4*, among several other commonly used signatures for the DPP4$^+$ FAP subset (such as *Pi16* and *Cd55*) (Fig 7C), was found to be enriched. Immunofluorescence staining revealed that DPP4$^+$ FAPs and LYVE1$^+$ SRRMs frequently locate in close proximity (Fig 7E). We found that the percentage of FAPs that are close to LYVE1$^+$ SRRMs expresses DPP4 is significantly higher than the occurrence of DPP4$^+$ cells among all FAPs (Fig 7F). This could be explained by the hypothesis that DPP4$^+$ FAPs must be involved in regulating the function of SRRMs in a paracrine manner (Fig 7F). This is because, if we hypothesize that DPP4$^+$ FAPs do not have any specific role on SRRMs, the frequency of FAPs located next to SRRMs being DPP4-positive, should be the same as the frequency of DPP4$^+$ FAPs among all FAPs (i.e. the implied null hypothesis when we performed the statistical test), which is being rejected. Hence, we concluded that DPP4$^+$ FAPs are likely to be a niche component for SRRMs. However, beyond CSF1, the exact signaling mechanisms on how DPP4$^+$ FAPs regulate SRRMs activity will require further examination.

It is worth mentioning that we only investigated the behavior of DPP4$^+$ FAPs from healthy mice. Different disease conditions are known to modify FAP numbers, activity, and proportion of different subsets (Camps et al., 2020; Farup et al., 2021; Malecova et al., 2018; Uezumi et al., 2011). It is therefore of great importance to test if the proportion of DPP4$^+$ and DPP4$^-$ FAPs, and their cellular activity, are altered in mdx mice, a widely used mouse model for DMD. In particular, given the known propensity of adipogenic differentiation of DPP4$^+$ FAPs from the *in vitro* data, it would be interesting to test if they are the source of ectopic fat in chronically injured skeletal

muscle, and if modulating their behavior could limit fatty infiltration. This could shed light on a potential therapy to mitigate muscle wasting by blocking fatty infiltration from the source (i.e. $DPP4^+$ FAPs).

It is notable that DPP4 is a proteolytic enzyme and participates in numerous signaling pathways. We did not address the role of DPP4 *per se* in $DPP4^+$ FAPs in this thesis, rather we simply consider it as a cell surface marker which allow us to isolate this subset of cells. It will be interesting to test if modulating DPP4 enzymatic activity would have any effect on $DPP4^+$ FAPs. An attractive candidate that could be implicated in the regeneration process is SDF1α, as it contains DPP4 cleavage site, has well-known function of mediating stem cell migration/recruitment through CXCR4-SDF1α axis, and its involvement in cardiac disease has been demonstrated (Batchu et al., 2018; Christopherson et al., 2002; Zaruba et al., 2009; Zhong & Rajagopalan, 2015). However, this hypothesis, alongside with hundreds of substrates that contain DPP4 cleavage sites (Boonacker & Van Noorden, 2003), remain to be experimentally tested. However, an exciting fact is that DPP4 inhibitor sitagliptin is an FDA-approved anti-diabetic drug widely available (Ahrén, 2019). Given its well-studied safety profile, it would be thrilling if we could repurpose the drug to attenuate hypothetical detrimental effects associated with DPP4 enzymatic activity in FAPs.

Together, this thesis provided a comprehensive characterization on a subset of fibroadipogenic progenitors in skeletal muscle labelled by DPP4 expression.

Bibliography

Acharyya, S., Sharma, S. M., Cheng, A. S., Ladner, K. J., He, W., Kline, W., Wang, H., Ostrowski, M. C., Huang, T. H., & Guttridge, D. C. (2010). TNF inhibits Notch-1 in skeletal muscle cells by Ezh2 and DNA methylation mediated repression: implications in duchenne muscular dystrophy. *PloS One*, *5*(8), e12479. https://doi.org/10.1371/journal.pone.0012479

Ahrén, B. (2019). DPP-4 Inhibition and the Path to Clinical Proof. *Frontiers in Endocrinology*, *10*. https://doi.org/10.3389/fendo.2019.00376

Alexander, K. A., Tseng, H.-W., Fleming, W., Jose, B., Salga, M., Kulina, I., Millard, S. M., Pettit, A. R., Genêt, F., & Levesque, J.-P. (2019). Inhibition of JAK1/2 Tyrosine Kinases Reduces Neurogenic Heterotopic Ossification After Spinal Cord Injury. *Frontiers in Immunology*, *10*, 377. https://doi.org/10.3389/fimmu.2019.00377

Almanzar, N., Antony, J., Baghel, A. S., Bakerman, I., Bansal, I., Barres, B. A., Beachy, P. A., Berdnik, D., Bilen, B., Brownfield, D., Cain, C., Chan, C. K. F. F., Chen, M. B., Clarke, M. F., Conley, S. D., Darmanis, S., Demers, A., Demir, K., de Morree, A., … Zou, J. (2020). A single-cell transcriptomic atlas characterizes ageing tissues in the mouse. *Nature*, *583*(7817), 590–595. https://doi.org/10.1038/s41586-020-2496-1

Amar, E., Sharfman, Z. T., & Rath, E. (2015). Heterotopic ossification after hip arthroscopy. *Journal of Hip Preservation Surgery*, *2*(4), 355–363. https://doi.org/10.1093/jhps/hnv052

Arrighi, N., Moratal, C., Clément, N., Giorgetti-Peraldi, S., Peraldi, P., Loubat, A., Kurzenne, J.-Y., Dani, C., Chopard, A., & Dechesne, C. A. (2015). Characterization of adipocytes derived from fibro/adipogenic progenitors resident in human skeletal muscle. *Cell Death & Disease*, *6*(4), e1733–e1733. https://doi.org/10.1038/cddis.2015.79

Au, Y. (2004). The muscle ultrastructure: a structural perspective of the sarcomere. *Cellular and Molecular Life Sciences*, *61*(24), 3016–3033. https://doi.org/10.1007/s00018-004-4282-x

Babaeijandaghi, F. (2021). *Dissecting the role of innate immunity in muscle regeneration* [University of British Columbia]. https://doi.org/10.14288/1.0401494

Babaeijandaghi, F., Cheng, R., Kajabadi, N., Soliman, H., Chang, C.-K., Smandych, J., Tung, L. W., Long, R., Ghassemi, A., & Rossi, F. M. V. (2022). Metabolic reprogramming of skeletal muscle by resident macrophages points to CSF1R inhibitors as muscular dystrophy therapeutics. *Science Translational Medicine*, *14*(651). https://doi.org/10.1126/scitranslmed.abg7504

Babaeijandaghi, F., Paiero, A., Long, R., Tung, L. W., Smith, S. P., Cheng, R., Smandych, J., Kajabadi, N., Chang, C.-K., Ghassemi, A., Kennedy, W. D. M., Soliman, H., Schutz, P. W., & Rossi, F. M. V. (2022). TNFα and IFNγ cooperate for efficient pro- to anti-inflammatory transition of macrophages during muscle regeneration. *Proceedings of the National Academy of Sciences of the United States of America*, *119*(44), e2209976119. https://doi.org/10.1073/pnas.2209976119

Bansal, D., Miyake, K., Vogel, S. S., Groh, S., Chen, C.-C., Williamson, R., McNeil, P. L., & Campbell, K. P. (2003). Defective membrane repair in dysferlin-deficient muscular dystrophy. *Nature*, *423*(6936), 168–172. https://doi.org/10.1038/nature01573

Bashir, R., Britton, S., Strachan, T., Keers, S., Vafiadaki, E., Lako, M., Richard, I., Marchand, S., Bourg, N., Argov, Z., Sadeh, M., Mahjneh, I., Marconi, G., Passos-Bueno, M. R., Moreira, E. de S., Zatz, M., Beckmann, J. S., & Bushby, K. (1998). A gene related to Caenorhabditis elegans spermatogenesis factor fer-1 is mutated in limb-girdle muscular dystrophy type 2B. *Nature Genetics*, *20*(1), 37–42. https://doi.org/10.1038/1689

Batchu, S. N., Thieme, K., Zadeh, F. H., Alghamdi, T. A., Yerra, V. G., Hadden, M. J., Majumder, S., Kabir, M. G., Bowskill, B. B., Ladha, D., Gramolini, A. O., Connelly, K. A., & Advani, A. (2018). The Dipeptidyl Peptidase 4 Substrate CXCL12 Has Opposing Cardiac Effects in Young Mice and Aged Diabetic Mice Mediated by Ca2+ Flux and Phosphoinositide 3-Kinase γ. *Diabetes*, *67*(11), 2443–2455. https://doi.org/10.2337/db18-0410

Berria, R., Wang, L., Richardson, D. K., Finlayson, J., Belfort, R., Pratipanawatr, T., De Filippis, E. A., Kashyap, S., & Mandarino, L. J. (2006). Increased collagen content in insulin-resistant skeletal muscle. *American Journal of Physiology-Endocrinology and Metabolism*, *290*(3), E560–E565. https://doi.org/10.1152/ajpendo.00202.2005

Bi, P., Ramirez-Martinez, A., Li, H., Cannavino, J., McAnally, J. R., Shelton, J. M., Sánchez-Ortiz, E., Bassel-Duby, R., & Olson, E. N. (2017). Control of muscle formation by the fusogenic micropeptide myomixer. *Science*, *356*(6335), 323–327. https://doi.org/10.1126/science.aam9361

Biftu, T., & SinhaRoy, R. (2017). DPP-4 Inhibitors. In *Comprehensive Medicinal Chemistry III* (pp. 512–555). Elsevier. https://doi.org/10.1016/B978-0-12-409547-2.12443-6

Biga, L. M., Dawson, S., Harwell, A., Hopkins, R., Kaufmann, J., LeMaster, M., Matern, P., Morrison-Graham, K., Quick, D., & Runyeon, J. (2020). *Anatomy & physiology*. OpenStax/Oregon State University.

Bodine, S. C., Stitt, T. N., Gonzalez, M., Kline, W. O., Stover, G. L., Bauerlein, R., Zlotchenko, E., Scrimgeour, A., Lawrence, J. C., Glass, D. J., & Yancopoulos, G. D. (2001). Akt/mTOR pathway is a crucial regulator of skeletal muscle hypertrophy and can prevent muscle atrophy in vivo. *Nature Cell Biology*, *3*(11), 1014–1019. https://doi.org/10.1038/ncb1101-

1014

Boonacker, E., & Van Noorden, C. J. F. F. (2003). The multifunctional or moonlighting protein CD26/DPPIV. *European Journal of Cell Biology*, *82*(2), 53–73. https://doi.org/10.1078/0171-9335-00302

Bosnakovski, D., Gearhart, M. D., Toso, E. A., Ener, E. T., Choi, S. H., & Kyba, M. (2018). Low level DUX4 expression disrupts myogenesis through deregulation of myogenic gene expression. *Scientific Reports*, *8*(1), 16957. https://doi.org/10.1038/s41598-018-35150-8

Bosnakovski, D., Shams, A. S., Yuan, C., da Silva, M. T., Ener, E. T., Baumann, C. W., Lindsay, A. J., Verma, M., Asakura, A., Lowe, D. A., & Kyba, M. (2020). Transcriptional and cytopathological hallmarks of FSHD in chronic DUX4-expressing mice. *Journal of Clinical Investigation*, *130*(5), 2465–2477. https://doi.org/10.1172/JCI133303

Buechler, M. B., Pradhan, R. N., Krishnamurty, A. T., Cox, C., Calviello, A. K., Wang, A. W., Yang, Y. A., Tam, L., Caothien, R., Roose-Girma, M., Modrusan, Z., Arron, J. R., Bourgon, R., Müller, S., & Turley, S. J. (2021). Cross-tissue organization of the fibroblast lineage. *Nature*, *593*(7860), 575–579. https://doi.org/10.1038/s41586-021-03549-5

Buras, E. D., Converso-Baran, K., Davis, C. S., Akama, T., Hikage, F., Michele, D. E., Brooks, S. V., & Chun, T.-H. (2019). Fibro-Adipogenic Remodeling of the Diaphragm in Obesity-Associated Respiratory Dysfunction. *Diabetes*, *68*(1), 45–56. https://doi.org/10.2337/db18-0209

Burzyn, D., Kuswanto, W., Kolodin, D., Shadrach, J. L., Cerletti, M., Jang, Y., Sefik, E., Tan, T. G., Wagers, A. J., Benoist, C., & Mathis, D. (2013). A Special Population of Regulatory T Cells Potentiates Muscle Repair. *Cell*, *155*(6), 1282–1295. https://doi.org/10.1016/j.cell.2013.10.054

Camps, J., Breuls, N., Sifrim, A., Giarratana, N., Corvelyn, M., Danti, L., Grosemans, H., Vanuytven, S., Thiry, I., Belicchi, M., Meregalli, M., Platko, K., MacDonald, M. E., Austin, R. C., Gijsbers, R., Cossu, G., Torrente, Y., Voet, T., & Sampaolesi, M. (2020). Interstitial Cell Remodeling Promotes Aberrant Adipogenesis in Dystrophic Muscles. *Cell Reports*, *31*(5), 107597. https://doi.org/10.1016/j.celrep.2020.107597

Chang, N. C., Chevalier, F. P., & Rudnicki, M. A. (2016). Satellite Cells in Muscular Dystrophy – Lost in Polarity. *Trends in Molecular Medicine*, *22*(6), 479–496. https://doi.org/10.1016/j.molmed.2016.04.002

Cheung, T. H., & Rando, T. A. (2013). Molecular regulation of stem cell quiescence. *Nature Reviews Molecular Cell Biology*, *14*(6), 329–340. https://doi.org/10.1038/nrm3591

Chooi, Y. C., Ding, C., & Magkos, F. (2019). The epidemiology of obesity. *Metabolism*, *92*, 6–10. https://doi.org/10.1016/j.metabol.2018.09.005

Christopherson, K. W., Hangoc, G., & Broxmeyer, H. E. (2002). Cell Surface Peptidase CD26/Dipeptidylpeptidase IV Regulates CXCL12/Stromal Cell-Derived Factor-1α-Mediated Chemotaxis of Human Cord Blood CD34 + Progenitor Cells . *The Journal of Immunology*, *169*(12), 7000–7008. https://doi.org/10.4049/jimmunol.169.12.7000

Christopherson, K. W., Hangoc, G., Mantel, C. R., & Broxmeyer, H. E. (2004). Modulation of hematopoietic stem cell homing and engraftment by CD26. *Science*, *305*(5686), 1000–1003. https://doi.org/10.1126/science.1097071

Collins, C. A., Olsen, I., Zammit, P. S., Heslop, L., Petrie, A., Partridge, T. A., & Morgan, J. E. (2005). Stem cell function, self-renewal, and behavioral heterogeneity of cells from the adult muscle satellite cell niche. *Cell*, *122*(2), 289–301. https://doi.org/10.1016/j.cell.2005.05.010

Consalvi, S., Tucciarone, L., Macrì, E., De Bardi, M., Picozza, M., Salvatori, I., Renzini, A., Valente, S., Mai, A., Moresi, V., & Puri, P. L. (2022). Determinants of epigenetic resistance to HDAC inhibitors in dystrophic fibro-adipogenic progenitors. *EMBO Reports*, *23*(6). https://doi.org/10.15252/embr.202254721

Contreras, O., Rebolledo, D. L., Oyarzún, J. E., Olguín, H. C., & Brandan, E. (2016). Connective tissue cells expressing fibro/adipogenic progenitor markers increase under chronic damage: relevance in fibroblast-myofibroblast differentiation and skeletal muscle fibrosis. *Cell and Tissue Research*, *364*(3), 647–660. https://doi.org/10.1007/s00441-015-2343-0

Contreras, O., Rossi, F. M. V., & Theret, M. (2021). Origins, potency, and heterogeneity of skeletal muscle fibro-adipogenic progenitors—time for new definitions. *Skeletal Muscle*, *11*(1), 16. https://doi.org/10.1186/s13395-021-00265-6

Cordani, N., Pisa, V., Pozzi, L., Sciorati, C., & Clementi, E. (2014). Nitric Oxide Controls Fat Deposition in Dystrophic Skeletal Muscle by Regulating Fibro-Adipogenic Precursor Differentiation. *Stem Cells*, *32*(4), 874–885. https://doi.org/10.1002/stem.1587

Cornelison, D. D., Olwin, B. B., Rudnicki, M. A., & Wold, B. J. (2000). MyoD(-/-) satellite cells in single-fiber culture are differentiation defective and MRF4 deficient. *Developmental Biology*, *224*(2), 122–137. https://doi.org/10.1006/dbio.2000.9682

Davie, J. K., Cho, J.-H., Meadows, E., Flynn, J. M., Knapp, J. R., & Klein, W. H. (2007). Target gene selectivity of the myogenic basic helix-loop-helix transcription factor myogenin in embryonic muscle. *Developmental Biology*, *311*(2), 650–664. https://doi.org/10.1016/j.ydbio.2007.08.014

Davis, R. L., Weintraub, H., & Lassar, A. B. (1987). Expression of a single transfected cDNA converts fibroblasts to myoblasts. *Cell*, *51*(6), 987–1000. https://doi.org/10.1016/0092-

8674(87)90585-x

De Micheli, A. J., Laurilliard, E. J., Heinke, C. L., Ravichandran, H., Fraczek, P., Soueid-Baumgarten, S., De Vlaminck, I., Elemento, O., & Cosgrove, B. D. (2020). Single-Cell Analysis of the Muscle Stem Cell Hierarchy Identifies Heterotypic Communication Signals Involved in Skeletal Muscle Regeneration. *Cell Reports*, *30*(10), 3583-3595.e5. https://doi.org/10.1016/j.celrep.2020.02.067

De Micheli, A. J., Spector, J. A., Elemento, O., & Cosgrove, B. D. (2020). A reference single-cell transcriptomic atlas of human skeletal muscle tissue reveals bifurcated muscle stem cell populations. *Skeletal Muscle*, *10*(1), 19. https://doi.org/10.1186/s13395-020-00236-3

Deng, B., Wehling-Henricks, M., Villalta, S. A., Wang, Y., & Tidball, J. G. (2012). IL-10 triggers changes in macrophage phenotype that promote muscle growth and regeneration. *Journal of Immunology (Baltimore, Md. : 1950)*, *189*(7), 3669–3680. https://doi.org/10.4049/jimmunol.1103180

Dey, D., Bagarova, J., Hatsell, S. J., Armstrong, K. A., Huang, L., Ermann, J., Vonner, A. J., Shen, Y., Mohedas, A. H., Lee, A., Eekhoff, E. M. W., van Schie, A., Demay, M. B., Keller, C., Wagers, A. J., Economides, A. N., & Yu, P. B. (2016). Two tissue-resident progenitor lineages drive distinct phenotypes of heterotopic ossification. *Science Translational Medicine*, *8*(366), 366ra163. https://doi.org/10.1126/scitranslmed.aaf1090

Di Pietro, L., Giacalone, F., Ragozzino, E., Saccone, V., Tiberio, F., De Bardi, M., Picozza, M., Borsellino, G., Lattanzi, W., Guadagni, E., Bortolani, S., Tasca, G., Ricci, E., & Parolini, O. (2022). Non-myogenic mesenchymal cells contribute to muscle degeneration in facioscapulohumeral muscular dystrophy patients. *Cell Death & Disease*, *13*(9), 793. https://doi.org/10.1038/s41419-022-05233-6

DiMario, J., Buffinger, N., Yamada, S., & Strohman, R. C. (1989). Fibroblast growth factor in the extracellular matrix of dystrophic (mdx) mouse muscle. *Science (New York, N.Y.)*, *244*(4905), 688–690. https://doi.org/10.1126/science.2717945

Dong, H., Sun, W., Shen, Y., Baláz, M., Balázová, L., Ding, L., Löffler, M., Hamilton, B., Klöting, N., Blüher, M., Neubauer, H., Klein, H., & Wolfrum, C. (2022). Identification of a regulatory pathway inhibiting adipogenesis via RSPO2. *Nature Metabolism*, *4*(1), 90–105. https://doi.org/10.1038/s42255-021-00509-1

Dong, R. P., Kameoka, J., Hegen, M., Tanaka, T., Xu, Y., Schlossman, S. F., & Morimoto, C. (1996). Characterization of adenosine deaminase binding to human CD26 on T cells and its biologic role in immune response. *Journal of Immunology (Baltimore, Md. : 1950)*, *156*(4), 1349–1355. http://www.ncbi.nlm.nih.gov/pubmed/8568233

Dowling, J. J., Weihl, C. C., & Spencer, M. J. (2021). Molecular and cellular basis of genetically inherited skeletal muscle disorders. *Nature Reviews Molecular Cell Biology*, *22*(11), 713–732. https://doi.org/10.1038/s41580-021-00389-z

Dulauroy, S., Di Carlo, S. E., Langa, F., Eberl, G., & Peduto, L. (2012). Lineage tracing and genetic ablation of ADAM12+ perivascular cells identify a major source of profibrotic cells during acute tissue injury. *Nature Medicine*, *18*(8), 1262–1270. https://doi.org/10.1038/nm.2848

Dumont, N. A., Bentzinger, C. F., Sincennes, M. C., & Rudnicki, M. A. (2015). Satellite Cells and Skeletal Muscle Regeneration. In *Comprehensive Physiology* (Vol. 5, Issue 3, pp. 1027–1059). Wiley. https://doi.org/10.1002/cphy.c140068

Eisner, C., Cummings, M., Johnston, G., Tung, L. W., Groppa, E., Chang, C., & Rossi, F. M. M. V. (2020). Murine Tissue-Resident PDGFRα+ Fibro-Adipogenic Progenitors

Spontaneously Acquire Osteogenic Phenotype in an Altered Inflammatory Environment. *Journal of Bone and Mineral Research : The Official Journal of the American Society for Bone and Mineral Research*, *35*(8), 1525–1534. https://doi.org/10.1002/jbmr.4020

Erbay, E., Park, I.-H., Nuzzi, P. D., Schoenherr, C. J., & Chen, J. (2003). IGF-II transcription in skeletal myogenesis is controlled by mTOR and nutrients. *The Journal of Cell Biology*, *163*(5), 931–936. https://doi.org/10.1083/jcb.200307158

Farup, J., Just, J., de Paoli, F., Lin, L., Jensen, J. B., Billeskov, T., Roman, I. S., Cömert, C., Møller, A. B., Madaro, L., Groppa, E., Fred, R. G., Kampmann, U., Gormsen, L. C., Pedersen, S. B., Bross, P., Stevnsner, T., Eldrup, N., Pers, T. H., … Jessen, N. (2021). Human skeletal muscle CD90+ fibro-adipogenic progenitors are associated with muscle degeneration in type 2 diabetic patients. *Cell Metabolism*, *33*(11), 2201-2214.e10. https://doi.org/10.1016/j.cmet.2021.10.001

Fernández-Eulate, G., Querin, G., Moore, U., Behin, A., Masingue, M., Bassez, G., Leonard-Louis, S., Laforêt, P., Maisonobe, T., Merle, P., Spinazzi, M., Solé, G., Kuntzer, T., Bedat-Millet, A., Salort-Campana, E., Attarian, S., Péréon, Y., Feasson, L., Graveleau, J., … Stojkovic, T. (2021). Deep phenotyping of an international series of patients with late-onset dysferlinopathy. *European Journal of Neurology*, *28*(6), 2092–2102. https://doi.org/10.1111/ene.14821

Fiore, D., Judson, R. N., Low, M., Lee, S., Zhang, E., Hopkins, C., Xu, P., Lenzi, A., Rossi, F. M. V., & Lemos, D. R. (2016). Pharmacological blockage of fibro/adipogenic progenitor expansion and suppression of regenerative fibrogenesis is associated with impaired skeletal muscle regeneration. *Stem Cell Research*, *17*(1), 161–169. https://doi.org/10.1016/j.scr.2016.06.007

Fitzgerald, G., Turiel, G., Gorski, T., Soro-Arnaiz, I., Zhang, J., Casartelli, N. C., Masschelein, E., Maffiuletti, N. A., Sutter, R., Leunig, M., Farup, J., & De Bock, K. (2023). MME+ fibro-adipogenic progenitors are the dominant adipogenic population during fatty infiltration in human skeletal muscle. *Communications Biology*, *6*(1), 111. https://doi.org/10.1038/s42003-023-04504-y

Forouhi, N. G., & Wareham, N. J. (2019). Epidemiology of diabetes. *Medicine*, *47*(1), 22–27. https://doi.org/10.1016/j.mpmed.2018.10.004

Genêt, F., Kulina, I., Vaquette, C., Torossian, F., Millard, S., Pettit, A. R., Sims, N. A., Anginot, A., Guerton, B., Winkler, I. G., Barbier, V., Lataillade, J.-J., Le Bousse-Kerdilès, M.-C., Hutmacher, D. W., & Levesque, J.-P. (2015). Neurological heterotopic ossification following spinal cord injury is triggered by macrophage-mediated inflammation in muscle. *The Journal of Pathology*, *236*(2), 229–240. https://doi.org/10.1002/path.4519

Ghorpade, D. S., Ozcan, L., Zheng, Z., Nicoloro, S. M., Shen, Y., Chen, E., Blüher, M., Czech, M. P., & Tabas, I. (2018). Hepatocyte-secreted DPP4 in obesity promotes adipose inflammation and insulin resistance. *Nature*, *555*(7698), 673–677. https://doi.org/10.1038/nature26138

Gilbert, M. P., & Pratley, R. E. (2020). GLP-1 Analogs and DPP-4 Inhibitors in Type 2 Diabetes Therapy: Review of Head-to-Head Clinical Trials. *Frontiers in Endocrinology*, *11*, 178. https://doi.org/10.3389/fendo.2020.00178

Giuliani, G., Vumbaca, S., Fuoco, C., Gargioli, C., Giorda, E., Massacci, G., Palma, A., Reggio, A., Riccio, F., Rosina, M., Vinci, M., Castagnoli, L., & Cesareni, G. (2021). SCA-1 micro-heterogeneity in the fate decision of dystrophic fibro/adipogenic progenitors. *Cell Death and Disease*, *12*(1), 1–24. https://doi.org/10.1038/s41419-021-03408-1

Golani, G., Leikina, E., Melikov, K., Whitlock, J. M., Gamage, D. G., Luoma-Overstreet, G., Millay, D. P., Kozlov, M. M., & Chernomordik, L. V. (2021). Myomerger promotes fusion pore by elastic coupling between proximal membrane leaflets and hemifusion diaphragm. *Nature Communications*, *12*(1), 495. https://doi.org/10.1038/s41467-020-20804-x

Goodpaster, B. H., & Wolf, D. (2004). Skeletal muscle lipid accumulation in obesity, insulin resistance, and type 2 diabetes. *Pediatric Diabetes*, *5*(4), 219–226. https://doi.org/10.1111/j.1399-543X.2004.00071.x

Grounds, M. D., Terrill, J. R., Radley-Crabb, H. G., Robertson, T., Papadimitriou, J., Spuler, S., & Shavlakadze, T. (2014). Lipid Accumulation in Dysferlin-Deficient Muscles. *The American Journal of Pathology*, *184*(6), 1668–1676. https://doi.org/10.1016/j.ajpath.2014.02.005

Hafemeister, C., & Satija, R. (2019). Normalization and variance stabilization of single-cell RNA-seq data using regularized negative binomial regression. *Genome Biology*, *20*(1), 296. https://doi.org/10.1186/s13059-019-1874-1

Halevy, O., Novitch, B. G., Spicer, D. B., Skapek, S. X., Rhee, J., Hannon, G. J., Beach, D., & Lassar, A. B. (1995). Correlation of terminal cell cycle arrest of skeletal muscle with induction of p21 by MyoD. *Science (New York, N.Y.)*, *267*(5200), 1018–1021. https://doi.org/10.1126/science.7863327

Hao, Y., Hao, S., Andersen-Nissen, E., Mauck, W. M., Zheng, S., Butler, A., Lee, M. J., Wilk, A. J., Darby, C., Zager, M., Hoffman, P., Stoeckius, M., Papalexi, E., Mimitou, E. P., Jain, J., Srivastava, A., Stuart, T., Fleming, L. M., Yeung, B., … Satija, R. (2021). Integrated analysis of multimodal single-cell data. *Cell*, *184*(13), 3573-3587.e29. https://doi.org/10.1016/j.cell.2021.04.048

Hatsell, S. J., Idone, V., Wolken, D. M. A., Huang, L., Kim, H. J., Wang, L., Wen, X., Nannuru, K. C., Jimenez, J., Xie, L., Das, N., Makhoul, G., Chernomorsky, R., D'Ambrosio, D., Corpina, R. A., Schoenherr, C. J., Feeley, K., Yu, P. B., Yancopoulos, G. D., … Economides, A. N. (2015). ACVR1R206H receptor mutation causes fibrodysplasia ossificans progressiva by imparting responsiveness to activin A. *Science Translational Medicine*, *7*(303), 303ra137. https://doi.org/10.1126/scitranslmed.aac4358

Heredia, J. E., Mukundan, L., Chen, F. M., Mueller, A. A., Deo, R. C., Locksley, R. M., Rando, T. A., & Chawla, A. (2013). Type 2 innate signals stimulate fibro/adipogenic progenitors to facilitate muscle regeneration. *Cell*, *153*(2), 376–388. https://doi.org/10.1016/j.cell.2013.02.053

Hogarth, M. W., Defour, A., Lazarski, C., Gallardo, E., Diaz Manera, J., Partridge, T. A., Nagaraju, K., & Jaiswal, J. K. (2019). Fibroadipogenic progenitors are responsible for muscle loss in limb girdle muscular dystrophy 2B. *Nature Communications*, *10*(1), 2430. https://doi.org/10.1038/s41467-019-10438-z

Hollenberg, S. M., Cheng, P. F., & Weintraub, H. (1993). Use of a conditional MyoD transcription factor in studies of MyoD trans-activation and muscle determination. *Proceedings of the National Academy of Sciences of the United States of America*, *90*(17), 8028–8032. https://doi.org/10.1073/pnas.90.17.8028

Hu, Y., & Smyth, G. K. (2009). ELDA: extreme limiting dilution analysis for comparing depleted and enriched populations in stem cell and other assays. *Journal of Immunological Methods*, *347*(1–2), 70–78. https://doi.org/10.1016/j.jim.2009.06.008

Huang, D. W., Sherman, B. T., & Lempicki, R. A. (2009). Systematic and integrative analysis of large gene lists using DAVID bioinformatics resources. *Nature Protocols*, *4*(1), 44–57.

https://doi.org/10.1038/nprot.2008.211

Janssen, I., Heymsfield, S. B., Wang, Z., & Ross, R. (2000). Skeletal muscle mass and distribution in 468 men and women aged 18–88 yr. *Journal of Applied Physiology*, *89*(1), 81–88. https://doi.org/10.1152/jappl.2000.89.1.81

Joe, A. W. B. B., Yi, L., Natarajan, A., Le Grand, F., So, L., Wang, J., Rudnicki, M. A., & Rossi, F. M. V. V. (2010). Muscle injury activates resident fibro/adipogenic progenitors that facilitate myogenesis. *Nature Cell Biology*, *12*(2), 153–163. https://doi.org/10.1038/ncb2015

Jones, N. C., Tyner, K. J., Nibarger, L., Stanley, H. M., Cornelison, D. D. W., Fedorov, Y. V., & Olwin, B. B. (2005). The p38α/β MAPK functions as a molecular switch to activate the quiescent satellite cell. *Journal of Cell Biology*, *169*(1), 105–116. https://doi.org/10.1083/jcb.200408066

Juban, G., & Chazaud, B. (2017). Metabolic regulation of macrophages during tissue repair: insights from skeletal muscle regeneration. *FEBS Letters*, *591*(19), 3007–3021. https://doi.org/10.1002/1873-3468.12703

Juban, G., Saclier, M., Yacoub-Youssef, H., Kernou, A., Arnold, L., Boisson, C., Ben Larbi, S., Magnan, M., Cuvellier, S., Théret, M., Petrof, B. J., Desguerre, I., Gondin, J., Mounier, R., & Chazaud, B. (2018). AMPK Activation Regulates LTBP4-Dependent TGF-β1 Secretion by Pro-inflammatory Macrophages and Controls Fibrosis in Duchenne Muscular Dystrophy. *Cell Reports*, *25*(8), 2163-2176.e6. https://doi.org/10.1016/j.celrep.2018.10.077

Kajabadi, N., Low, M., Jacques, E., Lad, H., Tung, L. W., Babaeijandaghi, F., Gamu, D., Zelada, D., Wong, C. K., Chang, C., Yi, L., Wosczyna, M. N., Rando, T. A., Henríquez, J. P., Gibson, W. T., Gilbert, P. M., & Rossi, F. M. V. (2023). Activation of β-catenin in

mesenchymal progenitors leads to muscle mass loss. *Developmental Cell*, *58*(6), 489-505.e7. https://doi.org/10.1016/j.devcel.2023.02.009

Kopinke, D., Roberson, E. C., & Reiter, J. F. (2017). Ciliary Hedgehog Signaling Restricts Injury-Induced Adipogenesis. *Cell*, *170*(2), 340-351.e12. https://doi.org/10.1016/j.cell.2017.06.035

Kotsaris, G., Qazi, T. H., Bucher, C. H., Zahid, H., Pöhle-Kronawitter, S., Ugorets, V., Jarassier, W., Börno, S., Timmermann, B., Giesecke-Thiel, C., Economides, A. N., Le Grand, F., Vallecillo-García, P., Knaus, P., Geissler, S., & Stricker, S. (2023). Odd skipped-related 1 controls the pro-regenerative response of fibro-adipogenic progenitors. *Npj Regenerative Medicine*, *8*(1), 19. https://doi.org/10.1038/s41536-023-00291-6

Kuang, S., Kuroda, K., Le Grand, F., & Rudnicki, M. A. (2007). Asymmetric Self-Renewal and Commitment of Satellite Stem Cells in Muscle. *Cell*, *129*(5), 999–1010. https://doi.org/10.1016/j.cell.2007.03.044

Kuswanto, W., Burzyn, D., Panduro, M., Wang, K. K., Jang, Y. C., Wagers, A. J., Benoist, C., & Mathis, D. (2016). Poor Repair of Skeletal Muscle in Aging Mice Reflects a Defect in Local, Interleukin-33-Dependent Accumulation of Regulatory T Cells. *Immunity*, *44*(2), 355–367. https://doi.org/10.1016/j.immuni.2016.01.009

Laurens, C., Louche, K., Sengenes, C., Coué, M., Langin, D., Moro, C., & Bourlier, V. (2016). Adipogenic progenitors from obese human skeletal muscle give rise to functional white adipocytes that contribute to insulin resistance. *International Journal of Obesity*, *40*(3), 497–506. https://doi.org/10.1038/ijo.2015.193

Lavin, Y., Mortha, A., Rahman, A., & Merad, M. (2015). Regulation of macrophage development and function in peripheral tissues. *Nature Reviews. Immunology*, *15*(12), 731–

744. https://doi.org/10.1038/nri3920

Lees-Shepard, J. B., Yamamoto, M., Biswas, A. A., Stoessel, S. J., Nicholas, S.-A. E., Cogswell, C. A., Devarakonda, P. M., Schneider, M. J., Cummins, S. M., Legendre, N. P., Yamamoto, S., Kaartinen, V., Hunter, J. W., & Goldhamer, D. J. (2018). Activin-dependent signaling in fibro/adipogenic progenitors causes fibrodysplasia ossificans progressiva. *Nature Communications*, *9*(1), 471. https://doi.org/10.1038/s41467-018-02872-2

Leikina, E., Gamage, D. G., Prasad, V., Goykhberg, J., Crowe, M., Diao, J., Kozlov, M. M., Chernomordik, L. V., & Millay, D. P. (2018). Myomaker and Myomerger Work Independently to Control Distinct Steps of Membrane Remodeling during Myoblast Fusion. *Developmental Cell*, *46*(6), 767-780.e7. https://doi.org/10.1016/j.devcel.2018.08.006

Leinroth, A. P., Mirando, A. J., Rouse, D., Kobayahsi, Y., Tata, P. R., Rueckert, H. E., Liao, Y., Long, J. T., Chakkalakal, J. V., & Hilton, M. J. (2022). Identification of distinct non-myogenic skeletal-muscle-resident mesenchymal cell populations. *Cell Reports*, *39*(6), 110785. https://doi.org/10.1016/j.celrep.2022.110785

Lemos, D. R., Babaeijandaghi, F., Low, M., Chang, C.-K. K., Lee, S. T., Fiore, D., Zhang, R.-H. H., Natarajan, A., Nedospasov, S. A., & Rossi, F. M. V. V. (2015). Nilotinib reduces muscle fibrosis in chronic muscle injury by promoting TNF-mediated apoptosis of fibro/adipogenic progenitors. *Nature Medicine*, *21*(7), 786–794. https://doi.org/10.1038/nm.3869

Leon, A. S. (2017). Attenuation of Adverse Effects of Aging on Skeletal Muscle by Regular Exercise and Nutritional Support. *American Journal of Lifestyle Medicine*, *11*(1), 4–16. https://doi.org/10.1177/1559827615589319

Li, Y.-P. (2003). TNF-alpha is a mitogen in skeletal muscle. *American Journal of Physiology.*

Cell Physiology, *285*(2), C370-6. https://doi.org/10.1152/ajpcell.00453.2002

Lounev, V. Y., Ramachandran, R., Wosczyna, M. N., Yamamoto, M., Maidment, A. D. A., Shore, E. M., Glaser, D. L., Goldhamer, D. J., & Kaplan, F. S. (2009). Identification of progenitor cells that contribute to heterotopic skeletogenesis. *The Journal of Bone and Joint Surgery. American Volume*, *91*(3), 652–663. https://doi.org/10.2106/JBJS.H.01177

Love, M. I., Huber, W., & Anders, S. (2014). Moderated estimation of fold change and dispersion for RNA-seq data with DESeq2. *Genome Biology*, *15*(12), 550. https://doi.org/10.1186/s13059-014-0550-8

Machida, S., Spangenburg, E. E., & Booth, F. W. (2003). Forkhead transcription factor FoxO1 transduces insulin-like growth factor's signal to p27Kip1 in primary skeletal muscle satellite cells. *Journal of Cellular Physiology*, *196*(3), 523–531. https://doi.org/10.1002/jcp.10339

Malecova, B., Gatto, S., Etxaniz, U., Passafaro, M., Cortez, A., Nicoletti, C., Giordani, L., Torcinaro, A., De Bardi, M., Bicciato, S., De Santa, F., Madaro, L., & Puri, P. L. (2018). Dynamics of cellular states of fibro-adipogenic progenitors during myogenesis and muscular dystrophy. *Nature Communications*, *9*(1). https://doi.org/10.1038/s41467-018-06068-6

Mauro, A. (1961). Satellite cell of skeletal muscle fibers. *The Journal of Biophysical and Biochemical Cytology*, *9*, 493–495. https://doi.org/10.1083/jcb.9.2.493

Mázala, D. A. G., Novak, J. S., Hogarth, M. W., Nearing, M., Adusumalli, P., Tully, C. B., Habib, N. F., Gordish-Dressman, H., Chen, Y.-W., Jaiswal, J. K., & Partridge, T. A. (2020). TGF-β–driven muscle degeneration and failed regeneration underlie disease onset in a DMD mouse model. *JCI Insight*, *5*(6). https://doi.org/10.1172/jci.insight.135703

Medici, D., Shore, E. M., Lounev, V. Y., Kaplan, F. S., Kalluri, R., & Olsen, B. R. (2010). Conversion of vascular endothelial cells into multipotent stem-like cells. *Nature Medicine*, *16*(12), 1400–1406. https://doi.org/10.1038/nm.2252

Megeney, L. A., Kablar, B., Garrett, K., Anderson, J. E., & Rudnicki, M. A. (1996). MyoD is required for myogenic stem cell function in adult skeletal muscle. *Genes & Development*, *10*(10), 1173–1183. https://doi.org/10.1101/gad.10.10.1173

Merrick, D., Sakers, A., Irgebay, Z., Okada, C., Calvert, C., Morley, M. P., Percec, I., & Seale, P. (2019). Identification of a mesenchymal progenitor cell hierarchy in adipose tissue. *Science*, *364*(6438), eaav2501. https://doi.org/10.1126/science.aav2501

Millay, D. P., O'Rourke, J. R., Sutherland, L. B., Bezprozvannaya, S., Shelton, J. M., Bassel-Duby, R., & Olson, E. N. (2013). Myomaker is a membrane activator of myoblast fusion and muscle formation. *Nature*, *499*(7458), 301–305. https://doi.org/10.1038/nature12343

Mogi, M., Kohara, K., Nakaoka, H., Kan-no, H., Tsukuda, K., Wang, X.-L., Chisaka, T., Bai, H.-Y., Shan, B.-S., Kukida, M., Iwanami, J., Miki, T., & Horiuchi, M. (2016). Diabetic mice exhibited a peculiar alteration in body composition with exaggerated ectopic fat deposition after muscle injury due to anomalous cell differentiation. *Journal of Cachexia, Sarcopenia and Muscle*, *7*(2), 213–224. https://doi.org/10.1002/jcsm.12044

Moore, C. W., Allen, M. D., Kimpinski, K., Doherty, T. J., & Rice, C. L. (2016). Reduced skeletal muscle quantity and quality in patients with diabetic polyneuropathy assessed by magnetic resonance imaging. *Muscle & Nerve*, *53*(5), 726–732. https://doi.org/10.1002/mus.24779

Moss, F., & Leblond, C. P. (1970). Nature of dividing nuclei in skeletal muscle of growing rats. *Journal of Cell Biology*, *44*(2), 459–462. https://doi.org/10.1083/jcb.44.2.459

Mozzetta, C., Consalvi, S., Saccone, V., Tierney, M., Diamantini, A., Mitchell, K. J., Marazzi, G., Borsellino, G., Battistini, L., Sassoon, D., Sacco, A., & Puri, P. L. (2013). Fibroadipogenic progenitors mediate the ability of HDAC inhibitors to promote regeneration in dystrophic muscles of young, but not old Mdx mice. *EMBO Molecular Medicine*, *5*(4), 626–639. https://doi.org/10.1002/emmm.201202096

Müller, T. D., Finan, B., Bloom, S. R., D'Alessio, D., Drucker, D. J., Flatt, P. R., Fritsche, A., Gribble, F., Grill, H. J., Habener, J. F., Holst, J. J., Langhans, W., Meier, J. J., Nauck, M. A., Perez-Tilve, D., Pocai, A., Reimann, F., Sandoval, D. A., Schwartz, T. W., … Tschöp, M. H. (2019). Glucagon-like peptide 1 (GLP-1). *Molecular Metabolism*, *30*, 72–130. https://doi.org/10.1016/j.molmet.2019.09.010

Murphy, M. M., Lawson, J. A., Mathew, S. J., Hutcheson, D. A., & Kardon, G. (2011). Satellite cells, connective tissue fibroblasts and their interactions are crucial for muscle regeneration. *Development*, *138*(17), 3625–3637. https://doi.org/10.1242/dev.064162

Nauth, A., Giles, E., Potter, B. K., Nesti, L. J., O'brien, F. P., Bosse, M. J., Anglen, J. O., Mehta, S., Ahn, J., Miclau, T., & Schemitsch, E. H. (2012). Heterotopic ossification in orthopaedic trauma. *Journal of Orthopaedic Trauma*, *26*(12), 684–688. https://doi.org/10.1097/BOT.0b013e3182724624

Ohnuma, K., Yamochi, T., Uchiyama, M., Nishibashi, K., Iwata, S., Hosono, O., Kawasaki, H., Tanaka, H., Dang, N. H., & Morimoto, C. (2005). CD26 mediates dissociation of Tollip and IRAK-1 from caveolin-1 and induces upregulation of CD86 on antigen-presenting cells. *Molecular and Cellular Biology*, *25*(17), 7743–7757. https://doi.org/10.1128/MCB.25.17.7743-7757.2005

Oprescu, S. N., Yue, F., Qiu, J., Brito, L. F., & Kuang, S. (2020). Temporal Dynamics and

Heterogeneity of Cell Populations during Skeletal Muscle Regeneration. *IScience*, *23*(4), 100993. https://doi.org/10.1016/j.isci.2020.100993

Pacheco, R., Martinez-Navio, J. M., Lejeune, M., Climent, N., Oliva, H., Gatell, J. M., Gallart, T., Mallol, J., Lluis, C., & Franco, R. (2005). CD26, adenosine deaminase, and adenosine receptors mediate costimulatory signals in the immunological synapse. *Proceedings of the National Academy of Sciences of the United States of America*, *102*(27), 9583–9588. https://doi.org/10.1073/pnas.0501050102

Park, I.-H., & Chen, J. (2005). Mammalian target of rapamycin (mTOR) signaling is required for a late-stage fusion process during skeletal myotube maturation. *The Journal of Biological Chemistry*, *280*(36), 32009–32017. https://doi.org/10.1074/jbc.M506120200

Pérez-Díaz, S., Koumaiha, Z., Borok, M. J., Aurade, F., Pini, M., Periou, B., Rouault, C., Baba-Amer, Y., Clément, K., Derumeaux, G., Authier, F. J., Lafuste, P., & Relaix, F. (2022). Obesity impairs skeletal muscle repair through NID-1 mediated extracellular matrix remodeling by mesenchymal progenitors. *Matrix Biology*, *112*, 90–115. https://doi.org/10.1016/j.matbio.2022.08.006

Perrone, C. E., Fenwick-Smith, D., & Vandenburgh, H. H. (1995). Collagen and stretch modulate autocrine secretion of insulin-like growth factor-1 and insulin-like growth factor binding proteins from differentiated skeletal muscle cells. *The Journal of Biological Chemistry*, *270*(5), 2099–2106. https://doi.org/10.1074/jbc.270.5.2099

Purslow, P. P. (2020). The Structure and Role of Intramuscular Connective Tissue in Muscle Function. *Frontiers in Physiology*, *11*. https://doi.org/10.3389/fphys.2020.00495

Quinn, M. E., Goh, Q., Kurosaka, M., Gamage, D. G., Petrany, M. J., Prasad, V., & Millay, D. P. (2017). Myomerger induces fusion of non-fusogenic cells and is required for skeletal

muscle development. *Nature Communications*, *8*(1), 15665. https://doi.org/10.1038/ncomms15665

Rajendran, V., & Jain, M. V. (2018). In Vitro Tumorigenic Assay: Colony Forming Assay for Cancer Stem Cells. *Methods in Molecular Biology (Clifton, N.J.)*, *1692*, 89–95. https://doi.org/10.1007/978-1-4939-7401-6_8

Rasmussen, D. G. K., Hansen, T. W., von Scholten, B. J., Nielsen, S. H., Reinhard, H., Parving, H.-H., Tepel, M., Karsdal, M. A., Jacobsen, P. K., Genovese, F., & Rossing, P. (2018). Higher Collagen VI Formation Is Associated With All-Cause Mortality in Patients With Type 2 Diabetes and Microalbuminuria. *Diabetes Care*, *41*(7), 1493–1500. https://doi.org/10.2337/dc17-2392

Reggio, A., Rosina, M., Krahmer, N., Palma, A., Petrilli, L. L., Maiolatesi, G., Massacci, G., Salvatori, I., Valle, C., Testa, S., Gargioli, C., Fuoco, C., Castagnoli, L., Cesareni, G., & Sacco, F. (2020). Metabolic reprogramming of fibro/adipogenic progenitors facilitates muscle regeneration. *Life Science Alliance*, *3*(3), e202000646. https://doi.org/10.26508/lsa.202000660

Roberts, E. W., Deonarine, A., Jones, J. O., Denton, A. E., Feig, C., Lyons, S. K., Espeli, M., Kraman, M., McKenna, B., Wells, R. J. B., Zhao, Q., Caballero, O. L., Larder, R., Coll, A. P., O'Rahilly, S., Brindle, K. M., Teichmann, S. A., Tuveson, D. A., & Fearon, D. T. (2013). Depletion of stromal cells expressing fibroblast activation protein-α from skeletal muscle and bone marrow results in cachexia and anemia. *The Journal of Experimental Medicine*, *210*(6), 1137–1151. https://doi.org/10.1084/jem.20122344

Rochlin, K., Yu, S., Roy, S., & Baylies, M. K. (2010). Myoblast fusion: When it takes more to make one. *Developmental Biology*, *341*(1), 66–83.

https://doi.org/10.1016/j.ydbio.2009.10.024

Rommel, C., Bodine, S. C., Clarke, B. A., Rossman, R., Nunez, L., Stitt, T. N., Yancopoulos, G. D., & Glass, D. J. (2001). Mediation of IGF-1-induced skeletal myotube hypertrophy by PI(3)K/Akt/mTOR and PI(3)K/Akt/GSK3 pathways. *Nature Cell Biology*, *3*(11), 1009–1013. https://doi.org/10.1038/ncb1101-1009

Rubenstein, A. B., Smith, G. R., Raue, U., Begue, G., Minchev, K., Ruf-Zamojski, F., Nair, V. D., Wang, X., Zhou, L., Zaslavsky, E., Trappe, T. A., Trappe, S., & Sealfon, S. C. (2020). Single-cell transcriptional profiles in human skeletal muscle. *Scientific Reports*, *10*(1), 229. https://doi.org/10.1038/s41598-019-57110-6

Rudnicki, M. A., Schnegelsberg, P. N., Stead, R. H., Braun, T., Arnold, H. H., & Jaenisch, R. (1993). MyoD or Myf-5 is required for the formation of skeletal muscle. *Cell*, *75*(7), 1351–1359. https://doi.org/10.1016/0092-8674(93)90621-v

Ryan, G. R., Dai, X. M., Dominguez, M. G., Tong, W., Chuan, F., Chisholm, O., Russell, R. G., Pollard, J. W., & Stanley, E. R. (2001). Rescue of the colony-stimulating factor 1 (CSF-1)-nullizygous mouse (Csf1(op)/Csf1(op)) phenotype with a CSF-1 transgene and identification of sites of local CSF-1 synthesis. *Blood*, *98*(1), 74–84. https://doi.org/10.1182/blood.v98.1.74

Sabourin, L. A., Girgis-Gabardo, A., Seale, P., Asakura, A., & Rudnicki, M. A. (1999). Reduced differentiation potential of primary MyoD-/- myogenic cells derived from adult skeletal muscle. *The Journal of Cell Biology*, *144*(4), 631–643. https://doi.org/10.1083/jcb.144.4.631

Sacco, A., Doyonnas, R., Kraft, P., Vitorovic, S., & Blau, H. M. (2008). Self-renewal and expansion of single transplanted muscle stem cells. *Nature*, *456*(7221), 502–506.

https://doi.org/10.1038/nature07384

Saclier, M., Yacoub-Youssef, H., Mackey, A. L., Arnold, L., Ardjoune, H., Magnan, M., Sailhan, F., Chelly, J., Pavlath, G. K., Mounier, R., Kjaer, M., & Chazaud, B. (2013). Differentially Activated Macrophages Orchestrate Myogenic Precursor Cell Fate During Human Skeletal Muscle Regeneration. *Stem Cells*, *31*(2), 384–396. https://doi.org/10.1002/stem.1288

Saito, Y., Chikenji, T. S., Matsumura, T., Nakano, M., & Fujimiya, M. (2020). Exercise enhances skeletal muscle regeneration by promoting senescence in fibro-adipogenic progenitors. *Nature Communications*, *11*(1), 889. https://doi.org/10.1038/s41467-020-14734-x

Sambasivan, R., Yao, R., Kissenpfennig, A., Van Wittenberghe, L., Paldi, A., Gayraud-Morel, B., Guenou, H., Malissen, B., Tajbakhsh, S., & Galy, A. (2011). Pax7-expressing satellite cells are indispensable for adult skeletal muscle regeneration. *Development (Cambridge, England)*, *138*(17), 3647–3656. https://doi.org/10.1242/dev.067587

Sampath, S. C., Sampath, S. C., & Millay, D. P. (2018). Myoblast fusion confusion: the resolution begins. *Skeletal Muscle*, *8*(1), 3. https://doi.org/10.1186/s13395-017-0149-3

Scadden, D. T. (2006). The stem-cell niche as an entity of action. *Nature*, *441*(7097), 1075–1079. https://doi.org/10.1038/nature04957

Schwalie, P. C., Dong, H., Zachara, M., Russeil, J., Alpern, D., Akchiche, N., Caprara, C., Sun, W., Schlaudraff, K.-U., Soldati, G., Wolfrum, C., & Deplancke, B. (2018). A stromal cell population that inhibits adipogenesis in mammalian fat depots. *Nature*, *559*(7712), 103–108. https://doi.org/10.1038/s41586-018-0226-8

Scott, R. W., Arostegui, M., Schweitzer, R., Rossi, F. M. V. V, & Underhill, T. M. (2019). Hic1

Defines Quiescent Mesenchymal Progenitor Subpopulations with Distinct Functions and Fates in Skeletal Muscle Regeneration. *Cell Stem Cell*, *25*(6), 797-813.e9. https://doi.org/10.1016/j.stem.2019.11.004

Seale, P., Sabourin, L. A., Girgis-Gabardo, A., Mansouri, A., Gruss, P., & Rudnicki, M. A. (2000). Pax7 is required for the specification of myogenic satellite cells. *Cell*, *102*(6), 777–786. https://doi.org/10.1016/s0092-8674(00)00066-0

Serrano, A. L., Baeza-Raja, B., Perdiguero, E., Jardí, M., & Muñoz-Cánoves, P. (2008). Interleukin-6 is an essential regulator of satellite cell-mediated skeletal muscle hypertrophy. *Cell Metabolism*, *7*(1), 33–44. https://doi.org/10.1016/j.cmet.2007.11.011

Sherman, B. T., Hao, M., Qiu, J., Jiao, X., Baseler, M. W., Lane, H. C., Imamichi, T., & Chang, W. (2022). DAVID: a web server for functional enrichment analysis and functional annotation of gene lists (2021 update). *Nucleic Acids Research*, *50*(W1), W216–W221. https://doi.org/10.1093/nar/gkac194

Shore, E. M., Xu, M., Feldman, G. J., Fenstermacher, D. A., Cho, T.-J., Choi, I. H., Connor, J. M., Delai, P., Glaser, D. L., LeMerrer, M., Morhart, R., Rogers, J. G., Smith, R., Triffitt, J. T., Urtizberea, J. A., Zasloff, M., Brown, M. A., & Kaplan, F. S. (2006). A recurrent mutation in the BMP type I receptor ACVR1 causes inherited and sporadic fibrodysplasia ossificans progressiva. *Nature Genetics*, *38*(5), 525–527. https://doi.org/10.1038/ng1783

Sohn, J., Lu, A., Tang, Y., Wang, B., & Huard, J. (2015). Activation of non-myogenic mesenchymal stem cells during the disease progression in dystrophic dystrophin/utrophin knockout mice. *Human Molecular Genetics*. https://doi.org/10.1093/hmg/ddv125

Soliman, H., Paylor, B., Scott, R. W., Lemos, D. R., Chang, C. K., Arostegui, M., Low, M., Lee, C., Fiore, D., Braghetta, P., Pospichalova, V., Barkauskas, C. E., Korinek, V., Rampazzo,

A., MacLeod, K., Underhill, T. M., & Rossi, F. M. V. V. (2020). Pathogenic Potential of Hic1-Expressing Cardiac Stromal Progenitors. *Cell Stem Cell*, *26*(2), 205-220.e8. https://doi.org/10.1016/j.stem.2019.12.008

Stanley, A., Tichy, E. D., Kocan, J., Roberts, D. W., Shore, E. M., & Mourkioti, F. (2022). Dynamics of skeletal muscle-resident stem cells during myogenesis in fibrodysplasia ossificans progressiva. *Npj Regenerative Medicine*, *7*(1), 5. https://doi.org/10.1038/s41536-021-00201-8

Stefkovich, M., Traynor, S., Cheng, L., Merrick, D., & Seale, P. (2021). Dpp4+ interstitial progenitor cells contribute to basal and high fat diet-induced adipogenesis. *Molecular Metabolism*, *54*, 101357. https://doi.org/10.1016/j.molmet.2021.101357

Stitt, T. N., Drujan, D., Clarke, B. A., Panaro, F., Timofeyva, Y., Kline, W. O., Gonzalez, M., Yancopoulos, G. D., & Glass, D. J. (2004). The IGF-1/PI3K/Akt Pathway Prevents Expression of Muscle Atrophy-Induced Ubiquitin Ligases by Inhibiting FOXO Transcription Factors. *Molecular Cell*, *14*(3), 395–403. https://doi.org/10.1016/S1097-2765(04)00211-4

Stumm, J., Vallecillo-García, P., Vom Hofe-Schneider, S., Ollitrault, D., Schrewe, H., Economides, A. N., Marazzi, G., Sassoon, D. A., & Stricker, S. (2018). Odd skipped-related 1 (Osr1) identifies muscle-interstitial fibro-adipogenic progenitors (FAPs) activated by acute injury. *Stem Cell Research*, *32*, 8–16. https://doi.org/10.1016/j.scr.2018.08.010

Sweeney, H. L., & Hammers, D. W. (2018). Muscle Contraction. *Cold Spring Harbor Perspectives in Biology*, *10*(2), a023200. https://doi.org/10.1101/cshperspect.a023200

Sweeney, H. L., & Holzbaur, E. L. F. (2018). Motor Proteins. *Cold Spring Harbor Perspectives in Biology*, *10*(5), a021931. https://doi.org/10.1101/cshperspect.a021931

Takada, N., Takasugi, M., Nonaka, Y., Kamiya, T., Takemura, K., Satoh, J., Ito, S., Fujimoto, K., Uematsu, S., Yoshida, K., Morita, T., Nakamura, H., Uezumi, A., & Ohtani, N. (2022). Galectin-3 promotes the adipogenic differentiation of PDGFRα+ cells and ectopic fat formation in regenerating muscle. *Development*, *149*(3). https://doi.org/10.1242/dev.199443

Tam, C. S., Covington, J. D., Bajpeyi, S., Tchoukalova, Y., Burk, D., Johannsen, D. L., Zingaretti, C. M., Cinti, S., & Ravussin, E. (2014). Weight Gain Reveals Dramatic Increases in Skeletal Muscle Extracellular Matrix Remodeling. *The Journal of Clinical Endocrinology & Metabolism*, *99*(5), 1749–1757. https://doi.org/10.1210/jc.2013-4381

Tatsumi, R., Anderson, J. E., Nevoret, C. J., Halevy, O., & Allen, R. E. (1998). HGF/SF is present in normal adult skeletal muscle and is capable of activating satellite cells. *Developmental Biology*, *194*(1), 114–128. https://doi.org/10.1006/dbio.1997.8803

Tawil, R., van der Maarel, S. M., & Tapscott, S. J. (2014). Facioscapulohumeral dystrophy: the path to consensus on pathophysiology. *Skeletal Muscle*, *4*(1), 12. https://doi.org/10.1186/2044-5040-4-12

Tidball, J. G. (2017). Regulation of muscle growth and regeneration by the immune system. *Nature Reviews. Immunology*, *17*(3), 165–178. https://doi.org/10.1038/nri.2016.150

Tonkin, J., Temmerman, L., Sampson, R. D., Gallego-Colon, E., Barberi, L., Bilbao, D., Schneider, M. D., Musarò, A., & Rosenthal, N. (2015). Monocyte/Macrophage-derived IGF-1 Orchestrates Murine Skeletal Muscle Regeneration and Modulates Autocrine Polarization. *Molecular Therapy : The Journal of the American Society of Gene Therapy*, *23*(7), 1189–1200. https://doi.org/10.1038/mt.2015.66

Torossian, F., Guerton, B., Anginot, A., Alexander, K. A., Desterke, C., Soave, S., Tseng, H.-W., Arouche, N., Boutin, L., Kulina, I., Salga, M., Jose, B., Pettit, A. R., Clay, D., Rochet, N.,

Vlachos, E., Genet, G., Debaud, C., Denormandie, P., … Le Bousse-Kerdilès, M.-C. (2017). Macrophage-derived oncostatin M contributes to human and mouse neurogenic heterotopic ossifications. *JCI Insight*, *2*(21). https://doi.org/10.1172/jci.insight.96034

Tseng, H.-W. W., Girard, D., Alexander, K. A., Millard, S. M., Torossian, F., Anginot, A., Fleming, W., Gueguen, J., Goriot, M.-E. E., Clay, D., Jose, B., Nowlan, B., Pettit, A. R., Salga, M., Genêt, F., Bousse-Kerdilès, M.-C. L. C. Le, Banzet, S., & Lévesque, J.-P. P. (2022). Spinal cord injury reprograms muscle fibroadipogenic progenitors to form heterotopic bones within muscles. *Bone Research*, *10*(1), 22. https://doi.org/10.1038/s41413-022-00188-y

Uezumi, A., Fukada, S. I., Yamamoto, N., Takeda, S., & Tsuchida, K. (2010). Mesenchymal progenitors distinct from satellite cells contribute to ectopic fat cell formation in skeletal muscle. *Nature Cell Biology*, *12*(2), 143–152. https://doi.org/10.1038/ncb2014

Uezumi, A., Fukada, S., Yamamoto, N., Ikemoto-Uezumi, M., Nakatani, M., Morita, M., Yamaguchi, A., Yamada, H., Nishino, I., Hamada, Y., & Tsuchida, K. (2014). Identification and characterization of PDGFRα+ mesenchymal progenitors in human skeletal muscle. *Cell Death & Disease*, *5*(4), e1186–e1186. https://doi.org/10.1038/cddis.2014.161

Uezumi, A., Ikemoto-Uezumi, M., Zhou, H., Kurosawa, T., Yoshimoto, Y., Nakatani, M., Hitachi, K., Yamaguchi, H., Wakatsuki, S., Araki, T., Morita, M., Yamada, H., Toyoda, M., Kanazawa, N., Nakazawa, T., Hino, J., Fukada, S., & Tsuchida, K. (2021). Mesenchymal Bmp3b expression maintains skeletal muscle integrity and decreases in age-related sarcopenia. *Journal of Clinical Investigation*, *131*(1). https://doi.org/10.1172/JCI139617

Uezumi, A., Ito, T., Morikawa, D., Shimizu, N., Yoneda, T., Segawa, M., Yamaguchi, M., Ogawa, R., Matev, M. M., Miyagoe-Suzuki, Y., Takeda, S., Tsujikawa, K., Tsuchida, K.,

Yamamoto, H., & Fukada, S. (2011). Fibrosis and adipogenesis originate from a common mesenchymal progenitor in skeletal muscle. *Journal of Cell Science*, *124*(21), 3654–3664. https://doi.org/10.1242/jcs.086629

Vallecillo-García, P., Orgeur, M., Vom Hofe-Schneider, S., Stumm, J., Kappert, V., Ibrahim, D. M., Börno, S. T., Hayashi, S., Relaix, F., Hildebrandt, K., Sengle, G., Koch, M., Timmermann, B., Marazzi, G., Sassoon, D. A., Duprez, D., & Stricker, S. (2017). Odd skipped-related 1 identifies a population of embryonic fibro-adipogenic progenitors regulating myogenesis during limb development. *Nature Communications*, *8*(1), 1218. https://doi.org/10.1038/s41467-017-01120-3

van Loon, L. J. C., & Goodpaster, B. H. (2006). Increased intramuscular lipid storage in the insulin-resistant and endurance-trained state. *Pflügers Archiv*, *451*(5), 606–616. https://doi.org/10.1007/s00424-005-1509-0

Villalta, S. A., Rinaldi, C., Deng, B., Liu, G., Fedor, B., & Tidball, J. G. (2011). Interleukin-10 reduces the pathology of mdx muscular dystrophy by deactivating M1 macrophages and modulating macrophage phenotype. *Human Molecular Genetics*, *20*(4), 790–805. https://doi.org/10.1093/hmg/ddq523

Webster, M. T., Manor, U., Lippincott-Schwartz, J., & Fan, C.-M. (2016). Intravital Imaging Reveals Ghost Fibers as Architectural Units Guiding Myogenic Progenitors during Regeneration. *Cell Stem Cell*, *18*(2), 243–252. https://doi.org/10.1016/j.stem.2015.11.005

Wosczyna, M. N., Biswas, A. A., Cogswell, C. A., & Goldhamer, D. J. (2012). Multipotent progenitors resident in the skeletal muscle interstitium exhibit robust BMP-dependent osteogenic activity and mediate heterotopic ossification. *Journal of Bone and Mineral Research*, *27*(5), 1004–1017. https://doi.org/10.1002/jbmr.1562

Wosczyna, M. N., Konishi, C. T., Perez Carbajal, E. E., Wang, T. T., Walsh, R. A., Gan, Q., Wagner, M. W., & Rando, T. A. (2019). Mesenchymal Stromal Cells Are Required for Regeneration and Homeostatic Maintenance of Skeletal Muscle. *Cell Reports*, *27*(7), 2029-2035.e5. https://doi.org/10.1016/j.celrep.2019.04.074

Wosczyna, M. N., & Rando, T. A. (2018). A Muscle Stem Cell Support Group: Coordinated Cellular Responses in Muscle Regeneration. *Developmental Cell*, *46*(2), 135–143. https://doi.org/10.1016/j.devcel.2018.06.018

Wu, C., Jin, X., Tsueng, G., Afrasiabi, C., & Su, A. I. (2016). BioGPS: building your own mash-up of gene annotations and expression profiles. *Nucleic Acids Research*, *44*(D1), D313–D316. https://doi.org/10.1093/nar/gkv1104

Yang, J., Vamvini, M., Nigro, P., Ho, L.-L., Galani, K., Alvarez, M., Tanigawa, Y., Renfro, A., Carbone, N. P., Laakso, M., Agudelo, L. Z., Pajukanta, P., Hirshman, M. F., Middelbeek, R. J. W., Grove, K., Goodyear, L. J., & Kellis, M. (2022). Single-cell dissection of the obesity-exercise axis in adipose-muscle tissues implies a critical role for mesenchymal stem cells. *Cell Metabolism*, *34*(10), 1578-1593.e6. https://doi.org/10.1016/j.cmet.2022.09.004

Zaruba, M.-M., Theiss, H. D., Vallaster, M., Mehl, U., Brunner, S., David, R., Fischer, R., Krieg, L., Hirsch, E., Huber, B., Nathan, P., Israel, L., Imhof, A., Herbach, N., Assmann, G., Wanke, R., Mueller-Hoecker, J., Steinbeck, G., & Franz, W.-M. (2009). Synergy between CD26/DPP-IV inhibition and G-CSF improves cardiac function after acute myocardial infarction. *Cell Stem Cell*, *4*(4), 313–323. https://doi.org/10.1016/j.stem.2009.02.013

Zhang, Q., Vashisht, A. A., O'Rourke, J., Corbel, S. Y., Moran, R., Romero, A., Miraglia, L., Zhang, J., Durrant, E., Schmedt, C., Sampath, S. C., & Sampath, S. C. (2017). The microprotein Minion controls cell fusion and muscle formation. *Nature Communications*,

8(1), 15664. https://doi.org/10.1038/ncomms15664

Zhong, J., & Rajagopalan, S. (2015). Dipeptidyl Peptidase-4 Regulation of SDF-1/CXCR4 Axis: Implications for Cardiovascular Disease. *Frontiers in Immunology*, *6*, 477. https://doi.org/10.3389/fimmu.2015.00477